

# **Identification and Functional Characterization of the RGM Family in Mouse**

**Inauguraldissertation**

zur Erlangung der Würde einer Doktorin der Philosophie  
vorgelegt der Philosophisch-Naturwissenschaftlichen Fakultät der Universität Basel  
von

**Vera Niederkofler**

aus Dornbirn / Österreich

Basel, März 2005

Genehmigt von der Philosophisch-Naturwissenschaftlichen Fakultät auf Antrag von

Prof. Dr. Silvia Arber  
(Dissertationsleiterin)

Prof. Dr. Esther Stöckli  
(Koreferentin)

Prof. Dr. Markus Rüegg  
(Vorsitzender)

Basel, 5. April 2005

Prof. Dr. Hans-Jakob Wirz  
(Dekan)

# Aims of the Thesis

This thesis is comprised of two distinct projects:

1.) The major goal of this work was to identify and subsequently characterize the murine family of Repulsive Guidance Molecules (RGMs). Initially discovered in chick, as a factor involved in guidance of retinal axons, we attempted to determine the function of the murine orthologues by generation and analysis of knockout animals for each of the three identified mouse *RGM* genes.

2.) The second project aimed at defining the neuronal cell type in which ER81 exerts its role in controlling the ingrowth of central projections of proprioceptive afferents into the ventral spinal cord. This was accomplished by the analysis of *Er81<sup>lox</sup>* mice (ETS domain flanked by loxP sites) crossed to various CRE-driver mouse lines and thereby generating cell type specific knockouts.

# Table of Contents

## Abstracts

### 1 Axon Guidance

1.1	Axon Guidance Molecules — an Overview.....	8-17
1.2	Patterning Molecules: Multitasking in the Nervous System.....	18-26
1.3	<i>RGM</i> Gene Function Is Required for Neural Tube Closure but not Retinal Topography in the Mouse Visual System.....	27-50
1.4	<i>In Vivo</i> Analysis of <i>mRGMb</i> Function in the Nervous System.....	51-61
	REFERENCES.....	62-78

### 2 Iron Homeostasis

2.1	Balancing Iron.....	80-88
2.2	<i>mRGMc</i> Acts as a Switch to Suppress Dietary Iron-Sensing during Inflammatory Response.....	89-102
	REFERENCES.....	103-109



### **3 Monosynaptic Stretch Reflex Circuit**

3.1	The Role of ETS Transcription Factors in Neuronal Circuit Formation.....	111-114
3.2	Peripheral NT3 Signaling Is Required for ETS Protein Expression and Central Patterning of Proprioceptive Sensory Afferent.....	115-143
	REFERENCES.....	144-151

### **Appendix**

A	Acknowledgments.....	153
B	Curriculum vitae.....	154-155

# Abstracts

## 1.) Identification and Functional Characterization of the Mouse RGM Family

The establishment of topographic projections in the developing visual system depends on spatially and temporally controlled expression of axon guidance molecules. In the developing chick tectum, the graded expression of Repulsive Guidance Molecule (*RGM*) has been proposed to be involved in controlling topography of retinal ganglion cell (RGC) axon termination zones along the anterior-posterior axis of the tectum. We show that there are three mouse proteins homologous to chick *RGM*, displaying similar proteolytic processing but exhibiting differential cell surface targeting by GPI anchor addition. Two members of this gene family (*mRGMa* and *mRGMb*) are expressed in complementary patterns in the nervous system, with *mRGMa* prominently expressed in the superior colliculus at the time of anterior-posterior targeting of RGC axons. The third member of the family (*mRGMc*) is expressed most strongly in skeletal muscles, but also in heart and liver.

Surprisingly, mice lacking *mRGMa* or *mRGMb* do not exhibit defects in anterior-posterior targeting of RGC axons to their stereotypic termination zones in the superior colliculus. Instead, *mRGMa* mutant mice show a defect in cephalic neural tube closure. The *in vivo* function of *mRGMb* still remains to be elucidated.

Mice lacking *mRGMc* mimic the phenotype observed in patients suffering from juvenile hereditary hemochromatosis, an iron overload disease caused by disruption of HFE2, the human ortholog of *mRGMc*. Moreover, *mRGMc* mutant mice exhibit a dramatic decrease in hepatic *Hamp*, a negative regulator of iron absorption, expression, yet retain *Hamp* inducibility via the inflammatory pathway. Our findings define a key role for *mRGMc* in the normal iron-sensing pathway and also reveal how this homeostatic pathway is uncoupled during inflammation, through the coordinate extinction of *mRGMc* and activation of *Hamp* expression.

## **2.) Peripheral NT3 Signaling Is Required for ETS Protein Expression and Central Patterning of Proprioceptive Sensory Afferents**

To study the role of NT3 in directing axonal projections of proprioceptive dorsal root ganglion (DRG) neurons,  $NT3^{-/-}$  mice were crossed with mice carrying a targeted deletion of the proapoptotic gene *Bax*. In  $Bax^{-/-}/NT3^{-/-}$  mice, NT3-dependent neurons survived and expressed the proprioceptive neuronal marker parvalbumin. Initial extension and collateralization of proprioceptive axons into the spinal cord occurred normally, but proprioceptive axons extended only as far as the intermediate spinal cord. This projection defect is similar to the defect in mice lacking the ETS transcription factor ER81. Few if any DRG neurons from  $Bax^{-/-}/NT3^{-/-}$  mice expressed ER81 protein. Expression of an *NT3* transgene in muscle restored ER81 expression in DRGs of  $NT3^{-/-}$  mice. Finally, addition of NT3 to DRG explant cultures resulted in induction of ER81 protein. Our data indicate that NT3 mediates the formation of proprioceptive afferent-motor neuron connections via regulation of ER81.

# **Chapter 1**

## **Axon Guidance**

# 1.1 Axon Guidance Molecules – an Overview

During development of the nervous system, growing axons find their targets by making use of a complex array of guidance signals that attract or repel growth cones (Tessier-Lavigne and Goodman, 1996; Dickson, 2002). These guidance cues, both attractants and repellents, include contact-mediated and secreted molecules, acting over short or long distances, respectively. The same signal at different points along a pathway can evoke a different response, depending on the complement of receptors expressed, on the intracellular state of active signaling molecules such as cyclic nucleotides, and on cross talk between intracellular signaling cascades (Song et al., 1997; Song et al., 1998; Song and Poo, 1999; Yu and Bargmann, 2001; Guan and Rao, 2003; Nishiyama et al., 2003).

## Steering of the Growth Cone

Guidance cues are perceived by the growth cone, which is a specialized and sensitive motile cytoskeletal structure located at the tips of developing neurites. Receptors on the surface of the growth cone sense guidance cues and transduce directional information by means of cytoskeletal changes. There are two filamentous components of the cytoskeleton common to all growth cones. Microtubules dominate the central domain (C-domain) of the growth cone, while an actin-based, microfilament system is concentrated in the peripheral domain (P-domain), where it forms the cytoskeletons of filopodia and lamellipodia (Smith, 1988; Huber et al., 2003; Zhou and Cohan, 2004) (Figure 1). Filopodia are stuffed with dense, parallel actin filaments, while lamellipodia contain actin filaments organized into a compact meshwork. Filopodial actin filaments are oriented with their fast-growing barbed ends toward the filopodium tip. The extension and retraction of a filopodium reflects the balance between the polymerization of actin at barbed ends and the retrograde flow of entire filaments. Retrograde flow is prevented when F-actin becomes immobilized through their attachment to adhesion sites on the growth cone membrane, which in turn enables myosin motors to exert the traction force for forward protrusive activity. Regulating the assembly and disassembly of

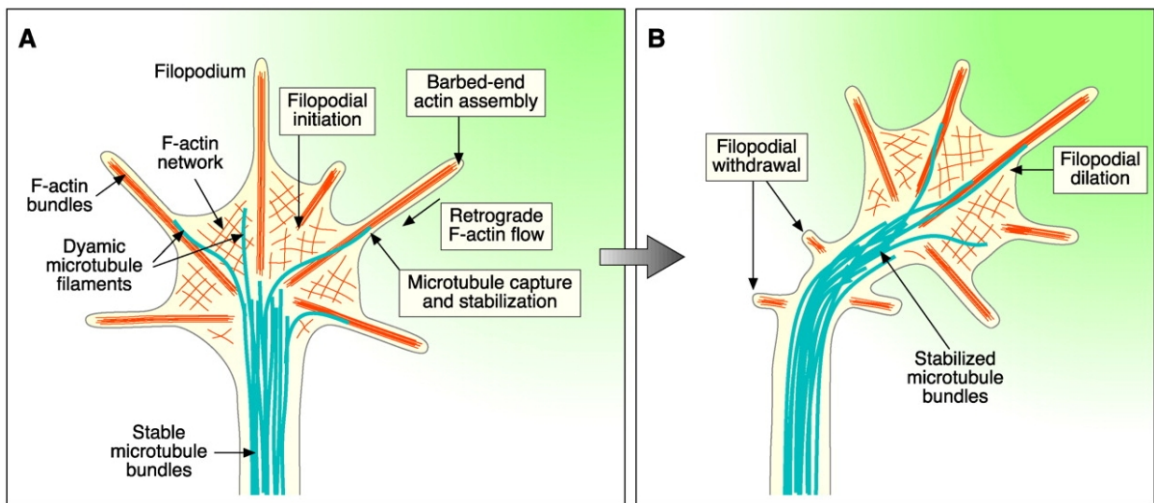


**Figure 1. Growth Cone Turning.**

(A, B) A model showing one way in which a growth cone might turn toward an attractant (green). (after Dickson, 2002)

the actinomyosin cytoskeleton, the attachment of F-actin to adhesion sites and myosin motor activity can influence growth cone extension and steering. Repulsive and attractive cues influence growth cone morphology by regulating these processes. The turning of the growth cones is tightly dependent upon the movement of the filopodia. In fact, without filopodia, correct pathfinding is disrupted (Chien et al., 1993; Zheng et al., 1996). Localized F-actin-based protrusive activity seems to be an initial step in growth cone navigation, because asymmetry in the protrusion of filopodia precedes growth cone turning (Bentley and Toroian-Raymond, 1986; Zheng et al., 1996; Isbister and O'Connor, 2000). Turning of the growth cone shaft (C-domain) requires asymmetric extension and stabilization of microtubule bundles in the new direction (Dent and Gertler, 2003; Gordon-Weeks, 2004) (Figure 1). Notably,  $\text{Ca}^{2+}$  signaling also plays an important role in growth cone turning since many effectors that regulate cytoskeletal rearrangements are  $\text{Ca}^{2+}$  dependent either directly or via intermediate events (Henley and Poo, 2004).

How do axon guidance cues regulate cytoskeletal dynamics within the growth cone? There is ample evidence that axon guidance cue signaling involves the action of proteins belonging to the Rho family of small GTP-binding proteins, key regulators of actin cytoskeletal dynamics (Hall, 1998; Luo, 2000; Dickson, 2001; Luo, 2002). Guidance receptors have been shown to interact directly or indirectly with Rho GTPases (Guan and Rao, 2003; Huber et al., 2003). These effector molecules in turn organize the response of receptor-expressing cells by regulating the structure and dynamics of the actin cytoskeleton through the control of actin polymerization, branching, and depolymerization. Moreover, Rho family members direct actin-myosin-dependent contractility, controlling the retrograde flow of F-actin within the growth cone (Huber et al., 2003).

## **Classical Axon Guidance Molecules**

Of the known axon guidance cues, four families have received the most attention: Slits, Netrin, Semaphorins, and Ephrins (Figure 2). All of these ligands and their receptors are evolutionarily conserved to various extents throughout the animal kingdom, as are their principal roles in the wiring of the nervous system (Chisholm and Tessier-Lavigne, 1999). The ligands from each family can act as both attractants and repellents, depending on the type

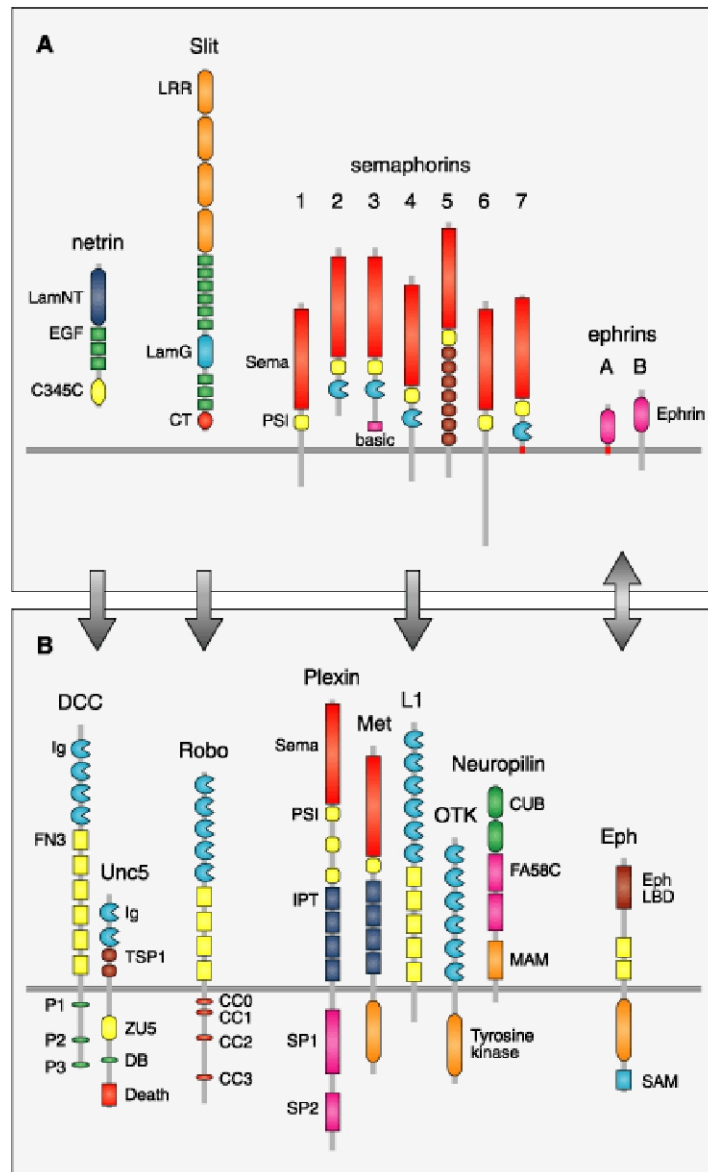


**Figure 2. Summary of the Four Best Studied Families of Guidance Molecules (A) and Their Receptors (B).** Domain names are from SMART (<http://smart.embl-heidelberg.de>). P1 to P3, DB (DCC-binding), CC0 to CC3, and SP1 and Sp2 indicate conserved regions in the cytoplasmic domains of DCC, UNC-5, Robo, and Plexin receptors, respectively. (after Dickson, 2002)



of the responding cell and on its developmental context (Yu and Bargmann, 2001; Huber et al., 2003; Wen et al., 2004).

### **Slits and Robos**

These molecules were first discovered through genetic experiments in *D. melanogaster*. Slits are large secreted proteins that signal through Robo (Roundabout) receptors in both vertebrates and invertebrates (Brose et al., 1999; Kidd et al., 1999; Li et al., 1999; Hao et al., 2001). Slits generally repel growing axons expressing Robo receptors. The Robo-Slit system has been extensively characterized with regards to ventral midline axon guidance in both *Drosophila* and vertebrates (Kidd et al., 1998; Seeger et al., 1993; Zou et al., 2000; Long et al., 2004; Sabatier et al., 2004), but also functions in guiding retinal projections in vertebrates (Karlstrom et al., 1996; Fricke et al., 2001; Plump et al., 2002). In addition to its repulsive guiding activity Slit was also purified as a factor that stimulates sensory axon branching and elongation (Van Vactor and Flanagan, 1999; Wang et al., 1999b; Zinn and Sun, 1999).

### **Netrins and Their Receptors**

A genetic screen in *C. elegans* isolated three mutants with defects in circumferential guidance of pioneer axons: *unc-5*, *unc-6/netrin* and *unc-40/DCC* (Hedgecock et al., 1990; Ishii et al., 1992; Leung-Hagesteijn et al., 1992; Chan et al., 1996). In parallel, biochemical purification of attractive signals for chick spinal commissural axons revealed Netrin-1 and Netrin-2, vertebrate homologues of UNC-6 (Kennedy et al., 1994; Serafini et al., 1994). The attractive activity of UNC-6/Netrin is transduced by the immunoglobulin superfamily receptor UNC-40/DCC (Keino-Masu et al., 1996). The best-understood role of Netrins is in attracting axons to the ventral midline in flies and vertebrates, acting in a complementary way to Slit repulsion (Harris et al., 1996; Mitchell et al., 1996; Serafini et al., 1996; Fazeli et al., 1997). Netrins can also act as chemorepellent (Colamarino and Tessier-Lavigne, 1995). This signal is mediated by the second Netrin receptor UNC-5, another immunoglobulin superfamily member, either alone or as a coreceptor for DCC (Leonardo et al., 1997; Hong et al., 1999; Keleman and Dickson, 2001; Guan and Rao, 2003).

Neogenin, a member of the DCC family, has also been shown to be a Netrin receptor (Wang et al., 1999a). *Neogenin* mutant mice do not appear to have an obvious axon guidance phenotype (Leighton et al., 2001). Recently, the first functional role for Netrin-Neogenin binding has been demonstrated during mammary gland morphogenesis (Srinivasan et al.,

2003). The authors suggest that Netrin-1 and its receptor Neogenin serve an adhesive function during nonneuronal organogenesis.

### **Semaphorins and Their Receptors**

Semaphorins are a large family of cell surface and secreted guidance molecules, defined by the presence of a conserved ~420-amino acid Sema domain at their NH<sub>2</sub>-termini. Semaphorins are divided into eight classes, on the basis of their structure. Classes 1 and 2 are found in invertebrates, classes 3 to 7 are found in vertebrates, and class V Semaphorins are encoded by viruses (Raper, 2000). The search for molecules expressed on specific axon fascicles in the grasshopper central nervous system (CNS) led to the discovery of the first Semaphorin, namely Semaphorin1/fasciculin IV (Kolodkin et al., 1992). Shortly after, Semaphorin3A/collapsin-1 was purified as potent inducer of vertebrate sensory ganglion growth cone collapse *in vitro* (Luo et al., 1993).

Semaphorins signal through multimeric receptor complexes. The composition of these receptor complexes is not fully known. Invertebrate Semaphorins, membrane-associated Semaphorins in vertebrates and viral Semaphorins have been shown to interact directly with Plexins (Comeau et al., 1998; Winberg et al., 1998; Tamagnone et al., 1999). Plexins comprise a large family of transmembrane proteins divided into four groups (A to D), on the basis of sequence similarity (Tamagnone et al., 1999). Vertebrate class 3 secreted Semaphorins however, generally utilize Neuropilin proteins (NP-1 and NP-2) as obligate ligand binding co-receptors, which assemble a Semaphorin/Neuropilin/Plexin signaling complex (Chen et al., 1997; He and Tessier-Lavigne, 1997; Kolodkin et al., 1997; Takahashi et al., 1999; Tamagnone et al., 1999). Experiments employing molecules with truncated cytoplasmic domains show that Plexins are essential to mediate repulsion, while Neuropilins do not appear to have a signaling function, but rather contribute to ligand specificity (Nakamura et al., 1998; Takahashi et al., 1999; Tamagnone et al., 1999; Cheng et al., 2001). To date, the only exception is Semaphorin3E, which has recently been shown to signal through PlexinD1, independent of Neuropilins, to perform its function in controlling vascular patterning (Gu et al., 2005). In addition to Plexins and Neuropilins, three other proteins have been implicated as either Semaphorin receptors or components of a holoreceptor complex in axon guidance: First, off-track (OtK), a catalytically inactive receptor tyrosine kinase, associates with *Drosophila* PlexinA to mediate Semaphorin1A repulsive function (Winberg et al., 2001; Whitford and Ghosh, 2001). Second, L1, a neuronal cell adhesion molecule plays a

role in repulsive responses to Semaphorin3A as part of the Neuropilin/Plexin receptor complex (Castellani et al., 2000; He, 2000). And third, a  $\beta$ 1-subunit-containing integrin receptor mediates growth promoting effects of Semaphorin7A on olfactory bulb axons (Pasterkamp et al., 2003). Outside the nervous system three more Semaphorin receptors or receptor components have been identified, namely Met (Giordano et al., 2002), CD72 (Kumanogoh et al., 2000) and Tim-2 (Kumanogoh et al., 2002).

Genetic analysis of Semaphorin function in flies and mice suggest that they primarily act as short-range inhibitory cues to deflect axons away from inappropriate regions, or guide them through repulsive corridors (Raper, 2000; Cheng et al., 2001). In contrast, several studies provide evidence that Semaphorins can also act as attractants (Wong et al., 1999; Raper, 2000; Kantor et al., 2004; Wolman et al., 2004). On top of their function in axon guidance, Semaphorins subserve diverse roles such as organogenesis, angiogenesis, neuronal apoptosis, neoplastic transformation, and immune system function (Spriggs, 1999; Bismuth and Boumsell, 2002; Neufeld et al., 2002; Trusolino and Comoglio, 2002; Kumanogoh and Kikutani, 2003; Neufeld et al., 2005).

### **Ephrins and Eph Receptors**

Eph receptors were initially cloned as orphan receptor tyrosine kinases, and the Ephrins identified as their ligands (Pandey et al., 1995). It was then discovered that Ephs and Ephrins are expressed in complementary gradients in the chick retina and optic tectum respectively, where they are important for retinotectal topography (Cheng and Flanagan, 1994; Cheng et al., 1995; Drescher et al., 1995). Ephrins and Ephs are each subdivided into two subclasses based on sequence conservation and their binding affinities: EphrinAs are anchored to the plasma membrane via a GPI linkage and each can bind the majority of the EphA subclass of receptors. In contrast, EphrinBs have a transmembrane domain and cytoplasmic region, and interact predominantly with members of the EphB subclass of receptors. There is little crosstalk between the two classes, except for EphA4, which can also bind with considerably high affinity to EphrinBs (Orioli and Klein, 1997), and EphB2, which was shown to bind to EphrinA5 (Barton et al., 2004). Although Ephrin/Eph signaling is now known to be involved in many biological processes, including vasculogenesis, formation of tissue borders and synaptic plasticity (Kullander and Klein, 2002), its function is still best understood in the visual system (McLaughlin et al., 2003a). Several functional *in vitro* and genetic *in vivo* studies have shown that EphrinAs, acting through their EphA receptors, partially control the

topographic mapping of the temporal-nasal retinal axis along the anterior-posterior tectal axis, by controlling topographically-specific interstitial branching of retinal axons (Yates et al., 2001). This branching is mediated by relative levels of EphA receptor repellent signaling. The dorsal-ventral retinal mapping along the lateral-medial tectal axis involves attractive signaling, mediated by EphrinB ligands and EphB receptors (Hindges et al., 2002; McLaughlin et al., 2003b). Correct mapping requires forward signaling, in which EphrinB ligands activate EphB receptors and EphrinB reverse signaling, in which EphBs serve as ligands to signal back through the transmembrane EphrinBs (Hindges et al., 2002; Mann et al., 2002).

The bidirectional signaling ability of Ephrins appears to be a common theme. In addition to their role in retinotopic map formation they control axon guidance in many other places. A well understood system for bidirectional EphrinB signaling is the vertebrate midline. Ipsilateral projecting axons of retinal ganglion cells expressing EphB1 are repelled by a source of EphrinB2 at the optic chiasm via forward signaling (Williams et al., 2003; Williams et al., 2004). In contrast, anterior commissure axons expressing EphrinB2, travel along territories rich in EphA4- and EphB2-positive cells. The fact that neither EphB2 nor EphA4 receptors require their catalytic activities to mediate this effect suggests that EphrinB2 is the signaling component partner in this process (Henkemeyer et al., 1996; Kullander et al., 2001).

### **RGMs and Neogenin**

In addition to the above discussed guidance molecules, recent work led to the discovery of a new axon guidance family, RGMs (Repulsive Guidance Molecule). RGM was initially discovered in a screen to identify molecules implicated in retinotectal guidance in chick: The posterior chick tectum has been shown to exhibit repulsive activity on temporal retinal ganglion cells (Walter et al., 1987a; Walter et al., 1987b). This led to the notion of a repulsive factor in the posterior tectum. The repulsive activity was diminished after heat treatment or incubation with the enzyme PI-PLC (phosphatidylinositol-specific phospholipase C), which cleaves GPI linked proteins from the cell surface (Walter et al., 1987a; Walter et al., 1990). A screen to identify molecules that were expressed in a higher concentration in the posterior tectum as compared to the anterior tectum, were sensitive to PI-PLC treatment and were developmentally regulated, revealed a 33 kDa, GPI-anchored protein fulfilling these requirements. Stripe and collapse assays using a protein fraction that contained this 33 kDa

molecule demonstrated guidance and collapse activity *in vitro* (Stahl et al., 1990). The 33 kDa molecule, called RGM (Repulsive Guidance Molecule), was later purified and cloned from the posterior part of the chick optic tectum and its function as a guiding and repelling factor *in vitro* was verified (Monnier et al., 2002).

Recently, we identified three mouse homologs, *mRGMa*, *mRGMb*, and *mRGMc* (Chapter 1.3; Niederkofler et al., 2004), two of which are expressed in the developing nervous system (*mRGMa* and *mRGMb*), the third, *mRGMc* is expressed mainly in skeletal muscle, heart and liver. The functional analysis of mice mutant in *mRGMa*, the closest homolog to the *RGM* identified in chick (*cRGM*), revealed no retinocollicular topography defect along the anterior-posterior axis. Instead, these mice exhibit a neural tube closure defect, known as exencephaly (Chapter 1.3; Niederkofler et al., 2004). This was somewhat surprising considering the *in vitro* guiding and collapsing activity of *cRGM*. *In vitro* experiments using hippocampal slice cultures suggest that *mRGMa* also functions as a repulsive guidance cue controlling the layer specific projection of entorhinal fibers to the dentate gyrus (Brinks et al., 2004).

*mRGMb/DRAGON* has been identified in parallel in a genetic screen for the promoter region of genes regulated by DRG11 (Samad et al., 2004), a paired homeodomain transcription factor, previously shown to play a role in the development of nociceptive sensory circuits in the spinal cord (Chen et al., 2001). In addition, *mRGMb/DRAGON* has been proposed by *in vitro* binding experiments to act as homophilic cell-cell neuronal adhesion molecule (Samad et al., 2004). Recently, *mRGMb/DRAGON* has also been suggested to act as BMP co-receptor (Samad et al., 2005). This was concluded from the fact that *mRGMb/DRAGON* can bind to BMP ligands and receptors, enhancing BMP signaling.

The non-neuronally expressed *mRGMc* has recently been linked to iron metabolism (Chapter 2.2). Mutation of *HFE2/HJV* (the human ortholog of *mRGMc*) has been shown to cause an iron overload disease called juvenile hereditary hemochromatosis (Papanikolaou et al., 2004).

Little is known about the signaling pathway of the RGM family of molecules. *cRGM* has been demonstrated to bind and transmit its guiding and collapsing activity *in vitro* through Neogenin (Rajagopalan et al., 2004), a formerly identified receptor for mouse Netrin (Wang et

al., 1999a; Srinivasan et al., 2003). Moreover, gene expression perturbation experiments in chick embryos showed that the ligand-receptor pair cRGM-Neogenin is also involved in cell survival (Matsunaga et al., 2004). While mRGMa binds to Neogenin, the receptor(s) for mRGMb and mRGMc still remain unidentified (Rajagopalan et al., 2004).

## **Molecular Multitasking**

Many members of the above discussed protein families, which were originally characterized in the nervous system as axon guidance molecules, have been recently demonstrated to contribute to the development of a variety of organs (for review see Hinck, 2004). Similarly, molecules known to act in patterning of embryonic tissue such as Hedgehogs, bone morphogenic proteins (BMPs), Wnts and fibroblast growth factors (FGFs) have been shown to play an important role in axon guidance and synaptogenesis. These “non-classical” axon guidance molecules will be described in the following chapter.

## 1.2 Patterning Molecules: Multitasking in the Nervous System

Rishard Salie\*, Vera Niederkofler\* & Silvia Arber (Neuron 45, 189-192, 2005)

### Summary

Classical patterning molecules previously implicated in controlling cell fate choices in the nervous system have recently been shown to play additional roles in axon guidance and synaptogenesis. Bone morphogenetic proteins (BMPs), Sonic hedgehog (Shh), Wnts and fibroblast growth factors (FGFs) all participate in multiple acts of controlling neuronal circuit assembly. Depending on the cellular context, they can provide instructive signals at the growth cone or synapse, or alternatively can elicit responses in the nucleus initiating transcriptional changes. Differences in signal transduction pathways may contribute to the diversity of the functional repertoire of these versatile molecules.

\* equal contribution

Precise spatiotemporal gene regulation governs nervous system development by controlling cell proliferation, migration and patterning as well as later events such as neuronal circuit formation and specificity in synaptogenesis. Gene families with evolutionarily conserved roles in patterning embryonic tissue such as Hedgehogs, bone morphogenetic proteins (BMPs), Wnts and fibroblast growth factors (FGFs) act by assigning cell fates through transcriptional control of gene expression (Anderson et al., 1997; Jessell, 2000; Patapoutian and Reichardt, 2000; Altmann and Brivanlou, 2001). Within the nervous system, they were long believed to play exclusive roles in regulating patterning processes. In contrast, many molecules involved in regulating axon guidance and synaptogenesis act preferentially at the growth cone or synapse (Tessier-Lavigne and Goodman, 1996; Yu and Bargmann, 2001; Scheiffele, 2003). Work from recent years however, has revealed several well-documented examples of molecular multitasking forcing us to reconsider this division.

When elucidating mechanisms by which multifunctional molecules exhibit their activities, two important aspects need to be considered. First, because of their inductive properties, determination of whether patterning molecules also control axonal outgrowth and neuronal circuit formation is inherently challenging. Consequently, direct and potential indirect activities are difficult to distinguish and need to be evaluated carefully. Second, the transduction mechanisms by which multifunctional molecules transmit their signals to result in appropriate cellular responses might depend significantly on whether they are acting in assigning cell fate or in controlling axonal targeting and synaptogenesis. In particular, it is well established that patterning molecules often result in the induction of transcriptional changes, whereas rapid integration of signals directly by the growth cone or synapse is a prerequisite for activity of molecules involved in axon guidance and synaptogenesis (Jessell, 2000; Yu and Bargmann, 2001; Scheiffele, 2003). This minireview focuses on recent studies of several families of classical patterning molecules and how their roles in cell fate assignment compare to their function in axon guidance and synaptogenesis. Particular emphasis will be given to the question of how signals are being transduced to elicit cellular responses.

### **Exploiting Shh and BMP Activities in the Spinal Cord to Function in Axon Guidance**

Two main signaling sources within the developing vertebrate spinal cord coordinately control the generation of distinct progenitor cell domains along the dorso-ventral axis. While the graded action of Shh released from the floor plate is a major determinant for the generation of cell types in the ventral spinal cord, BMP signals produced by the roof plate act to pattern the



dorsal spinal cord (Figure 3; Jessell, 2000; Altmann and Brivanlou, 2001). BMPs are also involved in the generation of neural crest cells and act to determine autonomic cell lineages (Anderson et al., 1997). Once generated, commissural neurons in the dorsal spinal cord extend axons towards and across the floor plate. The molecular mechanisms involved in these guidance decisions are well understood and classical guidance molecules such as Netrins and Slits play major roles in this process (Tessier-Lavigne and Goodman, 1996; Yu and Bargmann, 2001). Interestingly, recent studies have shown that members of the BMP and Hedgehog gene families also contribute to guidance of commissural axons towards the floor plate (Figure 3).

Experiments from the Dodd lab have provided evidence that the roof plate and select members of the BMP family possess repulsive activity capable of directing axons ventrally (Augsburger et al., 1999; Butler and Dodd, 2003). Analysis of roof plate activity from mice mutant in *BMP6*, *BMP7* or *GDF7* showed that only *BMP7* and *GDF7* contribute to this activity (Butler and Dodd, 2003). This result was somewhat surprising since *GDF7* lacked deflecting activity *in vitro* (Augsburger et al., 1999). Interestingly, roof plates from *BMP7/GDF7* double mutant mice showed no further reduction in repulsive activity in this assay when compared to roof plates from either the *BMP7* or *GDF7* single mutants (Butler and Dodd, 2003). These results pointed to the formation of active heterodimers of *BMP7* and *GDF7* functioning in repulsion *in vivo*. Indeed, co-culture experiments showed that *BMP7/GDF7* heterodimers exhibit stronger repulsive activity than *BMP7* homodimers and immunoprecipitation experiments confirmed physical interaction between *BMP7* and *GDF7* under these conditions (Butler and Dodd, 2003). It remains to be determined through which receptor complexes this repulsive signaling activity is mediated. At least part of the signal transduction machinery is likely to be distinct from that involved in controlling neuronal fate in the dorsal spinal cord since *BMP6* exhibits patterning activity but fails to guide commissural axons. It is also known that *BMP7* and *GDF7* influence axon guidance at concentrations below that required for neuronal specification (Augsburger et al., 1999). Moreover, the ability of *BMP7* to induce growth cone collapse in dissociated spinal cord neurons *in vitro* occurs over a time scale that excludes transcriptional mechanisms, implying a direct effect of BMPs at the growth cone. Together, these findings suggest that *BMP7/GDF7* heterodimers act at the growth cone in a repulsive manner to direct commissural axons away from the roof plate.

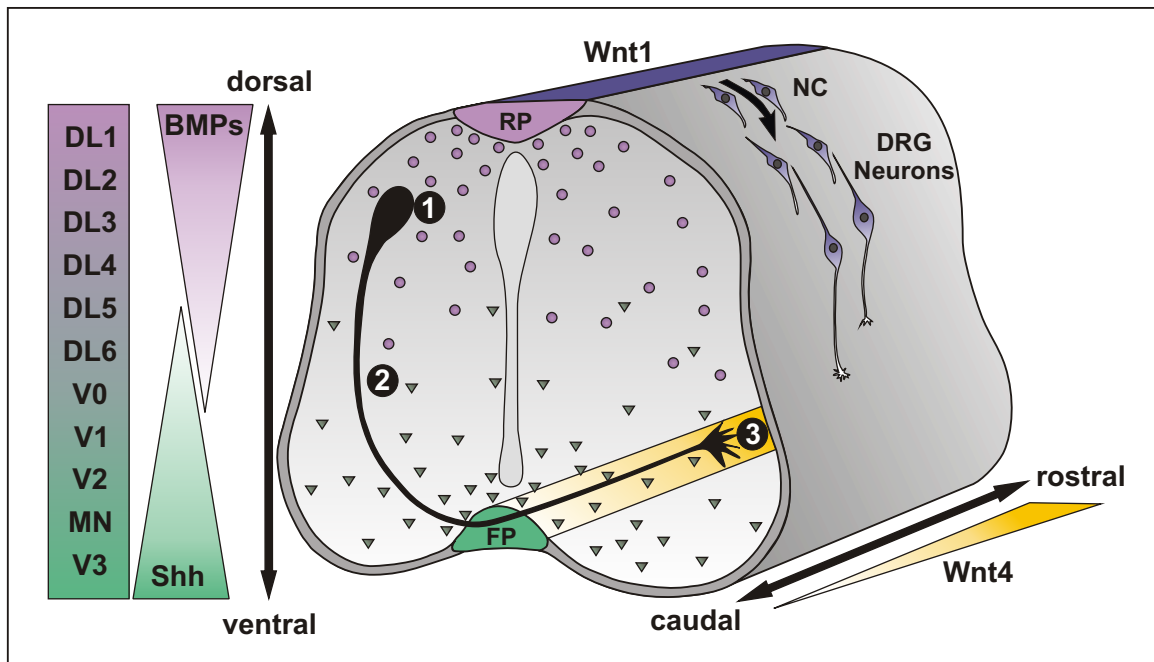


**Figure 3. Control of Commissural Axon Guidance by Patterning Molecules.**

(Left) At early stages, BMPs (purple) from the roof plate (RP) control the generation of distinct neuronal subtypes in the dorsal spinal cord (DL1-DL6) whereas Shh (green) from the floor plate (FP) acts to pattern the ventral spinal cord (V0-V3, MN).

(Right) At later stages, commissural axon guidance is influenced sequentially by (1) BMPs (purple) from the RP to direct axons ventrally, (2) combinatorial activities of Netrin-1 and Shh (green) to attract axons to the FP and (3) Wnt4 (yellow) expression in a caudal-low rostral-high gradient to control rostral turning towards the brain. BMP and Shh signals are shown only on the cross sectional face of the three-dimensional schematic drawing of the spinal cord but are expressed along the entire rostro-caudal length of the spinal cord. Wnt1 signals (blue) derived from the roof plate act to instruct neural crest (NC) cells to acquire DRG sensory neuron identity. Dorsal-ventral and rostro-caudal axes are indicated by black arrows.

The establishment of the further trajectory of commissural axons towards the ventral midline is influenced by attractive cues derived from the floor plate (Figure 3). While the role of Netrin-1 in this process is well established (Tessier-Lavigne and Goodman, 1996), the fact that floor plates from *Netrin-1* mutant mice still show some residual ability to attract commissural axons *in vitro* suggested that other floor plate derived factors might collaborate with Netrin-1. Moreover, while most commissural axons do not reach the ventral midline in mice mutant in either *Netrin-1* or its receptor *DCC*, some axons still arrive at the floor plate. Indeed, a recent study suggests that Shh acts in concert with Netrin-1 as a chemoattractant in a manner independent of its initial role in patterning to draw commissural axons toward the midline (Charron et al., 2003). Using collagen gel co-culture assays, this study shows that commissural axons reorient towards a source of Shh, establishing the sufficiency of Shh in this process. The action of Shh in patterning cell types in the ventral spinal cord is mediated through Smoothed (Smo), the activity of which can be blocked efficiently by application of cyclopamine. Since the remaining attractive activity of *Netrin-1* mutant floor plates is diminished upon application of cyclopamine, at least part of the signaling cascade responsible for interacting with the cytoskeleton to mediate chemoattraction is most likely conserved between patterning and guidance activities downstream of Shh.

What effects do BMPs and Shh have on commissural axon outgrowth *in vivo*? Both *BMP7* and *GDF7* mutant commissural neurons exhibit transient defects in axonal polarization at early stages of axon extension, but at later stages their axons revert to a normal ventral trajectory (Butler and Dodd, 2003). The *in vivo* impact of Shh on guidance of commissural axons towards the midline was assessed in mice with conditional inactivation of *Smo* in the dorsal spinal cord including commissural neurons. While axons in these mice reach the midline, axonal trajectories towards the floor plate appear more widespread and irregular than in wild-type (Charron et al., 2003). Together, these findings suggest that rather than being primary axon outgrowth and guidance forces for commissural axons, BMPs and Shh might act to fine tune trajectories of commissural axons growing towards the floor plate in response to Netrin-1 (Figure 3).

### **Evolutionary and Cell Type Specific Divergence in Wnt Signaling**

Apart from their well-characterized roles in influencing cell proliferation, Wnts were recently also shown to be involved in specification of dorsal root ganglia (DRG) sensory neurons at

early developmental stages (Figure 3; Lee et al., 2004). Moreover, several studies have addressed the role of Wnt signaling in axon guidance, neurite outgrowth (see below) and synaptogenesis (Packard et al., 2003). Wnts are not only versatile in regards to their biological functions, but also with respect to the mechanisms by which Wnt signals are transduced and integrated. Interestingly, phylogenetically distant species appear to use distinct signaling strategies to do so.

Commissural neurons in the *Drosophila* embryonic ventral nerve cord project their axons towards and across the midline. Axon guidance towards the midline also involves chemoattraction by Netrins, but there is currently no evidence that either BMP homologues or Hh proteins are involved in these events in *Drosophila*. Axons crossing the midline in *Drosophila* have to choose between two alternative routes: the anterior or the posterior commissure. Initial details regarding the mechanism responsible for this choice were revealed when Derailed (Drl; an atypical receptor tyrosine kinase with homology to vertebrate Ryk) was discovered to be both necessary and sufficient to direct axons through the anterior commissure (Bonkowsky et al., 1999). Drl is selectively expressed on axons choosing the anterior commissure and ectopic expression of Drl in neurons normally choosing the posterior commissure forces them to the anterior path. An elegant genetic screen identified Wnt5 as a ligand for Drl (Yoshikawa et al., 2003). *Wnt5* is expressed by neurons adjacent to the posterior commissure and in *wnt5* mutants, as in *drl* mutants, anterior commissural axons project abnormally through the posterior commissure. Furthermore, Wnt5 misexpression in midline glia leads to a marked reduction or complete loss of the anterior commissure. Since no genetic interaction between Drl and the well-established Wnt receptor component Frizzled could be detected in control of midline guidance in *Drosophila*, Drl seems to transduce the chemorepellant Wnt5 signal in a Frizzled independent manner (Yoshikawa et al., 2003). Despite the fact that the intracellular region of Drl is not predicted to possess catalytic activity, this domain appears to be functionally essential in *Drosophila* (Yoshikawa et al., 2003). In contrast, the *C.elegans* Ryk ortholog LIN-18 functions in parallel to Frizzled/LIN-17 signaling during vulval cell fate specification, and the kinase domain of LIN-18 is dispensable for its function (Inoue et al., 2004).

In vertebrates, commissural axons turn rostrally after crossing the floor plate, projecting toward their targets in the brain. Wnt signaling has been implicated in controlling this decision (Lyuksyutava et al., 2003; Figure 3). *Wnt4* is expressed in a high-anterior to low-

posterior gradient along the spinal cord in the floor plate throughout the time window when commissural neurons make the decision to turn towards the brain. Wnt4 expressed from COS cell aggregates can induce postcrossing commissural axons to turn either anteriorly or posteriorly, depending on the position these cells are placed. Interestingly, the observed activity of Wnt4 selectively affects postcrossing but not precrossing commissural axons. While it is currently not known how sensitivity to Wnts is induced after midline crossing, commissural neurons have also been shown to switch their responsiveness to Netrin-1 and Slit after crossing the midline (Stein and Tessier-Lavigne, 2001). In functional experiments *in vitro*, the addition of secreted Frizzled-related proteins (sFRPs) to block Wnt binding to its receptor is able to randomize the turning event of commissural axons after crossing the midline. *In vivo*, commissural axons from mice mutant in *Frizzled3* lose anterior preference in turning after midline crossing. Since mammalian Ryk is not expressed by dorsal commissural neurons, it does not appear to be involved in transduction of the Wnt4 signal in this system. These findings suggest that an anterior-posterior gradient of *Wnt4* expression is read by Frizzled3 on commissural axons and converted into an instructive, attractive guidance cue to efficiently steer these axons towards the brain (Figure 3; Lyuksyutava et al., 2003). A recent study from the Baltimore lab shows that mammalian Ryk forms a complex with Frizzled-8 and binds directly to Wnt-1 and Wnt3a (Lu et al., 2004). Furthermore, it provides evidence for direct binding of the intracellular domain of mammalian Ryk to Dishevelled, thus activating the canonical Wnt pathway downstream of the receptor complex.

Many interesting questions remain in resolving how Wnts act in different cellular contexts and/or species to transduce Wnt signals into appropriate cellular responses. Mammalian Wnt signals have been shown to influence axon growth positively for both commissural axons signaling through Frizzled-3 (Lyuksyutava et al., 2003) and cultured DRG neurons signaling through Ryk (Lu et al., 2004). It can be anticipated that other neuronal populations might respond to Wnt signals in a repulsive manner, analogous to the *Drosophila* Wnt5 signal read by Drl (Yoshikawa et al., 2003). In support of this, the activity of several classes of axon guidance molecules depends both on the complement of receptors expressed by a neuron as well as on the intracellular state of active signaling molecules such as cyclic nucleotides (Yu and Bargmann, 2001). For example, Netrin-1 acts as a chemoattractant for commissural axons in the spinal cord whereas it repels trochlear motor axons at hindbrain levels (Tessier-Lavigne and Goodman, 1996). Exactly how Wnts, and in particular gradients of Wnts, are transduced at different stages of neuronal differentiation will be of great interest

in future studies. Interspecies comparison of Wnt signaling cascades and their activities within distinct classes of neurons will certainly help to reveal the full breadth of effects mediated by Wnt signaling.

### **FGFs Determine Rostro-Caudal Identity and Act as Presynaptic Organizers**

Recent evidence implicates FGFs as important upstream signaling molecules in assigning anterior-posterior identity to spinal motor neurons (Dasen et al., 2003). This study demonstrates that spinal progenitors can read graded FGF signals resulting in the expression of defined Hox-c proteins at distinct rostro-caudal levels of the spinal cord. In turn, Hox-c proteins impose columnar fate upon spinal motor neurons, acting upstream in the determination of motor neuron fate, which specifies the expression of downstream genes involved in execution of axon pathfinding decisions. Whereas Hoxc6 expression determines lateral motor column fate at forelimb levels, Hoxc9 acts at thoracic levels to determine the fate of column of terni motor neurons (Dasen et al., 2003). In future experiments, it will be interesting to define whether not only motor neurons are responsive to FGF signaling to generate rostro-caudal diversity, but whether interneurons and DRG neurons also use the same strategy.

Acting at the growth cone and synapse, members of the FGF family of proteins have not only been implicated in the establishment of trochlear motor neuron trajectories (Irving et al., 2002), but have also recently been isolated as important players in presynaptic organization during synaptogenesis (Umemori et al., 2004). To identify target-derived molecules influencing differentiation of presynaptic nerve terminals, extracts derived from forebrain of postnatal mice were added to cultured chick embryonic motor neurons. Such cultures showed a significant increase in presynaptic differentiation when compared to control cultures. This assay was subsequently used for the purification of active components derived from postnatal forebrain extracts, resulting in the identification of FGF22 as one active component. In a survey of 12 different purified FGFs, not only FGF22, but also the two closely related family members FGF10 and FGF7, had very similar activities in inducing vesicle aggregation and neurite branching. The findings were extended to study the role of FGF signaling in controlling presynaptic neuronal differentiation of cerebellar mossy fibers *in vivo*. In support of the *in vitro* experiments, conditional elimination of FGFR2 postnatally resulted in a significant reduction in presynaptic mossy fiber specializations within the cerebellum. While the current study mainly focuses on vesicle aggregation and neurite

branching, other members of the FGF family appear to have distinct and diverse combinations of activities, at least when added to motor neurons in culture (Umemori et al., 2004). It will be interesting to characterize these activities as well as the types of neurons responsive to these factors in future studies.

## **Outlook**

The use of patterning molecules for multiple, important tasks during nervous system formation is a prominent, recurring theme. The recycling of signaling sources established at early developmental stages to independently direct later steps of development represents a wonderful way to further exploit complex signaling systems. Much attention in the future must be given to define distinctions and similarities of signaling pathways involved in the translation of extracellular signals into downstream cellular responses. It will be of particular interest to identify which actions permanently change cellular identity by initiating transcriptional responses and which events act at defined subcellular sites without altering permanently neuronal identity. Finally, given the recent exciting discoveries of molecular multitasking it seems unlikely that patterning molecules retire at the end of development and it will be intriguing to determine their functions in mature neuronal circuits.

# 1.3 *RGM* Gene Function Is Required for Neural Tube Closure but not Retinal Topography in the Mouse Visual System

Vera Niederkofler<sup>\*</sup>, Rishard Salie<sup>\*</sup>, Markus Sigrist & Silvia Arber (J. Neurosci 24, 808-18, 2004)

## Abstract

The establishment of topographic projections in the developing visual system depends on spatially and temporally controlled expression of axon guidance molecules. In the developing chick tectum, the graded expression of Repulsive Guidance Molecule (*RGM*) has been proposed to be involved in controlling topography of retinal ganglion cell (RGC) axon termination zones along the anterior-posterior axis of the tectum. We now show that there are three mouse proteins homologous to chick *RGM* displaying similar proteolytic processing but exhibiting differential cell surface targeting by GPI anchor addition. Two members of this gene family (*mRGMa* and *mRGMb*) are expressed in complementary patterns in the nervous system, and *mRGMa* is expressed prominently in the superior colliculus at the time of anterior-posterior targeting of RGC axons. The third member of the family (*mRGMc*) is expressed almost exclusively in skeletal muscles. Functional studies in the mouse reveal a role for *mRGMa* in controlling cephalic neural tube closure thus defining an unexpected role for *mRGMa* in early embryonic development. In contrast, *mRGMa* mutant mice do not exhibit defects in anterior-posterior targeting of RGC axons to their stereotypic termination zones in the superior colliculus.

<sup>\*</sup> equal contribution



## Introduction

The precise temporal and spatial interplay of different extracellular proteins is essential for the establishment of correct morphology and patterning of the nervous system at early developmental stages as well as for the assembly of neuronal circuits later in development. Many extracellular proteins have been studied for their role in controlling axon outgrowth to target regions in an attempt to address the question of how axonal projections of different neuronal populations achieve precise targeting to the region they innervate in the mature nervous system. These studies have led to the concept that extracellular guidance molecules can act in both attractive and repulsive manners (Tessier-Lavigne and Goodman, 1996) and much is known about the mechanisms by which these molecules direct axons towards their targets (Yu and Bargmann, 2001; Dickson, 2002).

One system where the underlying molecular mechanisms controlling the development of precise axonal projections have been studied extensively is the projection of retinal ganglion cells (RGCs) to either the chick tectum or the rodent superior colliculus (Sperry, 1963; McLaughlin et al., 2003a). The anatomical arrangement of retinocollicular projections during rodent development and in the mature system has been well-defined (Simon and O'Leary, 1992). In the mature retinocollicular system there is a precise topography of projections from the retina to the superior colliculus: Temporal RGC axons consistently terminate in the anterior superior colliculus whereas nasal RGC axons project to the posterior superior colliculus (Sperry, 1963; McLaughlin et al., 2003a). This observation has led to the proposal that RGC axons terminating in the anterior superior colliculus may be repelled by molecular cues found at a higher concentration in the posterior relative to the anterior superior colliculus (Sperry, 1963). Consistent with this model, temporal RGCs are repelled by membranes isolated from the posterior chick tectum and grow preferentially on anterior tectal membranes (Walter et al., 1987). The isolation of molecules expressed in a low anterior to high posterior gradient in the chick tectum led to the discovery that members of the Ephrin family (in particular EphrinA2 and EphrinA5) possess such a repulsive activity (Drescher et al., 1995; Nakamoto et al., 1996; Monschau et al., 1997). Both *EphrinA2* and *EphrinA5* are expressed in a gradient in the chick tectum and the mouse superior colliculus (Drescher et al., 1995; Cheng et al., 1995; Feldheim et al., 2000). Functional evidence supports the idea that EphrinA2 and EphrinA5 act as repulsive guidance cues confining the termination zones of

temporal RGCs to more anterior positions (Nakamoto et al., 1996; Feldheim et al., 2000; McLaughlin et al., 2003a).

Chick RGM (cRGM) has been reported to possess an *in vitro* activity similar to the Ephrins, causing growth cone collapse and preferential guidance of temporal RGC axons (Monnier et al., 2002). In contrast to Ephrins however, the *in vivo* role of RGM remains unclear. To determine whether *RGM* does indeed play a role in the establishment of retinocollicular projections *in vivo* we decided to isolate the corresponding mouse gene and examine the neural phenotype of mice lacking *RGM* gene function.

We discovered three genes with homology to *cRGM* within the mouse genome. All three murine members of this protein family – *mRGMa*, *mRGMb* and *mRGMc* – show a carboxy terminal GPI-anchor consensus sequence, but the efficiency of cell surface transport of the different family members is highly variable. The expression of *mRGMa* and *mRGMb* is largely confined to the nervous system where they are expressed in complementary patterns. In contrast, the most prominent expression of *mRGMc* is found in skeletal muscles. Analysis of *mRGMa* mutant mice demonstrates that the development of RGC projections from the retina to the colliculus and topographic mapping of these projections to defined anterior-posterior positions within the superior colliculus is normal. In contrast, ~ 50% of *mRGMa* mutant mice show defects in cephalic neural tube closure. Together, these findings identify a novel family of extracellular GPI anchored proteins in the mouse with homology to cRGM and reveal an unexpected role for *mRGMa* in the process of neural tube closure.

## Results

### Isolation of Three Genes in the Mouse Genome Homologous to *cRGM*

To isolate genes homologous to *cRGM* (Monnier et al., 2002) in the mouse genome, we searched the database for mouse expressed sequence tags (ESTs) and genomic sequences with a high degree of identity to *cRGM*. We found that the mouse genome contains three genes with homology to *cRGM* (in this paper now referred to as *cRGMa*). Mouse *RGMa* (*mRGMa*) is most closely related to *cRGMa* and shows an identity of 80% to *cRGMa* at the amino acid level (Figure 4A). The two more distantly related members of the RGM family of proteins, which we called *mRGMb* and *mRGMc*, show identities to *cRGMa* of 50% and 42%, respectively (Figure 4A). Additional evidence that *mRGMb* may be more closely related to *mRGMa* than *mRGMc* comes from an analysis of the organization of the respective genomic loci. The positions of intron-exon junctions as well as the sizes of introns are highly conserved between *mRGMa* (chromosome 7) and *mRGMb* (chromosome 17; data not shown). In addition, two homologous genes – chromodomain helicase DNA binding protein 1 (*CHD1*) and chromodomain helicase DNA binding protein 2 (*CHD2*) – are located in close proximity to *mRGMb* (*mRGMb/CHD1*) and *mRGMa* (*mRGMa/CHD2*) respectively, suggesting that *mRGMa* and *mRGMb* may have evolved by gene duplication. In contrast, the genomic organization of *mRGMc* is highly divergent to *mRGMa* or *mRGMb* (data not shown).

We found that like *cRGMa*, all three members of the mouse family of RGM proteins contain an amino terminal consensus signal peptide for targeting to the endoplasmic reticulum (Figure 4A, grey box) and a carboxy terminal GPI anchor consensus sequence (Figure 4A). However, the quality and score of the best site predicted for the addition of a GPI anchor varied significantly amongst the three mouse homologues of RGM and *cRGMa* (*cRGMa*: 7.93; *mRGMa*: 1.14; *mRGMb*: 2.72; *mRGMc*: 6.63), raising the possibility that not all members of the RGM family are processed by the addition of a carboxy terminal GPI anchor with the same efficiency. Since differential processing could affect the efficiency of protein targeting to the plasma membrane where GPI anchored proteins are usually localized to lipid rafts (Sharom and Lehto, 2002), we assessed the subcellular localization of *cRGMa*, *mRGMa*, *mRGMb* and *mRGMc* by transfecting full-length RGMs and a cDNA encoding nuclear  $\beta$ -galactosidase from a bicistronic mRNA into COS-7 cells. To label cell surface accumulated proteins, we incubated live transfected cells with primary antibodies specific to individual

RGM family members before fixation and permeabilization of cells. For the identification of transfected cells we stained them with an antibody to  $\beta$ -galactosidase after fixation and permeabilization. While strong cell surface labeling was detected on cells transfected with cRGMa and mRGMc, mRGMa expressing cells were labeled less intensely, and very low if any staining was detected on the plasma membrane of cells transfected with mRGMb (Figure 5A-D). When transfected cells were fixed and permeabilized before incubation with the primary antibody, all four RGMs displayed strong labeling (Figure 5E-H). However, mRGMb protein was highly concentrated in the perinuclear endoplasmic reticulum/Golgi compartment, consistent with the observation that mRGMb protein is not efficiently targeted to the cell surface (Figure 5G). To determine whether this differential subcellular distribution was also found in neurons *in vivo* we electroporated embryonic day 3 (E3) chick spinal cords with vectors expressing mRGMa, mRGMb or mRGMc. Whereas mRGMa and mRGMc proteins were expressed and efficiently transported into neuronal processes by embryonic day 5 (E5), mRGMb appeared to be concentrated predominantly in neuronal cell bodies and proximal axonal processes, consistent with our findings in transfected COS-7 cells (Figure 5I-O).

It has been shown previously that in addition to the proteolytic processing of the amino terminal signal peptide, cRGMa is cleaved once more to yield two proteolytic fragments – an amino terminal fragment containing an integrin binding RGD motif and a carboxy terminal GPI anchored fragment (Monnier et al., 2002). To determine whether this is also the case for mRGM proteins, we expressed mRGMa, mRGMb and mRGMc in COS-7 cells replacing the GPI anchor consensus sequence by a Myc labeled hexahistidine tag. The molecular weights of these mRGM proteins collected from COS-7 cell supernatants were ~42kD whereas the molecular weight of cRGMa expressed using the same strategy was ~35kD (Figure 4B). Nevertheless, amino terminal end sequencing using Edman degradation showed identical cleavage sites within cRGMa, mRGMa, mRGMb and mRGMc (Figure 4A). The difference in the detected molecular weight is most likely due to glycosylation (Figure 4A, green boxes) or other posttranslational modifications. In summary, the three murine members of the RGM family are proteolytically processed in a manner analogous to cRGMa, but whereas mRGMa and mRGMc are transported to the plasma membrane, mRGMb appears to be predominantly accumulated in intracellular compartments.

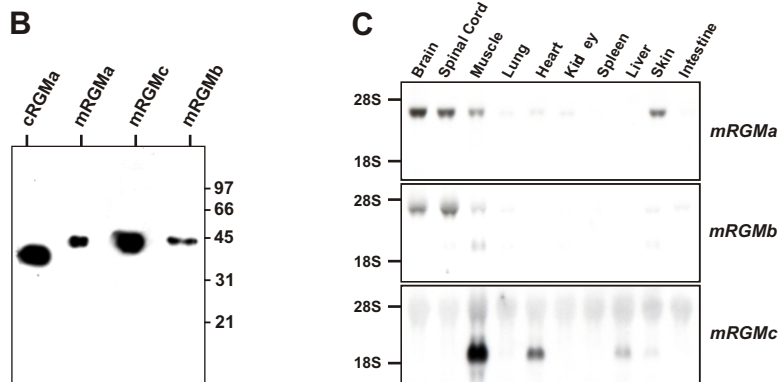
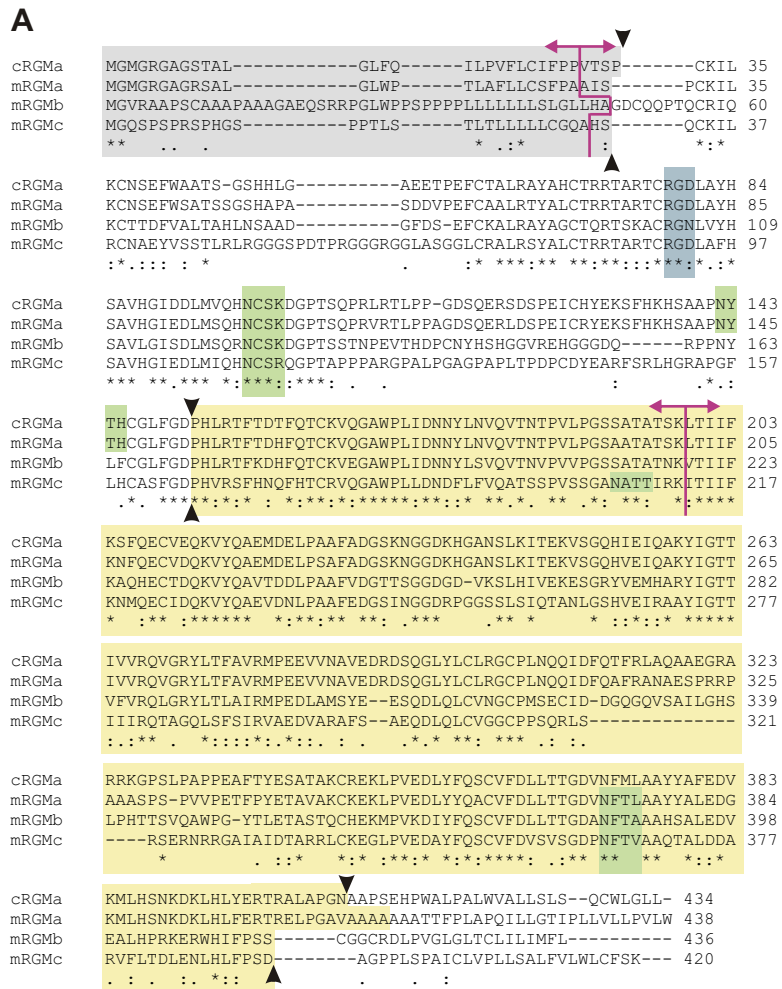


**Figure 4. Characterization of the Murine RGM Protein Family.**  
 (A) Protein sequence alignment of cRGMa, mRGMa, mRGMb and mRGMc. Stars indicate identical amino acids, pink lines: intron-exon junctions, the grey box: predicted signal peptides, the blue box: potential integrin binding sites (RGD), green boxes: predicted N-glycosylation sites, the yellow box: mature carboxy terminal RGM fragments after full proteolytic cleavage and carboxy terminal GPI anchor addition (proteolytic cleavage sites indicated by arrowheads).  
 (B) Western blot analysis of supernatant collected from COS-7 cells transfected with carboxy terminally truncated Histidine-Myc labelled cRGMa, mRGMa, mRGMc and mRGMb detected with an anti-Myc antibody. MW standards are indicated to the right.  
 (C) Northern blot analysis on total RNA from a variety of postnatal day 3 (P3) mouse tissues as indicated, using *mRGMa*, *mRGMb* and *mRGMc* as probes.

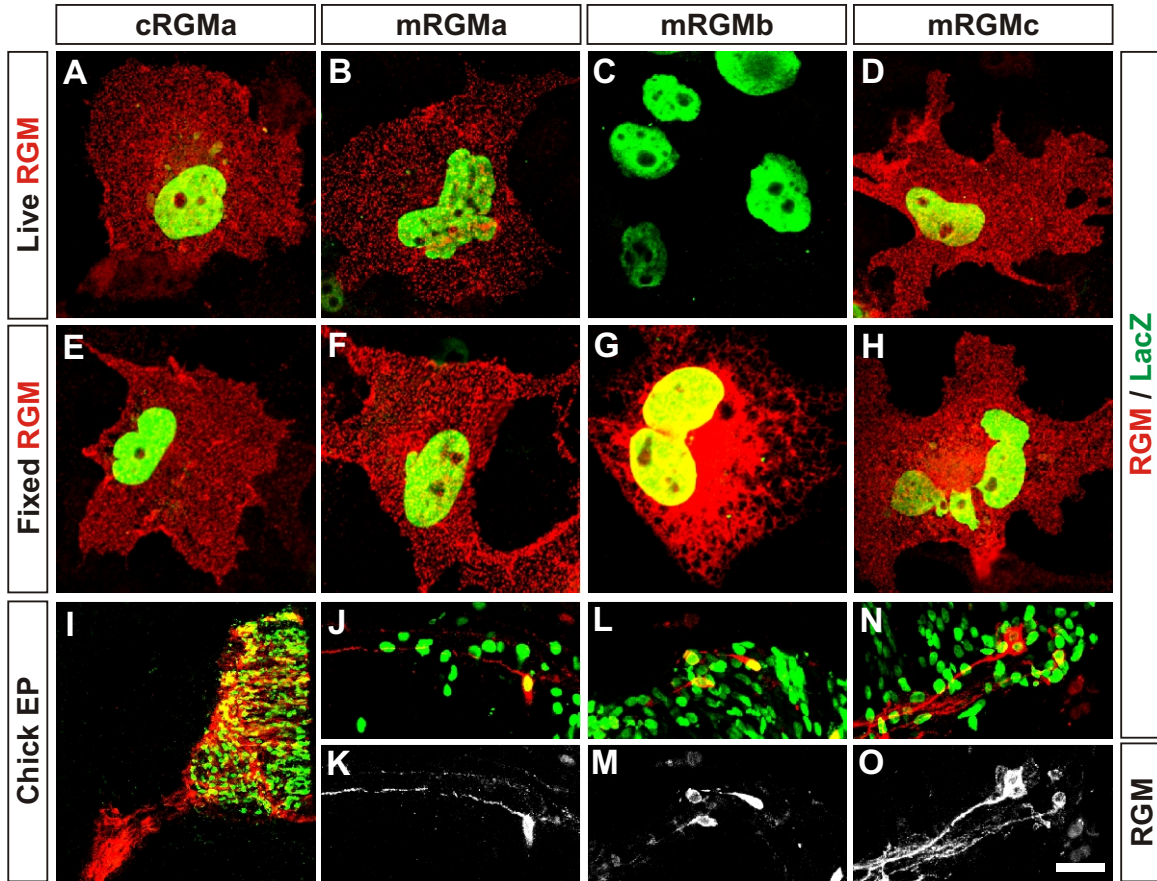


**Figure 5. Differential Cell Surface Targeting of mRGMs.**

(A-H) Expression of full length cDNAs coding for *cRGMa* (A, E), *mRGMa* (B, F), *mRGMb* (C, G) and *mRGMc* (D, H) and  $\beta$ -galactosidase on the same plasmid using an IRES in COS-7 cells. Transfected COS-7 cells are identified by staining for  $\beta$ -galactosidase after fixation and permeabilization of cells (green). RGMs (red) are detected either before fixation and permeabilization of cells (A-D) to detect cell surface accumulated RGM or after fixation and permeabilization of cells (E-H) to detect all RGM in transfected cells.

(I-O) Chick spinal cords electroporated with cDNAs coding for *cRGMa* (I), *mRGMa* (J, K), *mRGMb* (L, M) and *mRGMc* (N, O) and  $\beta$ -galactosidase on the same plasmid using an IRES. Sections were stained for either RGM (red) and  $\beta$ -galactosidase (green; I, J, L, N) or RGM (white; K, M, O). Note extensive labeling of axonal processes in (I, J, K, N, O) and predominant cell body and proximal axonal labeling in (L, M).

Scale bar: (A-H)=15 $\mu$ m, (I)=150 $\mu$ m, (J-O)=60 $\mu$ m.

### Differential Expression of *mRGM* Family Members During Development

Using a Northern blot analysis we found that the most abundant expression of *mRGMa* and *mRGMb* was detected in the nervous system whereas *mRGMc* was expressed predominantly in striated muscle tissues, with the highest level of expression detected in skeletal muscles (Figure 4C). To determine the specific sites of expression of *mRGMa* and *mRGMb* during embryonic development, we performed *in situ* hybridization experiments. Both *mRGMa* and *mRGMb* are expressed specifically at the tips of the neural folds of mouse embryos from E8 to E9, coincident with the expression of *mEphrinA5* (Figure 6A-C; Holmberg et al., 2000). Later, both *mRGMa* and *mRGMb* are expressed at discrete sites in the developing CNS, but in non-overlapping and highly complementary patterns. *mRGMa* expression in the brain is found surrounding the ventricles, whereas *mRGMb* expression is often found laterally apposed to *mRGMa* in early postmitotic neurons (e.g. E12.5 spinal cord, Figure 6E-G; E14.5 thalamus, Figure 6H-K). In addition, a high level of *mRGMb* expression was also detected in developing dorsal root ganglia (DRG; Figure 6F, G) and at later developmental stages, *mRGMa* and *mRGMb* are also expressed in distinct nuclei of the brain (E17.5; data not shown). Consistent with the data from our Northern blot analysis, expression of *mRGMc* is confined to striated muscles where it is found in both the muscles of the extremities, (Figure 6L-O) and of the face (Figure 6J, K). No expression of *mRGMc* was detected in embryonic brain or spinal cord (Figure 6J, data not shown).

In summary, the most striking feature revealed by this *in situ* hybridization analysis was an essentially complete lack of overlap and a strong complementarity in the expression of *mRGMa* and *mRGMb* in the developing nervous system. Whereas *mRGMa* expression is consistently found in subventricular zones surrounding the ventricles, *mRGMb* expression is often found laterally apposed to *mRGMa* and *mRGMc* is expressed predominantly in skeletal muscles.

### Expression Analysis of Mouse *RGMs* in the Visual System

To address which of the mouse *RGM* family members might play a dominant role in the development of the retinocollicular system, we performed *in situ* hybridization experiments in the mouse superior colliculus at P0, a stage just before targeting of RGC axons to defined anterior-posterior positions occurs (Simon and O'Leary, 1992). We found that *mRGMa*, the closest homologue of *cRGMa*, was prominently expressed in the superior colliculus at this stage (Figure 7A, D). However, in contrast to chick (Monnier et al., 2002; Figure 7F), we



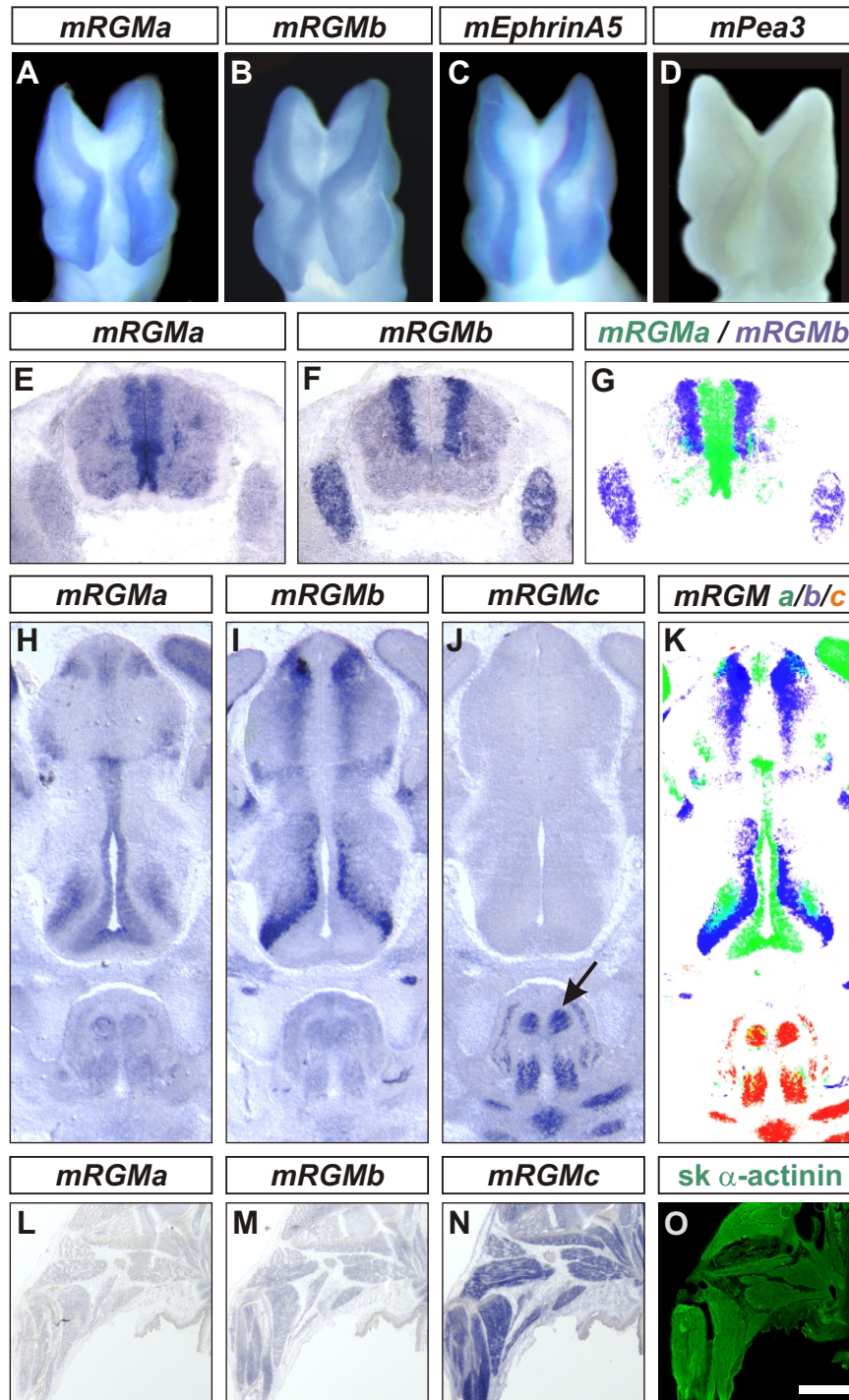


**Figure 6. Embryonic Expression of *mRGMs* in Complementary Patterns.**

(A-D) Whole-mount *in situ* hybridization of E8.5 mouse embryos using *mRGMa* (A), *mRGMb* (B), *mEphrinA5* (C) and *mPea3* (D) as probes. Note absence of *mPea3* expression from the tips of neural folds.

(E-G) Expression of *mRGMa* (E) and *mRGMb* (F) in E12.5 mouse spinal cord and dorsal root ganglia detected by *in situ* hybridization on transverse sections. (G) shows an artificial overlay (*mRGMa* in green, *mRGMb* in blue) to demonstrate complementarity of expression patterns.

(H-K) Expression of *mRGMa* (H), *mRGMb* (I) and *mRGMc* (J) in E14.5 mouse thalamus by *in situ* hybridization on coronal brain sections. Arrow in (J) points to signal of *mRGMc* in skeletal muscles. (K) shows an artificial overlay (*mRGMa* in green, *mRGMb* in blue and *mRGMc* in red) to demonstrate complementarity of expression patterns.

(L-O) Expression of *mRGMa* (L), *mRGMb* (M) and *mRGMc* (N) by *in situ* hybridization and skeletal  $\alpha$ -actinin (O) by immunocytochemistry on E17.5 mouse hindlimbs.

Scale bar: (A-D)=0.15mm, (E-G)=0.35mm, (H-K)=0.32mm, (L-O)=1.8mm.



failed to detect a gradient in the level of *mRGMa* expression along the anterior-posterior axis of the superior colliculus (Figure 7A, D). In addition, and as described previously, *mEphrinA5* was expressed in a clear anterior-posterior gradient in the mouse superior colliculus (Figure 7B, E; Frisen et al., 1998; Feldheim et al., 2000). At earlier developmental stages (E15.5), *mRGMa* is also expressed prominently in the superior colliculus, whereas only faint expression of *mRGMb* was detected (Figure 7G-I). In the retina, *mRGMb* but not *mRGMa* or *mRGMc* is expressed in RGCs (Figure 7J-L). Thus the *mRGM* family member expressed most prominently in the superior colliculus, at a time just before targeting of RGC axons to defined anterior-posterior positions occurs, is *mRGMa*.

### Generation of *mRGMa* Mutant Mice

To investigate the function of *mRGMa* in retinocollicular topographic mapping, we performed homologous recombination in embryonic stem cells to eliminate *mRGMa* gene function. We replaced the exon encoding the amino terminal signal peptide responsible for targeting mRGMa protein to the endoplasmic reticulum with a TK-Neomycin cassette (Figure 8A). The transfection of a cDNA construct coding for the remaining carboxy terminal exons of mRGMa into COS-7 cells showed that none of the transfected (eGFP<sup>+</sup>) COS-7 cells expressed the carboxy terminal fragment of mRGMa, thus demonstrating that all cell-surface targeted mRGMa protein is eliminated with this targeting strategy (Figure 8E-H).

Successful homologous recombination in embryonic stem cells using this targeting construct was detected at a very low frequency (~1:2000). Heterozygous *mRGMa*<sup>+/-</sup> mice were phenotypically normal and interbreeding resulted in the generation of homozygous viable *mRGMa*<sup>-/-</sup> mice (Figure 8I; data not shown). Both PCR from genomic DNA as well as RT-PCR from total RNA of homozygous *mRGMa*<sup>-/-</sup> mice showed successful elimination of the exon encoding the signal peptide of mRGMa (Figure 8D). While *mRGMa*<sup>-/-</sup> mice were detected at postnatal stages, the frequency of recovered viable mutants was non-Mendelian (Figure 8I).

### Mutation in *mRGMa* Results in an Exencephalic Phenotype *in Utero*

To assess whether a fraction of *mRGMa*<sup>-/-</sup> embryos die *in utero*, we examined the frequency and appearance of *mRGMa*<sup>-/-</sup> embryos at various prenatal stages. At E16.5, we recovered two

phenotypically different types of *mRGMa*<sup>-/-</sup> embryos: ~ 50% of *mRGMa*<sup>-/-</sup> embryos had an appearance indistinguishable from wild type embryos (Figure 8I; data not shown) whereas in the remaining ~ 50% of *mRGMa*<sup>-/-</sup> embryos, the brain was exposed to the exterior environment and cranial skull tissue was absent (Figure 8I, Figure 9D). Dissection of the brains from these affected *mRGMa*<sup>-/-</sup> embryos revealed that the ventral side of the brains as well as the brainstem and spinal cord were anatomically normal when compared to wild type brains and spinal cords (Figure 9E, F). In contrast, dorsal and lateral views of the brain from affected *mRGMa*<sup>-/-</sup> embryos revealed major defects in the morphogenesis of dorsal brain structures (Figure 9B, E; data not shown).

In order to define the nature of the observed defects more precisely, we performed a time course analysis at different embryonic stages. At E8, all *mRGMa*<sup>-/-</sup> embryos were indistinguishable from wild type embryos (data not shown). By E8.5 to E9, when the closure of neural folds in wild type embryos has been initiated at both cephalic and spinal cord levels (Theiler, 1989), ~ 50% of *mRGMa*<sup>-/-</sup> embryos did not show signs of efficient cephalic closure leading to a lack of closure at the cephalic level by E10.5 (Figure 9G-J; data not shown). In contrast, the closure of the neural folds at the level of the spinal cord was never affected in *mRGMa*<sup>-/-</sup> embryos (Figure 9I, J; data not shown). This defect has previously been described as exencephaly (Harris and Juriloff, 1997). Exencephaly is caused by a failure of the cephalic neural folds to fuse, resulting in an exvagination of the developing cephalic tissue at later developmental stages when many neurons are born and brain size increases (Harris and Juriloff, 1997). By E14.5, exencephalic *mRGMa*<sup>-/-</sup> embryos show a pronounced exposure of the developing brain structures and third ventricle to the external environment, as well as a lack of development of cranial skull tissue (Figure 9K-N). In addition, the exencephalic tissue of *mRGMa*<sup>-/-</sup> embryos was highly vascularized (Figure 9E, L), another feature frequently observed in exencephalic brains (Harris and Juriloff, 1997). Exencephalic *mRGMa*<sup>-/-</sup> embryos removed surgically immediately prior to birth (E19) displayed reflexive motion and breathing behavior but died shortly thereafter (data not shown). In contrast, exencephalic *mRGMa*<sup>-/-</sup> embryos delivered by natural birth were stillborn and anencephalic (lacking brain tissue entirely), presumably due to a lack of protection of the brain by the overlying skull during the process of birth (data not shown).

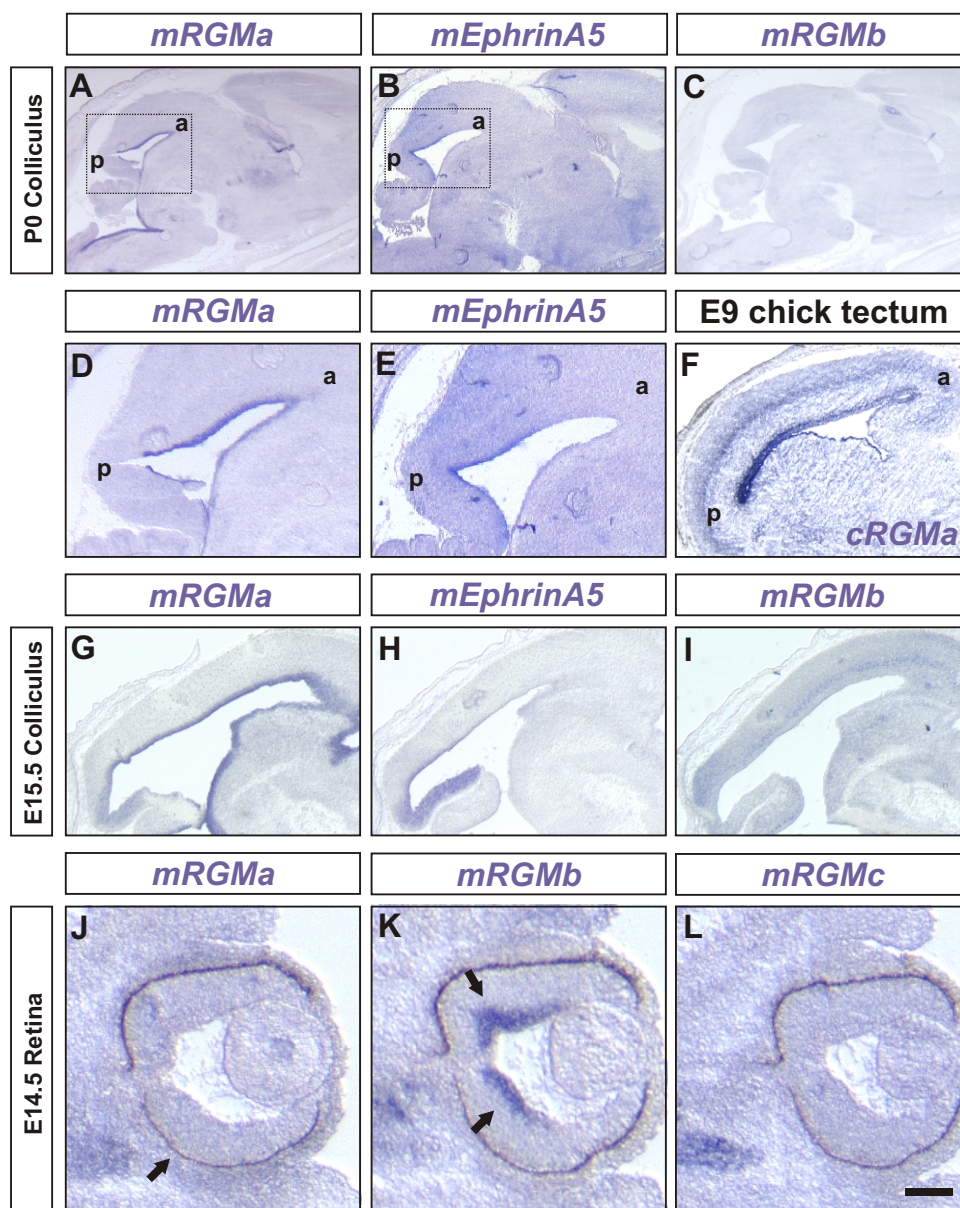


**Figure 7. Expression of *mRGMs* in the Developing Retinocollicular System.**

(A–E) Expression of *mRGMa* (A, D), *mEphrinA5* (B, E), and *mRGMb* (C) in the superior colliculus of P0 sagittal brain sections detected by *in situ* hybridization. Boxes in (A) and (B) indicate regions shown in higher magnification in (D) and (E). a, anterior; p, posterior.

(F) Expression of *cRGMa* in E9 chick tectum detected by *in situ* hybridization.

(G–I) Expression of *mRGMa* (G), *mEphrinA5* (H), and *mRGMb* (long exposure to detect faint expression; I) in the superior colliculus of E15.5 sagittal brain sections detected by *in situ* hybridization.

(J–L) Expression of *mRGMa* (J), *mRGMb* (K), and *mRGMc* (L) in E14.5 retina detected by *in situ* hybridization. Note the expression of *mRGMb* in RGCs (K, arrows). Pigment epithelium is marked by an arrow in (J).

Scale bar: (in L) (A–C)=1mm; (D, E)=0.4 mm; (F)=0.85 mm; (G–I)=0.25 mm; (J–L)=0.13 mm.

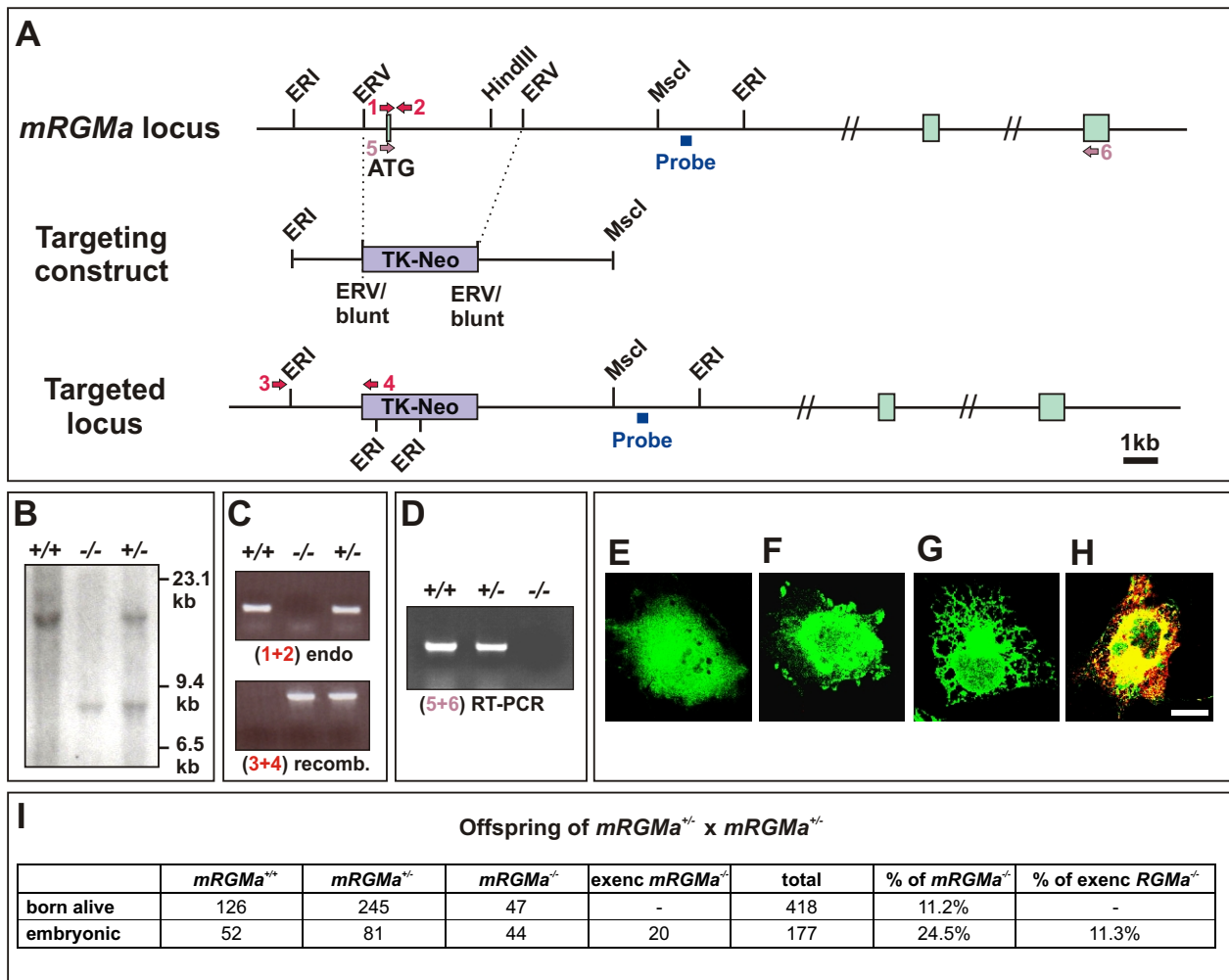


**Figure 8. Generation of  $mRGMa$  Mutant Mice.**

(A-C) Targeting strategy for homologous recombination in ES cells to eliminate  $mRGMa$  gene function. An EcoRV fragment including the exon containing the methionine of the signal peptide for targeting of  $mRGMa$  to the endoplasmic reticulum was replaced by a TK-Neomycin resistant cassette (purple). Coding exons for  $mRGMa$  are indicated in green, the probe used for genomic Southern analysis (B) in blue, oligonucleotides to determine absence of methionine containing exon in red (arrows 1 and 2; C), oligonucleotides to verify 5' homologous recombination in red (arrows 3 and 4; C) and oligonucleotides used for RT-PCR in pink (arrows 5 and 6; D).

(D) RT-PCR analysis to verify absence of exon containing signal peptide on  $mRGMa$  mRNA in  $mRGMa$  mutant mice (arrows 5 and 6 in A).

(E-H) Immunocytochemistry of COS-7 cells transfected with a cDNA construct containing  $mRGMa$  exons 3' of the targeted exon and eGFP on a bicistronic plasmid (E, F) or a cDNA construct containing an additional artificial in-frame amino terminal methionine and an eGFP containing a signal peptide for targeting to the endoplasmic reticulum (G, H). Cells were stained for eGFP (green) and mRGMa (red). In (E, G), incubation of cells with antibody to mRGMa was performed before fixation and permeabilization of cells to label cell-surface associated mRGMa. In (F, H), fixation and permeabilization of cells was performed before incubation with antibodies. Note that even the addition of an artificial amino terminal methionine in frame with the carboxy terminal  $mRGMa$  exons did not result in cell-surface exposed mRGMa after transfection (G, H). Scale bar = 15µm.

(I) Statistical analysis of the offspring recovered from matings of  $mRGMa^{+/+}$  breeder pairs. Exencephalic  $mRGMa^{+/-}$  embryos are indicated as exenc in the table.

These findings suggest that an early function of *mRGMa* at the site of neural tube closure where both *mRGMa* and *mRGMb* are expressed at this time may be responsible for the exencephalic phenotype observed in ~ 50% of *mRGMa*<sup>-/-</sup> embryos.

### **Exencephalic *mRGMa* Mutants Show no Defects in Early Brain Patterning**

Does the absence of *mRGMa* lead to defects in neuronal patterning, cell proliferation or apoptosis? We first performed BrdU pulse labeling experiments to assess proliferation and neuronal differentiation in *mRGMa*<sup>-/-</sup> embryos. We found that the amount of cellular proliferation was not obviously changed in either exencephalic or anatomically normal *mRGMa*<sup>-/-</sup> embryos when compared to wild type brains or spinal cords (Figure 10A-H; data not shown). However, due to the lack of brain closure in exencephalic *mRGMa*<sup>-/-</sup> embryos proliferating cells in dorsal brain structures now appeared on the outside of the brain whereas GAP43<sup>+</sup> differentiating neurons were facing the lumen (Figure 10B, D, F, H). BrdU<sup>+</sup> and GAP43<sup>+</sup> cells were not intermingled in exencephalic *mRGMa*<sup>-/-</sup> embryos, indicating that *mRGMa* is not required for initial segregation of proliferating cells and differentiating neurons in the brain. We also did not find defects in cellular proliferation and pan-neuronal differentiation in spinal cords of *mRGMa*<sup>-/-</sup> embryos (data not shown). Similarly, many genes expressed in defined cell types of the brain and spinal cord were expressed normally in *mRGMa*<sup>-/-</sup> embryos (data not shown). In addition, no aberrant increase or decrease in apoptotic cell death could be observed in cephalic neural folds of exencephalic *mRGMa*<sup>-/-</sup> embryos at E8.5 (Figure 10I, J). Together these findings suggest that the exencephalic phenotype observed in a subpopulation of *mRGMa*<sup>-/-</sup> embryos is most likely not caused by defects in neuronal patterning or cell proliferation, nor does the exencephalic phenotype caused by absence of *mRGMa* lead to such defects.

### **Viable *mRGMa* Mutants Show no Defects in Retinocollicular Projections**

To determine whether the surviving *mRGMa*<sup>-/-</sup> mice show defects in the anterior-posterior mapping of retinocollicular projections as suggested from *in vitro* studies in the developing chick embryo (Monnier et al., 2002), we first injected the lipophilic tracer DiI into the eyes of postnatal day 0 (P0) mice, attempting to label many RGC axons projecting from the retina to the brain. In viable *mRGMa*<sup>-/-</sup> as in wild type mice, the entire superior colliculus was filled with axons and, as expected at this developmental stage (Simon and O'Leary, 1992), a significant number of axons also projected into the inferior colliculus (n=5; Figure 11A, B).



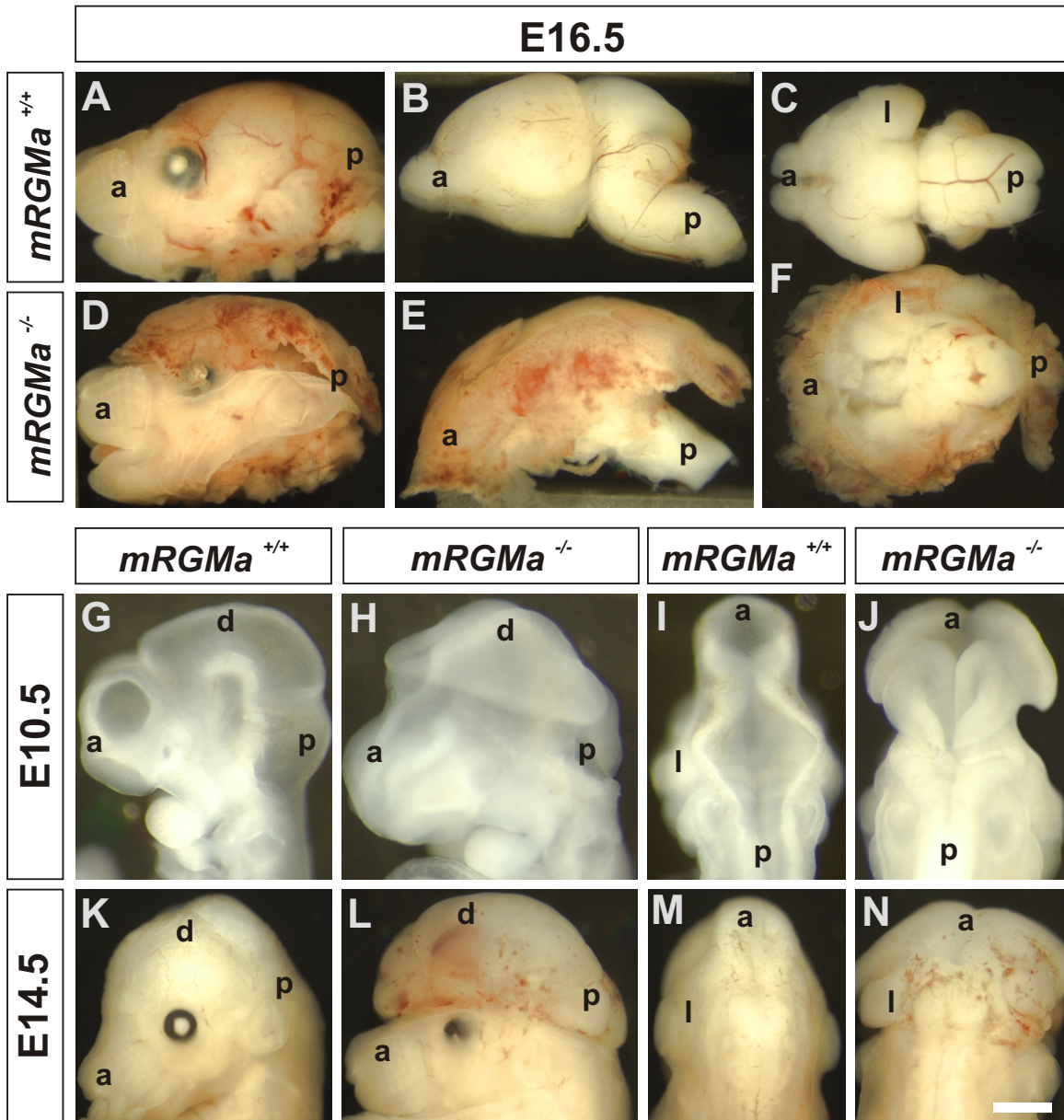


**Figure 9. *mRGMa* Mutant Mice Show an Exencephalic Phenotype.**

(A-F) Lateral (A, B, D, E) or ventral (C, F) view of E16.5 heads (A, D) or dissected brains (B, C, E, F) from *mRGMa*<sup>+/+</sup> (A-C) and exencephalic *mRGMa*<sup>-/-</sup> (D-F) embryos.

(G-J) Lateral (G, H) or dorsal (I, J) head view of E10.5 *mRGMa*<sup>+/+</sup> (G, I) and *mRGMa*<sup>-/-</sup> (H, J) embryos.

(K-N) Lateral (K, L) or dorsal (M, N) head view of E14.5 *mRGMa*<sup>+/+</sup> (K, M) and *mRGMa*<sup>-/-</sup> (L, N) embryos  
a, anterior; p, posterior; d, dorsal; l, lateral.

Scale bar: (A, D)=1.5mm, (B, E)=1mm, (C, F)=1.1mm, (G-J)=0.6mm, (K-N)=1.2mm

By postnatal day 8 (P8) RGC axons within the superior colliculus have segregated into defined anterior-posterior positions, reaching topographic positions found in the mature superior colliculus (Simon and O'Leary, 1992; Frisen et al., 1998). To determine whether in viable *mRGMa*<sup>-/-</sup> mice, retinocollicular axonal projections terminate in the appropriate anterior-posterior position within the superior colliculus we focally injected DiI into specific regions of the retina of postnatal day 9 to 12 (P9-P12) animals. In this analysis we first focused our attention on injections into the temporal RGC population known to normally project to the anterior and to be repelled by the posterior superior colliculus (Walter et al., 1987; Godement and Bonhoeffer, 1989; Roskies and O'Leary, 1994). Analysis of the projections of these DiI<sup>+</sup> temporal RGC axons showed a single focal termination zone, in the predicted anterior posterior position of both wild type and viable *mRGMa*<sup>-/-</sup> mice (n≥15, Figure 11C, D). In addition, focal injections of DiI into the nasal retina of both wild type and viable *mRGMa*<sup>-/-</sup> mice revealed that these axons also project and terminate normally in the posterior superior colliculus (n=10, Figure 11E, F). To assess whether the lack of phenotype observed in retinocollicular projections of viable *mRGMa*<sup>-/-</sup> mice could be due to compensatory upregulation of either other *mRGM* family members, or members of the *Ephrin* family of genes, we performed *in situ* hybridization experiments. We found that expression of *mRGMb*, *mRGMc*, *EphrinA2*, *EphrinA5* in the superior colliculus of *mRGMa*<sup>-/-</sup> mice was not altered when compared to wild-type littermates (Figure 11G-J). Taken together these findings suggest that the lack of *mRGMa* gene function does not seem to impair anterior-posterior mapping of RGC axons to the superior colliculus.

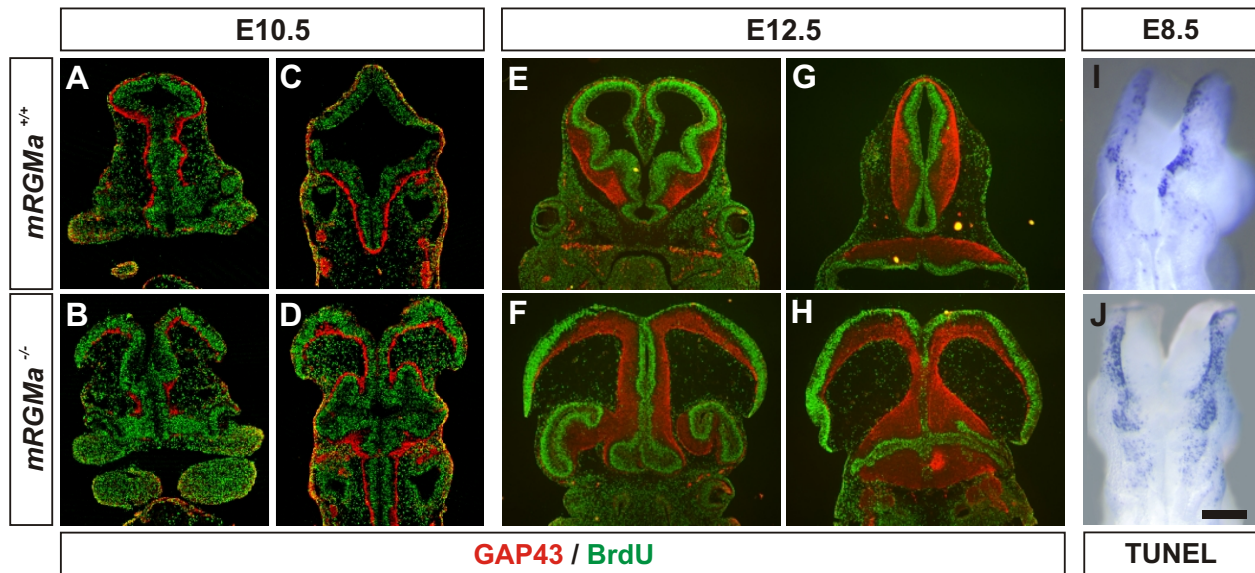


**Figure 10. Exencephalic *mRGMa* Mutant Embryos Do Not Show Defects in Proliferation in the Brain.**

(A-H) Immunocytochemical analysis (GAP-43: red; BrdU: green) of coronal brain sections from E10.5 (A-D) and E12.5 (E-H) BrdU pulse labelled *mRGMa*<sup>+/+</sup> (A, C, E, G) and exencephalic *mRGMa*<sup>-/-</sup> (B, D, F, H) embryos.

(I, J) Whole-mount TUNEL labeling of E8.5 *mRGMa*<sup>+/+</sup> (I) and exencephalic *mRGMa*<sup>-/-</sup> (J) embryos in dorsal view.

Scale bar: (A, B, E, F)=0.38mm, (C, D, G, H)=0.5mm, (I, J)=0.13mm



## Discussion

In this study we found that *cRGMa* is a member of a novel family of GPI-anchored proteins of which we identified and characterized three murine members – *mRGMa*, *mRGMb* and *mRGMc*. Two members of this gene family are expressed predominantly in the developing nervous system in non-overlapping and distinct expression patterns (*mRGMa* and *mRGMb*) whereas the third member is expressed most abundantly in skeletal muscles (*mRGMc*). Previous *in vitro* studies in the chick have suggested that *cRGMa* may play a role in the establishment of appropriate anterior-posterior RGC termination zones within the tectum. Our functional studies in the mouse now show that *mRGMa* mutant mice do not exhibit defects in the development of topographically appropriate projections in the anterior-posterior dimension of the superior colliculus. Instead, a significant proportion of *mRGMa* mutant mice show an exencephalic defect due to failure of the cephalic neural tube to close during development. We will discuss these findings in the context of (1) the distinct sites of expression and subcellular localization of different RGM family members and (2) the *in vivo* function of *mRGMa* in the developing mouse nervous system.

### Identification of a Novel Family of GPI-Anchored Proteins Homologous to *cRGMa*

The identification of three genes homologous to *cRGMa* in the mouse genome has allowed us to study the precise developmental time course of expression, subcellular targeting and proteolytic processing of these proteins. Two members of this gene family – *mRGMa* and *mRGMb* – show abundant expression in the developing mouse nervous system. It is interesting to note that the two genes expressed in the nervous system appear to have evolutionarily arisen by gene duplication. Preliminary evidence suggests that there is a homologue of *mRGMb* in the chick genome with an expression pattern confined to the nervous system (R. Salie, V. Niederkofler, and S. Arber, unpublished observations), indicating that this gene duplication must have occurred evolutionarily earlier than in the chick. A striking feature we observed in the expression of *mRGMa* and *mRGMb* within the nervous system is that their sites of expression are highly distinct and non-overlapping. While *mRGMa* is consistently expressed in ventricular zones where proliferating cells are found, the expression of *mRGMb* is almost exclusive to domains where early postmitotic neurons are found and not in ventricular zones. In addition to these sites of expression, distinct groups of postmitotic neurons also express *mRGMa* or *mRGMb* in non-overlapping patterns. In contrast,

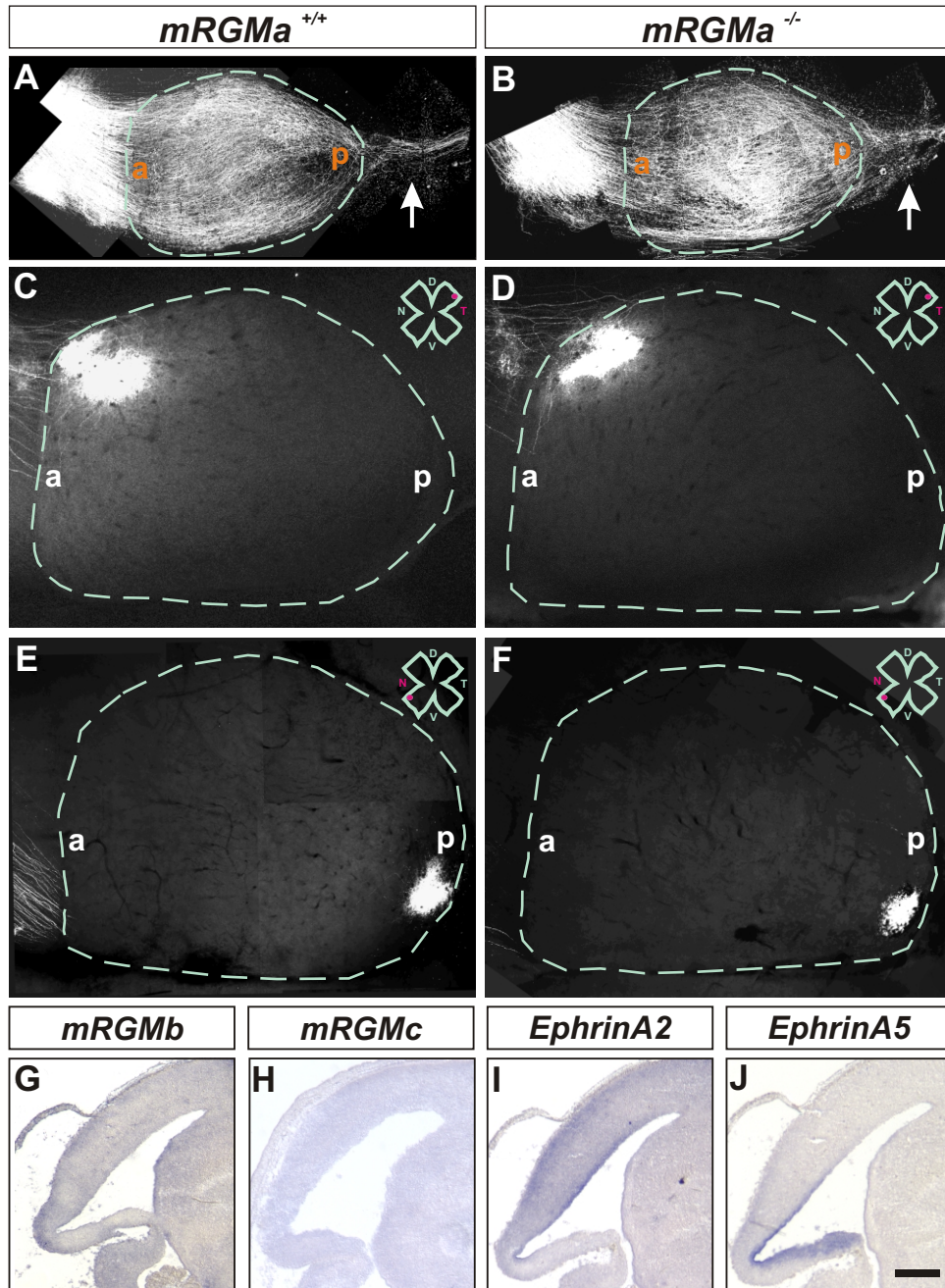


**Figure 11. Lack of Retinocollicular Projection Phenotype in *mRGMa* Mutant Mice.**

(A, B) Dorsal views of superior and inferior colliculi from *mRGMa*<sup>+/+</sup> (A) and *mRGMa*<sup>-/-</sup> (B) mice after anterograde DiI labeling from the retina at P0 to label many RGC axons. Green dashed line outlines the superior colliculus (a=anterior, p=posterior), arrows point to RGC axons projecting to the inferior colliculus.

(C-F) Anterograde DiI labeling from the temporal (C, D) or nasal (E, F) retina to the superior colliculus (outlined by green dashed lines) after focal DiI injection into the retina of *mRGMa*<sup>+/+</sup> (C, E) and *mRGMa*<sup>-/-</sup> (D, F) mice at P10 (injection point in the retina indicated by red dot in the top right corner). (T=temporal, N=nasal, D=dorsal, V=ventral).

(G-J) Expression of *mRGMb* (G), *mRGMc* (H), *EphrinA2* (I) and *EphrinA5* (J) in superior colliculi of E16.5 sagittal brain sections from *mRGMa*<sup>-/-</sup> mice detected by *in situ* hybridization.

Scale bar: (A, B)=0.5mm, (C-F)=0.33mm, (G-J)=0.3mm

the third member of the family (*mRGMc*) is expressed in skeletal muscles and is evolutionarily more distantly related to *mRGMa* and *mRGMb*. Given the function of *mRGMa* in controlling the process of alignment of dorsal neural folds ultimately leading to neural tube closure, it is tempting to speculate that *mRGMc* might be involved in the process of myogenesis where mononucleated myoblasts fuse to form multinucleated myotubes. Consistent with this idea, *mRGMc* expression is upregulated during the process of myogenic differentiation *in vitro* (V. Niederkofler, R. Salie, and S. Arber, unpublished observations).

All three mouse homologues of *cRGMa* have predicted GPI anchor consensus sequences and undergo proteolytic cleavage at several sites within the protein raising the question of the subcellular localization of the mature mRGM proteins. Our analysis revealed that there is an internal cleavage site within all three mRGM proteins that is highly conserved in sequence between the three mRGM members and *cRGMa*. This internal protein cleavage produces two fragments, one amino-terminal fragment containing an integrin-binding RGD site and a carboxy terminal fragment with a GPI anchor consensus site. To our knowledge, the sequence of this cleavage site has not been previously described in other proteins and it will be interesting to determine which protease(s) recognize(s) this cleavage site and whether similar proteolytic cleavage sites are present in other proteins. In addition, such a protease may be expressed differentially in different cell types leading to variable efficiencies in proteolytic processing depending on the amount and activity of protease present in a given cell type.

In contrast to the proteolytic cleavage reactions in the amino-terminal region detected in all mRGM proteins, subcellular targeting of different mRGM members to the cell surface does not occur with equal efficiency for all RGM family members. While *mRGMc* is as efficiently targeted to the cell surface as *cRGMa*, less *mRGMa* and almost no *mRGMb* appears to reach the cell surface. This differential subcellular localization of the RGM family of proteins could be due to differential efficiency in the addition of GPI anchors and may have important implications for the function of individual RGM family members in the extracellular space. Differential subcellular targeting has recently been suggested as a mechanism by which several proteins with proposed extracellular functions regulate their activities. For example, only small amounts of NogoA protein reach the cell surface of

oligodendrocytes and the most prominent localization of NogoA is found in the endoplasmic reticulum (Chen et al., 2000; GrandPre et al., 2000). It has been suggested that NogoA protein may only be released from oligodendrocytes after lesion of the nervous system, thus preventing NogoA from acting under normal circumstances (Brittis and Flanagan, 2001). Moreover, Comm in *Drosophila* has recently been described to sort Robo, the receptor for the repulsive guidance molecule Slit, to the endosomal compartment in order to prevent commissural neurons from responding to Slit before midline crossing (Keleman et al., 2002). Similarly, differential *in vivo* processing and subcellular localization of different members of the RGM family of proteins could regulate the degree of activity in a particular cell.

### ***In Vivo* Function of *mRGMa* in the Developing Nervous System**

Two major candidate protein families have been implicated in anterior-posterior topographic mapping in the retinocollicular system (McLaughlin et al., 2003a). Ephrins and cRGMa have both been shown to exhibit comparable *in vitro* activities guiding RGC axons (Drescher et al., 1995; Cheng et al., 1995; Monschau et al., 1997). However, whereas genetic evidence supports a role for *Ephrins* in anterior-posterior topographic mapping in the superior colliculus (Feldheim et al., 2000; McLaughlin et al., 2003a), our data on *mRGMa*<sup>-/-</sup> mice suggest that *mRGMa* is not essential for this process. Our findings reveal however, that while there does not appear to be a similarity in the phenotype of *EphrinA5*<sup>-/-</sup> and *mRGMa*<sup>-/-</sup> mice in the retinocollicular system, both *mRGMa* and *EphrinA5* are involved in the process of cephalic neural tube closure albeit at a different level of genetic penetrance (Holmberg et al., 2000). Consistent with this phenotype, both *EphrinA5* (Holmberg et al., 2000) and *mRGMa* are expressed in the dorsal edges of the cranial neural folds.

Why do *mRGMa*<sup>-/-</sup> mice not show a defect in the establishment of anterior-posterior retinocollicular topographic mapping? It is unlikely that a compensatory upregulation of gene expression of other *mRGM* or *Ephrin* family member(s) can account for the lack of phenotype in retinocollicular mapping of *mRGMa*<sup>-/-</sup> mice since the expression of both *mRGMb* and *mRGMc* as well as *EphrinA2* and *EphrinA5* is unchanged in *mRGMa*<sup>-/-</sup> mice. Moreover, *mRGMa* appears to be the member of the *mRGM* gene family expressed at the highest level in the mouse superior colliculus at the time RGC axons segregate into their final anterior-posterior position within the target region suggesting that *mRGMa* should play the dominant role amongst *mRGM* family members in controlling RGC targeting. In contrast, developing RGCs express high levels of *mRGMb* and no or only low levels of *mRGMa*. Since previous

evidence suggests that the expression of Ephrins does not only contribute to the development of retinocollicular projections through expression in the target region itself but also through expression in RGCs (Hornberger et al., 1999), it will be interesting to determine in future experiments how *mRGMb* gene function contributes to the development of retinocollicular projections. Another possible explanation for a lack of phenotype in *mRGMa*<sup>-/-</sup> mice could come from the observation that while the expression of *EphrinA2* and *EphrinA5* in the mouse superior colliculus is graded (Feldheim et al., 2000), *mRGMa* exhibits no such anterior-posterior gradient. Thus the function of *mRGMa* may have changed during evolution, maybe because the chick tectum is significantly bigger than the mouse superior colliculus (McLaughlin et al., 2003a) potentially requiring additional cues to acquire precision in the development of projections from the retina to the tectum. Alternatively, *mRGMa* may only function in combination with *EphrinA2* and *EphrinA5* present in the superior colliculus of the mouse and to reveal a retinocollicular phenotype may require the generation of *mRGMa*<sup>-/-</sup>/*EphrinA2*<sup>-/-</sup>/*EphrinA5*<sup>-/-</sup> mice. It has indeed been suggested that in addition to *EphrinA2* and *EphrinA5* other guidance cues ought to be present in the mouse to explain the anterior-posterior topographic mapping in the superior colliculus since disruption of both *EphrinA2* and *EphrinA5* does not lead to a complete loss in anterior-posterior retinocollicular topography (Feldheim et al., 2000). Future work will determine whether *mRGMa* does indeed act as a cofactor in combination with other guidance molecules to restrict RGC axons to their correct anterior-posterior position in the superior colliculus.

## Materials and Methods

### Characterization of *mRGM* Gene Family and Histology

The three members of the *mRGM* gene family were isolated by database searches (Accession numbers: *mRGMa*: AI118914; *mRGMb*: BG519283; *mRGMc*: AA656608). Signal peptide and GPI anchor cleavage sites were determined using the following programs (<http://www.cbs.dtu.dk/services/SignalP-2.0/#submission>; Nielsen et al., 1999 and [http://mendel.imp.univie.ac.at/gpi/gpi\\_server.html](http://mendel.imp.univie.ac.at/gpi/gpi_server.html); Eisenhaber et al., 1999). Percentages of identities of *mRGM* family members to *cRGMa* were determined using NCBI BlastP version 2.2.6. To determine amino-terminal proteolytic cleavage sites, *cRGMa* (Monnier et al., 2002) and *mRGMs* were cloned into pSecTag2A (Invitrogen, San Diego, CA) in frame with the His-tag (*cRGMa*: bp 93-1217; *mRGMa*: bp 91-1232; *mRGMb*: bp 144-1243; *mRGMc*: bp 94-1178). COS-7 cell conditioned medium was collected 2-5 days after transfection and proteins were purified over a Ni-NTA-column (Qiagen, Basel, Switzerland). Amino-terminal sequencing was performed by Edman degradation (ARS, University of Bern, Switzerland).

For *in situ* hybridization analysis, sections were hybridized with digoxigenin-labelled probes (Schäeren-Wiemers et al., 1993) directed against mouse *mRGMa*, *mRGMb*, *mRGMc*, *cRGMa* (Monnier et al., 2002), *mEphrinA5* (BG921710), *mEphrinA2* (AA170896) and *mPea3* (Livet et al., 2002). Antibodies used in this study were: rabbit anti-GAP-43 (Arber et al., 1999), rabbit anti-*mRGMa* (peptide antibody to aa 316 to 331), rabbit anti-*mRGMb* (peptide antibody to aa 256 to 270), rabbit anti-*mRGMc* (peptide antibody to aa 314 to 328), rabbit anti-*cRGMa* (peptide antibody to aa 319 to 332), mouse anti-BrdU (Beckton Dickinson, San Jose, CA), mouse anti-Myc (9E10; ATTC), mouse anti-skeletal  $\alpha$ -actinin (Sigma, Buchs, Switzerland), goat anti- $\beta$ -Galactosidase (Arnel, New York, NY) and sheep anti-eGFP (Biogenesis, Kingston, NH). Chick electroporations were performed as previously described (Briscoe et al., 2000). Cryostat sections were processed for immunohistochemistry as previously described (Arber et al., 1999) using fluorophore-conjugated secondary antibodies (Molecular Probes, Eugene, OR) (1:1000).

### Generation and Analysis of *mRGMa* Mutant Mice

A mouse genomic library was screened using a *mRGMa* specific probe (Incyte Genomics, Palo Alto, CA). An EcoRV genomic fragment containing the exon coding for the amino-

terminal methionine and signal peptide was replaced by a TK-Neomycin cassette using homologous recombination in ES cells (targeting frequency ~1:2000). ES cell recombinants were screened by genomic Southern blot (EcoRI digest; 3' probe (~ 200bp): oligonucleotides (A) 5'TTGACCTGCCGCTGAGCACA 3' and (B) 5'CTGGGCACTGAGTGGTAAGG 3') and verified by PCR (see Figure 8 for position of oligonucleotides: [3]: 5'CATCCAACAAGGCTCCACTGGAAGG 3', [4]: 5'TGCGAAGTGGACCTGGGACCGCG 3'). The identification of *mRGMa*<sup>-/-</sup> mice was performed by genomic Southern blot and PCR (see Figure 8 for position of oligonucleotides: [1]: 5'CAGGTAGGCACAACCTCCTTGGTGG 3' and [2]: 5'TTAGCACGTCTGAGCCTGTGTCCG 3'). RT-PCR was performed following the instructions of the manufacturer (Promega, Madison, WI) using P0 mouse brain total RNA and the following oligonucleotides: [5]: 5'CTTCCTTCTCTGCAGCTTCCCCGC 3' and [6]: 5'CTGGCGCGCCAGCTTGGTAGACTTTCTGGTCC 3'. Lack of antibodies recognizing endogenous mRGMa prohibited us from confirming the absence of mRGMa protein in *mRGMa*<sup>-/-</sup> mice.

BrdU experiments were performed by intraperitoneal injection of BrdU (Sigma, Buchs, Switzerland; 50µg/g body weight) 2 hr before sacrifice and detection of BrdU was performed as previously described (Arber et al., 1999). TUNEL labeling to detect apoptotic cells in whole-mount embryos was performed as described by the manufacturer (Roche, Rotkreuz, Switzerland). Anterograde labeling of retinocollicular projections was done essentially as described (Simon and O'Leary, 1992). Briefly, 5% DiI (Molecular Probes, Eugene, OR) in dimethyl formamide solution was injected into the retina at P0 or the nasal or temporal extreme of the retina at P9-P12 with a fine glass micropipette using a Picospritzer III (Parker, Fairfield, NJ). One day later for fills at P0 or two days later for focal injections, colliculi were analyzed blind to genotype with confocal microscopy (Olympus, Hamburg, Germany). Retinas were examined to verify a single injection point for focal injections.

## 1.4 A Potential Role for *mRGMb* in Axon Guidance and Establishment of Cutaneous Afferent Projections

### 1.4.1 *mRGMb* Mutant Mice Do Not Exhibit Defects in Retinocollicular Topography

#### Introduction

Retinal ganglion cells (RGCs) from the eye extend axons to their target, the chick tectum or the rodent superior colliculus, in a stereotypical manner. Axons from the nasal retina consistently project to the posterior tectum/colliculus whereas axons from the temporal retina project to the anterior tectum/colliculus. EphrinA2 and EphrinA5 have been implicated in the establishment of this topographic map as guidance factors, both *in vitro* and *in vivo*. In addition, chick RGM (cRGM) has been reported to possess an *in vitro* activity similar to the Ephrins, causing growth cone collapse and preferential guidance of temporal RGC axons (Monnier et al., 2002). Surprisingly, the *in vivo* analysis of its closest ortholog in mouse, *mRGMa*, revealed that *mRGMa* mutant mice do not exhibit defects in retinocollicular topography along the anterior-posterior axis (Chapter 1.3; Niederkofler et al., 2004).

In mouse, the RGM family of GPI anchored molecules comprises three members, two of which are expressed in the developing nervous system, *mRGMa* and *mRGMb*, the third, *mRGMc* is most abundant in skeletal muscle (Chapter 1.3; Niederkofler et al., 2004). *mRGMa* and *mRGMb* are both expressed in the developing visual system, although in different patterns. *mRGMb* is expressed in the superior colliculus at much lower level than *mRGMa*. Moreover, *mRGMb* is the only member of the RGM family expressed in the developing RGC



layer. The lack of retinocollicular guidance defects in *mRGMa* mutant mice along with the expression of *mRGMb* in the developing mouse visual system raises the question: Does *mRGMb* contribute to the development of the retinocollicular map? The discovery that Ephrins not only contribute to the retinocollicular trajectory by acting in the target region itself, but also by functioning in RGCs, makes this question especially interesting (Hornberger et al., 1999).

## Results and Discussion

To investigate the function of mRGMb in retinocollicular topographic mapping, we performed homologous recombination in embryonic stem cells to eliminate *mRGMb* gene function. We disrupted the second coding exon with a eGFP-IRES-NLZ-pA-TK-neomycin cassette (Figure 12A). Successful homologous recombination in embryonic stem cells using this targeting construct was confirmed by southern blotting (Figure 12B). Heterozygous *mRGMb*<sup>+/-</sup> mice were phenotypically normal and interbreeding resulted in the generation of homozygous *mRGMb*<sup>-/-</sup> offspring at a Mendelian frequency. Mice homozygous for the disrupted *mRGMb* allele showed a complete absence of *mRGMb* mRNA in total brain extracts of perinatal mice (P0) providing evidence for a complete null mutation (Figure 12C).

Topographic projections of RGCs along the anterior-posterior axis were analyzed by focal DiI injections into the temporal and nasal extreme of the retina of postnatal day 9 to 12 (P9-P12) animals. Temporal RGCs axons are known to project to the anterior part of the superior colliculus, whereas nasal RGC axons project to the posterior part. Focal termination zones were detected in the predicted location in the superior colliculus in both *wild-type* and *mRGMb* mutant mice. (Figure 13) (temporal: n<sub>≥</sub>3; nasal: n<sub>≥</sub>6). No shift in location or ectopic termination zones could be detected.

Here we show that *mRGMb* mutant mice do not have a defect in the retinal projection mapping of RGCs to the superior colliculus along the anterior-posterior axis. The absence of such a defect in both *mRGMa* and *mRGMb* mutant mice suggests a potential functional redundancy between those two molecules. The analysis of *mRGMa/mRGMb* double mutants will elucidate this issue. It is also possible that mRGMa and mRGMb only reveals their function in combination with EphrinA2 or EphrinA5 or both. Alternatively, the function of mRGMa and mRGMb became extinct in setting up a topographic map during evolution, since the chick tectum is significantly bigger than the mouse superior colliculus, and thus probably requires additional guidance cues for proper precise mapping.

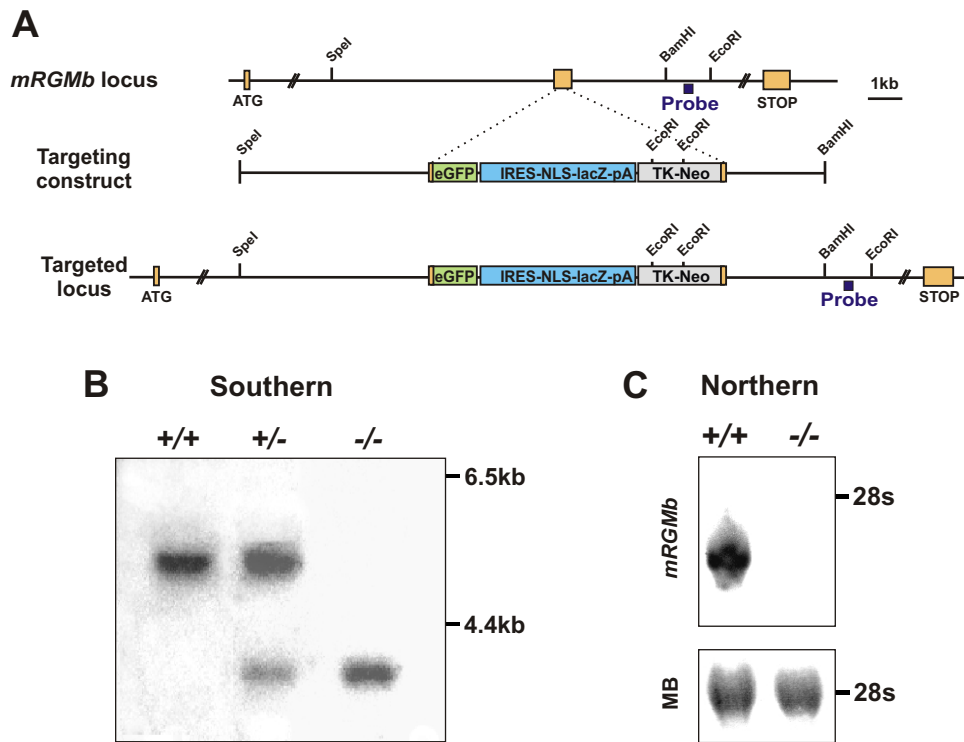


**Figure 12. Generation of *mRGMb* Mutant Mice.**

(A, B) Targeting strategy for homologous recombination in ES cells to eliminate *mRGMb* gene function. The second coding exon was disrupted with an eGFP-IRES-NLS-lacZ-pA-TK-Neo cassette. Exons are indicated in yellow. Probe used for genomic Southern analysis (B) is depicted in dark blue.

(C) Northern blot analysis demonstrates the absence of *mRGMb* mRNA in *mRGMb* mutant animals. Methylene Blue (MB) staining served as a loading control.

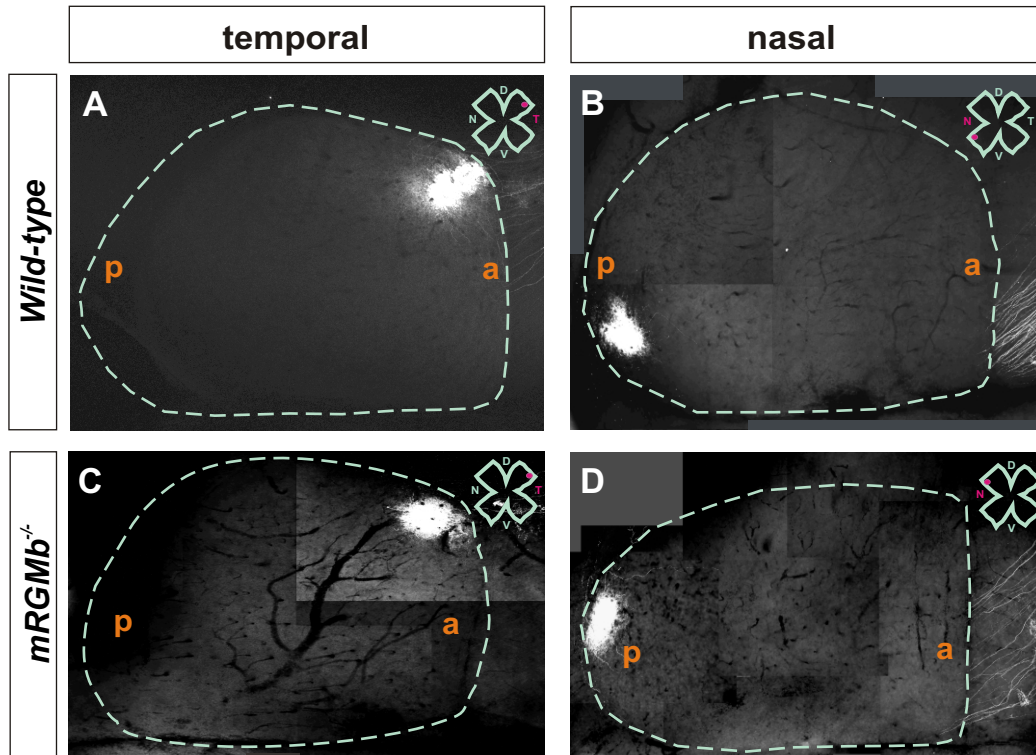


**Figure 13. Lack of Retinocollicular Projection Defects in *mRGMb* Mutant Mice.**

(A-D) Dorsal view of anterograde DiI tracing from temporal (A, C) or nasal (B, D) RGCs to the superior colliculus (outlined by green dashed lines) after focal DiI injection into the retina of *wild-type* (A, B) or *mRGMb*<sup>-/-</sup> (C, D) mice at P10 (injection points indicated by pink dot in top right corner). (T=temporal, N=nasal, D=dorsal, V=ventral, a=anterior, p=posterior)

## **1.4.2 *mRGMB* Mutant Mice Do Not Exhibit Defects in Establishment of Cutaneous Afferent Projections**

### **Introduction**

Primary somatosensory neurons in mammalian dorsal root ganglia (DRG) are a heterogeneous population subserving diverse sensory modalities, including pain, touch and body position. Different types of sensory inputs are associated with specifically localized terminations of the projections within the spinal cord. While proprioceptive (muscle) sensory neurons project to the ventral spinal cord, cutaneous (skin) sensory neurons terminate in superficial laminae I and II of the dorsal horn. It has been suggested that this specificity is determined by differential expression of transcription factors in one or the other class of sensory neurons and their corresponding targets. For example, the ETS transcription factor, *Er81*, has been shown to be expressed specifically in proprioceptive afferents and the motor neurons to which they connect (Lin et al., 1998; Arber et al., 2000). The same principle holds true for the paired homeodomain transcription factor *DRG11*, which is expressed in cutaneous afferents and in the dorsal horn of the spinal cord (Chen et al., 2001). This model is supported by the phenotypes of the *Er81* and the *DRG11* mutant mice, both of which exhibit connectivity defects in the spinal cord (Arber et al., 2000; Chen et al., 2001).

Recently, a genetic screen for the promoter regions of genes regulated by DRG11 identified *mRGMB/DRAGON* as being transcriptionally regulated by DRG11 (Samad et al., 2004). Furthermore, the same study shows that *mRGMB* is coexpressed with *DRG11* in embryonic DRG and spinal cord and that its expression is reduced in *DRG11* null mutants. Taken together, this suggests a potential role for *mRGMB* in establishment of cutaneous afferent projections.

## Results and Discussion

To address the functional implications of *mRGMb* regulation by DRG11, we assessed *mRGMb* mutant mice for defects observed in the *DRG11* mutant animals. Mouse embryos deficient in *DRG11* display abnormalities in the spatio-temporal patterning of cutaneous sensory afferent projections into the dorsal horn, as well as dorsal horn morphogenesis (Chen et al., 2001).

### Projection Pattern of Primary Sensory Afferents in the Dorsal Horn

To check whether there were any gross central projection defects in *mRGMb* mutant mice we immunostained spinal cords of embryonic day 15.5 (E15.5) animals, three days after the initial ingrowth of sensory fibers into the gray matter, for parvalbumin, which marks proprioceptive afferents, and TrkA, which marks for cutaneous afferents (Figure 14C, D; data not shown). We could not detect an obvious sensory projection defect in *mRGMb* mutant mice compared to *wild-type* littermates, for either proprioceptive or cutaneous afferents. In contrast, *DRG11* mutant animals exhibit a delayed ingrowth of TrkA positive afferent fibers into the gray matter relative to *wild-type* littermates. In addition, these fibers are also biased toward the medial region and depleted from the lateral region in *DRG11* mutant animals.

To assess more subtle potential projection defects, we examined subsets of cutaneous afferents. First we analyzed nonpeptidergic nociceptive fibers (IB4+), known to project specifically to lamina III in the dorsal horn, by utilizing a transgenic mouse line expressing *eGFP* under the control of the *Thy1* promoter selectively in this sensory afferent subpopulation (Caroni, 1997; M. Sigrist and S. Arber, unpublished observation). The projection pattern was indistinguishable between *mRGMb* mutant and *wild-type* mice. (Figure 14E, F). In contrast, *DRG11* mutant embryos have reduced nonpeptidergic nociceptive fibers with incorrectly localized terminations within the gray matter.

In addition, we stained for Calbindin which marks another subset of cutaneous afferents. These projections start to invade the dorsal horn at E12.5-E13.5 in *wild-type* embryos. Interestingly, no Calbindin positive fibers have been detected in the dorsal horn of

*DRG11*<sup>-/-</sup> embryos at E13.5 (Chen et al., 2001). This defect in *DRG11* mutant animals appears to be transient, since later in development the majority of Calbindin positive fibers project into the dorsal horn, although their trajectory is slightly disturbed. In contrast, no delay in invasion was observed in Calbindin positive cutaneous projections in *mRGMb* mutant mice when compared to *wild-type* littermates (Figure 14A, B).

### Dorsal Horn Morphogenesis

*DRG11* mutant embryos have been reported to exhibit increased cell death in the dorsal horn at E17.5, which results in an altered dorsal horn morphology. Furthermore, these mice lack PKC- $\gamma$  (protein kinase C- $\gamma$ ) positive neurons, which have been previously implicated in pain sensation. TUNEL labeling at E17.5 did not show an increase in apoptotic cells in *mRGMb* mutant embryos compared to *wild-type* littermates (Figure 15A, B). Moreover, no decrease in PKC- $\gamma$  positive neurons in the dorsal horn was detectable in early postnatal *mRGMb* mutant mice (Figure 15C, D).

Together, our data do not provide any evidence for a function of *mRGMb* in the establishment of cutaneous afferent projections. Interestingly, although *mRGMb* is coexpressed with *DRG11* in embryonic DRG and spinal cord *mRGMb* is expressed earlier than *DRG11* in the neural tube and is, unlike *DRG11*, also present in the brain (Chen et al., 2001). This suggests that also other regulatory elements must play a role in controlling *mRGMb* expression. Furthermore, *DRG11* likely regulates several genes. It could thus affect neuronal differentiation via other molecules than *mRGMb*.

Interestingly, both *mRGMb* and *DRG11* mutant mice die within the first postnatal month. Backcrosses into the outbred CD-1 genetic background extended the life span of *DRG11* mutant animals significantly (Chen et al., 2001). Behavioral analysis revealed a reduced sensitivity to nociceptive and mechanical stimuli in *DRG11* deficient mice compared to *wild-type*. It still remains to be determined whether a change of genetic background would extend the life of *mRGMb* mutant mice, and whether they would exhibit similar behavioral defects to the *DRG11* mutant mice.

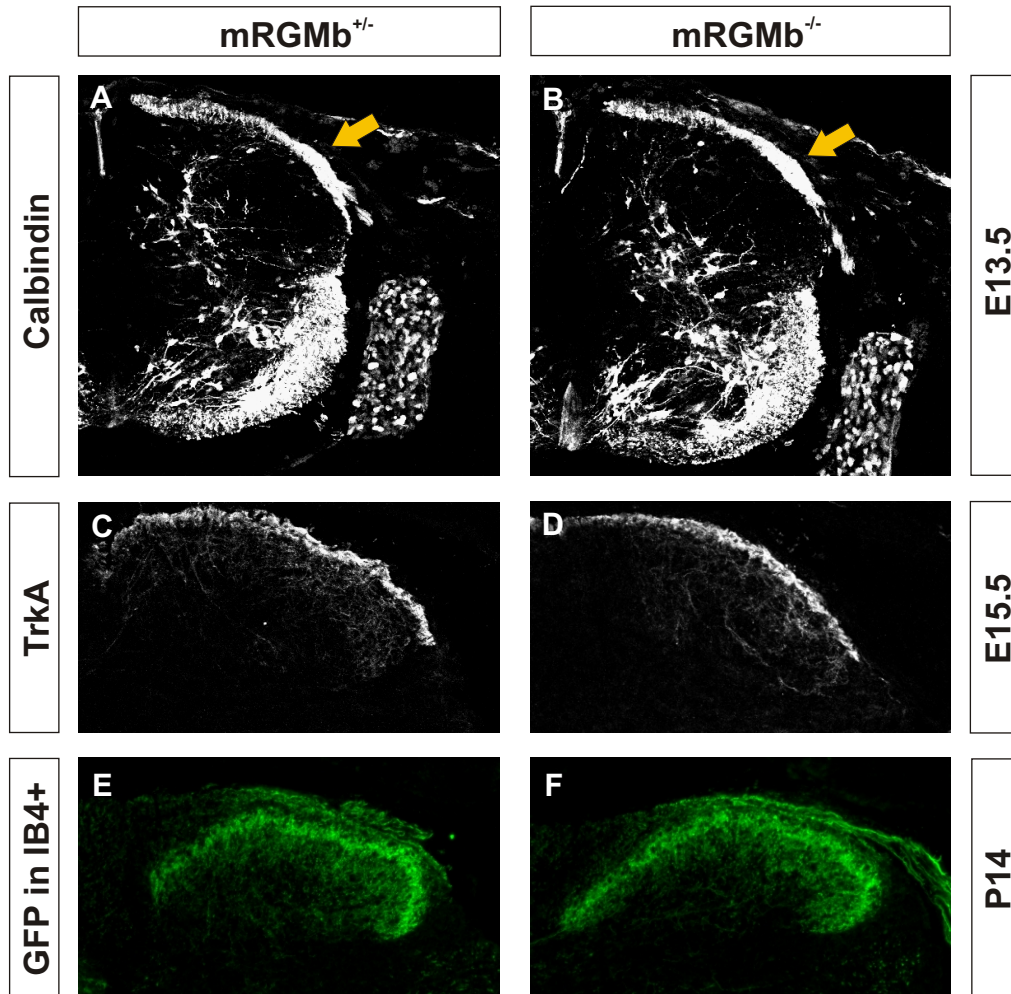


**Figure 14. *mRGMb* Mutant Mice Do Not Exhibit a Defect in Cutaneous Afferent Projections.**  
 (A-D) Spinal cords of *mRGMb*<sup>+/-</sup> (A, C) and *mRGMb*<sup>-/-</sup> (B, D) embryos were immunostained with Calbindin-28K (A, B) or TrkA (C, D). Arrows in (A, B) indicate Calbindin positive cutaneous afferents.  
 (E, F) GFP driven by the *Thy1* promoter labels specifically IB4 positive cutaneous afferents.



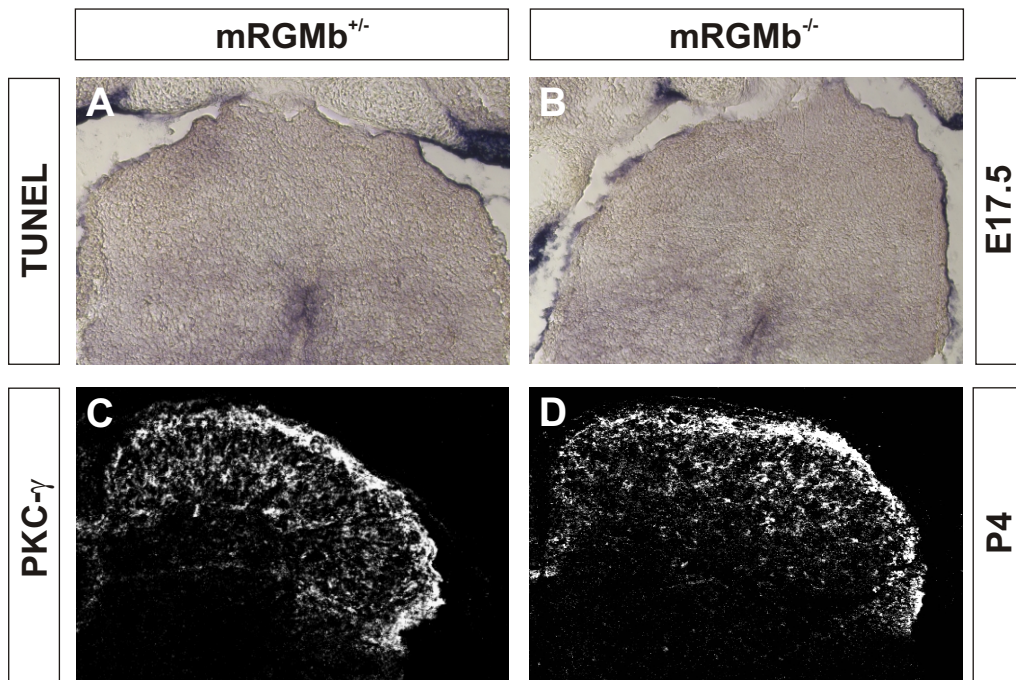


**Figure 15. Dorsal Horn Morphogenesis Is Not Affected in *mRGMb* Mutant Mice.**

(A, B) TUNEL labeling does not reveal increased apoptosis in *mRGMb*<sup>-/-</sup> (B) compared to *mRGMb*<sup>+/-</sup> (A) embryos.

(C, D) PKC-γ positive neurons are unchanged in *mRGMb*<sup>-/-</sup> (D) compared to *mRGMb*<sup>+/-</sup> (C) animals.

## Material and Methods

### Generation of *mRGMB* Mutant Mice

A mouse genomic library was screened using a *mRGMB* specific probe (Incyte Genomics, Palo Alto, CA). The second coding exon of *mRGMB* was disrupted by inserting a cassette containing an *eGFP* in frame with the endogenous ATG, followed by an *IRES-NLS-LacZ-pA* and a thymidine kinase (TK)-neomycin cassette using homologous recombination in embryonic stem (ES) cells (targeting frequency, ~1:50). ES cell recombinants were screened by genomic Southern blot (EcoRI digest; 3' probe (~250bp): oligonucleotides (A) 5' cca tgc tgc tca gcc ctg c-3' and (B) 5' ctt aga acg tgt ttt gta agg 3'). The identification of *mRGMB* mutant mice was performed by genomic Southern blotting and PCR ([1] 5'-gtt cct agg gag aat agc gtc tcc-3'; [2] 5'-aca ggc acg ttc gtc act tga acc-3'). Northern blot analysis confirmed the absence of *mRGMB* mRNA in *mRGMB*<sup>-/-</sup>, using a *mRGMB* specific probe (BG519283)

### Analysis of Retinocollicular Projections

Anterograde labeling of retinocollicular projections was done as described (Simon and O'Leary, 1992). Briefly, 5% DiI (Molecular Probes, Eugene, OR) in dimethyl formamide solution was injected into the retina at P0 or the nasal or temporal extreme of the retina at P9-P12 with a fine glass micropipette using a Picospritzer III (Parker, Fairfield, NJ). One day later for fills at P0 or two days later for focal injections, colliculi were analyzed blind to genotype with confocal microscopy (Olympus, Hamburg, Germany). Retinas were examined to verify a single injection point for focal injections.

### Histotology

Antibodies used in this study were: rabbit anti-parvalbumin (Swant), rabbit anti-TrkA (Upstate), rabbit anti-PKC- $\gamma$  (C19) (Santa Cruz), rabbit anti-Calbindin D-28k (Swant), sheep anti-GFP (Biogenesis). Cryostat sections were processed for immunohistochemistry as previously described (Arber et al., 1999) using fluorophore-conjugated secondary antibodies (Molecular Probes, Eugene, OR) (1:1000). TUNEL labeling to detect apoptotic cells was performed as described by the manufacturer (Roche, Rotkreuz, Switzerland)

## REFERENCES

Altmann, C. R., and Brivanlou, A. H. (2001). Neural patterning in the vertebrate embryo. *Int Rev Cytol* 203, 447-482.

Anderson, D. J., Groves, A., Lo, L., Ma, Q., Rao, M., Shah, N. M., and Sommer, L. (1997). Cell lineage determination and the control of neuronal identity in the neural crest. *Cold Spring Harb Symp Quant Biol* 62, 493-504.

Arber S., Han B., Mendelsohn M., Smith M., Jessell T. M., Sockanathan S. (1999). Requirement for the homeobox gene Hb9 in the consolidation of motor neuron identity. *Neuron* 23:659-674.

Arber, S., Ladle, D. R., Lin, J. H., Frank, E., and Jessell, T. M. (2000). ETS gene Er81 controls the formation of functional connections between group Ia sensory afferents and motor neurons. *Cell* 101, 485-498.

Augsburger, A., Schuchardt, A., Hoskins, S., Dodd, J., and Butler, S. (1999). BMPs as mediators of roof plate repulsion of commissural neurons. *Neuron* 24, 127-141.

Barton, W. A., Himanen, J. P., Antipenko, A., and Nikolov, D. B. (2004). Structures of axon guidance molecules and their neuronal receptors. *Adv Protein Chem* 68, 65-106.

Bentley, D., and Toroian-Raymond, A. (1986). Disoriented pathfinding by pioneer neurone growth cones deprived of filopodia by cytochalasin treatment. *Nature* 323, 712-715.

Bismuth, G., and Bomsell, L. (2002). Controlling the immune system through semaphorins. *Sci STKE* 2002, RE4.

Bonkowsky, J. L., Yoshikawa, S., O'Keefe, D. D., Scully, A. L., and Thomas, J. B. (1999). Axon routing across the midline controlled by the *Drosophila* Derailed receptor. *Nature* 402, 540-544.

Brinks, H., Conrad, S., Vogt, J., Oldekamp, J., Sierra, A., Deitinghoff, L., Bechmann, I., Alvarez-Bolado, G., Heimrich, B., Monnier, P. P., *et al.* (2004). The repulsive guidance molecule RGMA is involved in the formation of afferent connections in the dentate gyrus. *J Neurosci* 24, 3862-3869.

Briscoe J., Pierani A., Jessell T. M., Ericson J. (2000). A homeodomain protein code specifies progenitor cell identity and neuronal fate in the ventral neural tube. *Cell* 101:435-445.

Brittis P. A., Flanagan J. G. (2001). Nogo domains and a Nogo receptor: implications for axon regeneration. *Neuron* 30:11-14.

Brose, K., Bland, K. S., Wang, K. H., Arnott, D., Henzel, W., Goodman, C. S., Tessier-Lavigne, M., and Kidd, T. (1999). Slit proteins bind Robo receptors and have an evolutionarily conserved role in repulsive axon guidance. *Cell* 96, 795-806.

Butler, S. J., and Dodd, J. (2003). A role for BMP heterodimers in roof plate-mediated repulsion of commissural axons. *Neuron* 38, 389-401.

Caroni, P. (1997). Overexpression of growth-associated proteins in the neurons of adult transgenic mice. *J Neurosci Methods* 71, 3-9.

Charron, F., Stein, E., Jeong, J., McMahon, A. P., and Tessier-Lavigne, M. (2003). The morphogen sonic hedgehog is an axonal chemoattractant that collaborates with netrin-1 in midline axon guidance. *Cell* 113, 11-23.

Castellani, V., Chedotal, A., Schachner, M., Faivre-Sarrailh, C., and Rougon, G. (2000). Analysis of the L1-deficient mouse phenotype reveals cross-talk between Sema3A and L1 signaling pathways in axonal guidance. *Neuron* 27, 237-249.

Chan, S. S., Zheng, H., Su, M. W., Wilk, R., Killeen, M. T., Hedgecock, E. M., and Culotti, J. G. (1996). UNC-40, a *C. elegans* homolog of DCC (Deleted in Colorectal Cancer), is required in motile cells responding to UNC-6 netrin cues. *Cell* 87, 187-195.

Chen, H., Chedotal, A., He, Z., Goodman, C. S., and Tessier-Lavigne, M. (1997). Neuropilin-2, a novel member of the neuropilin family, is a high affinity receptor for the semaphorins Sema E and Sema IV but not Sema III. *Neuron* 19, 547-559.

Chen, Z. F., Rebelo, S., White, F., Malmberg, A. B., Baba, H., Lima, D., Woolf, C. J., Basbaum, A. I., and Anderson, D. J. (2001). The paired homeodomain protein DRG11 is required for the projection of cutaneous sensory afferent fibers to the dorsal spinal cord. *Neuron* 31, 59-73.

Chen M. S., Huber A. B., van der Haar M. E., Frank M., Schnell L., Spillmann A. A., Christ F., Schwab M. E. (2000). Nogo-A is a myelin-associated neurite outgrowth inhibitor and an antigen for monoclonal antibody IN-1. *Nature* 403:434-439.

Cheng, H. J., Bagri, A., Yaron, A., Stein, E., Pleasure, S. J., and Tessier-Lavigne, M. (2001). Plexin-A3 mediates semaphorin signaling and regulates the development of hippocampal axonal projections. *Neuron* 32, 249-263.

Cheng, H. J., and Flanagan, J. G. (1994). Identification and cloning of ELF-1, a developmentally expressed ligand for the Mek4 and Sek receptor tyrosine kinases. *Cell* 79, 157-168.

Cheng, H. J., Nakamoto, M., Bergemann, A. D., and Flanagan, J. G. (1995). Complementary gradients in expression and binding of ELF-1 and Mek4 in development of the topographic retinotectal projection map. *Cell* 82, 371-381.

Chien, C. B., Rosenthal, D. E., Harris, W. A., and Holt, C. E. (1993). Navigational errors made by growth cones without filopodia in the embryonic *Xenopus* brain. *Neuron* 11, 237-251.

Chisholm, A., and Tessier-Lavigne, M. (1999). Conservation and divergence of axon guidance mechanisms. *Curr Opin Neurobiol* 9, 603-615.

Colamarino, S. A., and Tessier-Lavigne, M. (1995). The axonal chemoattractant netrin-1 is also a chemorepellent for trochlear motor axons. *Cell* 81, 621-629.

- Comeau, M. R., Johnson, R., DuBose, R. F., Petersen, M., Gearing, P., VandenBos, T., Park, L., Farrah, T., Buller, R. M., Cohen, J. I., *et al.* (1998). A poxvirus-encoded semaphorin induces cytokine production from monocytes and binds to a novel cellular semaphorin receptor, VESPR. *Immunity* 8, 473-482.
- Dasen, J. S., Liu, J. P., and Jessell, T. M. (2003). Motor neuron columnar fate imposed by sequential phases of Hox-c activity. *Nature* 425, 926-933.
- Dent, E. W., and Gertler, F. B. (2003). Cytoskeletal dynamics and transport in growth cone motility and axon guidance. *Neuron* 40, 209-227.
- Dickson, B. J. (2001). Rho GTPases in growth cone guidance. *Curr Opin Neurobiol* 11, 103-110.
- Dickson, B. J. (2002). Molecular mechanisms of axon guidance. *Science* 298, 1959-1964.
- Drescher, U., Kremoser, C., Handwerker, C., Loschinger, J., Noda, M., and Bonhoeffer, F. (1995). In vitro guidance of retinal ganglion cell axons by RAGS, a 25 kDa tectal protein related to ligands for Eph receptor tyrosine kinases. *Cell* 82, 359-370.
- Eisenhaber B., Bork P., Eisenhaber F. (1999). Prediction of potential GPI-modification sites in proprotein sequences. *J Mol Biol* 292, 741-758.
- Fazeli, A., Dickinson, S. L., Hermiston, M. L., Tighe, R. V., Steen, R. G., Small, C. G., Stoeckli, E. T., Keino-Masu, K., Masu, M., Rayburn, H., *et al.* (1997). Phenotype of mice lacking functional Deleted in colorectal cancer (Dcc) gene. *Nature* 386, 796-804.
- Feldheim D. A., Kim Y. I., Bergemann A. D., Frisen J., Barbacid M., Flanagan J. G. (2000). Genetic analysis of ephrin-A2 and ephrin-A5 shows their requirement in multiple aspects of retinocollicular mapping. *Neuron* 25, 563-574
- Fricke, C., Lee, J. S., Geiger-Rudolph, S., Bonhoeffer, F., and Chien, C. B. (2001). *astray*, a zebrafish roundabout homolog required for retinal axon guidance. *Science* 292, 507-510.

- Frisen J., Yates P. A., McLaughlin T., Friedman G. C., O'Leary D. D., Barbacid M. (1998). Ephrin-A5 (AL-1/RAGS) is essential for proper retinal axon guidance and topographic mapping in the mammalian visual system. *Neuron* 20, 235-243.
- Giordano, S., Corso, S., Conrotto, P., Artigiani, S., Gilestro, G., Barberis, D., Tamagnone, L., and Comoglio, P. M. (2002). The semaphorin 4D receptor controls invasive growth by coupling with Met. *Nat Cell Biol* 4, 720-724.
- Godement P., Bonhoeffer F. (1989). Cross-species recognition of tectal cues by retinal fibers in vitro. *Development* 106, 313-320.
- Gordon-Weeks, P. R. (2004). Microtubules and growth cone function. *J Neurobiol* 58, 70-83.
- GrandPre T., Nakamura F., Vartanian T., Strittmatter S. M. (2000) Identification of the Nogo inhibitor of axon regeneration as a Reticulon protein. *Nature* 403, 439-444.
- Gu, C., Yoshida, Y., Livet, J., Reimert, D. V., Mann, F., Merte, J., Henderson, C. E., Jessell, T. M., Kolodkin, A. L., and Ginty, D. D. (2005). Semaphorin 3E and plexin-D1 control vascular pattern independently of neuropilins. *Science* 307, 265-268.
- Guan, K. L., and Rao, Y. (2003). Signalling mechanisms mediating neuronal responses to guidance cues. *Nat Rev Neurosci* 4, 941-956.
- Hall, A. (1998). Rho GTPases and the actin cytoskeleton. *Science* 279, 509-514.
- Hao, J. C., Yu, T. W., Fujisawa, K., Culotti, J. G., Gengyo-Ando, K., Mitani, S., Moulder, G., Barstead, R., Tessier-Lavigne, M., and Bargmann, C. I. (2001). *C. elegans* slit acts in midline, dorsal-ventral, and anterior-posterior guidance via the SAX-3/Robo receptor. *Neuron* 32, 25-38.
- Harris, R., Sabatelli, L. M., and Seeger, M. A. (1996). Guidance cues at the *Drosophila* CNS midline: identification and characterization of two *Drosophila* Netrin/UNC-6 homologs. *Neuron* 17, 217-228.

Harris M. J., Juriloff D. M. (1997). Genetic landmarks for defects in mouse neural tube closure. *Teratology* 56, 177-187.

He, Z. (2000). Crossed wires: L1 and neuropilin interactions. *Neuron* 27, 191-193.

He, Z., and Tessier-Lavigne, M. (1997). Neuropilin is a receptor for the axonal chemorepellent Semaphorin III. *Cell* 90, 739-751.

Hedgecock, E. M., Culotti, J. G., and Hall, D. H. (1990). The *unc-5*, *unc-6*, and *unc-40* genes guide circumferential migrations of pioneer axons and mesodermal cells on the epidermis in *C. elegans*. *Neuron* 4, 61-85.

Henkemeyer, M., Orioli, D., Henderson, J. T., Saxton, T. M., Roder, J., Pawson, T., and Klein, R. (1996). Nuk controls pathfinding of commissural axons in the mammalian central nervous system. *Cell* 86, 35-46.

Henley, J., and Poo, M. M. (2004). Guiding neuronal growth cones using Ca<sup>2+</sup> signals. *Trends Cell Biol* 14, 320-330.

Hinck, L. (2004). The versatile roles of "axon guidance" cues in tissue morphogenesis. *Dev Cell* 7, 783-793.

Hindges, R., McLaughlin, T., Genoud, N., Henkemeyer, M., and O'Leary, D. D. (2002). EphB forward signaling controls directional branch extension and arborization required for dorsal-ventral retinotopic mapping. *Neuron* 35, 475-487.

Holmberg J., Clarke D. L., Frisen J. (2000). Regulation of repulsion versus adhesion by different splice forms of an Eph receptor. *Nature* 408, 203-206.

Hong, K., Hinck, L., Nishiyama, M., Poo, M. M., Tessier-Lavigne, M., and Stein, E. (1999). A ligand-gated association between cytoplasmic domains of UNC5 and DCC family receptors converts netrin-induced growth cone attraction to repulsion. *Cell* 97, 927-941.



Hornberger, M. R., Dutting, D., Ciossek, T., Yamada, T., Handwerker, C., Lang, S., Weth, F., Huf, J., Wessel, R., Logan, C., *et al.* (1999). Modulation of EphA receptor function by coexpressed ephrinA ligands on retinal ganglion cell axons. *Neuron* 22, 731-742.

Huber, A. B., Kolodkin, A. L., Ginty, D. D., and Cloutier, J. F. (2003). Signaling at the growth cone: ligand-receptor complexes and the control of axon growth and guidance. *Annu Rev Neurosci* 26, 509-563.

Inoue, T., Oz, H. S., Wiland, D., Gharib, S., Deshpande, R., Hill, R. J., Katz, W. S., and Sternberg, P. W. (2004). *C. elegans* LIN-18 is a Ryk ortholog and functions in parallel to LIN-17/Frizzled in Wnt signaling. *Cell* 118, 795-806.

Irving, C., Malhas, A., Guthrie, S., and Mason, I. (2002). Establishing the trochlear motor axon trajectory: role of the isthmus organizer and Fgf8. *Development* 129, 5389-5398.

Isbister, C. M., and O'Connor, T. P. (2000). Mechanisms of growth cone guidance and motility in the developing grasshopper embryo. *J Neurobiol* 44, 271-280.

Ishii, N., Wadsworth, W. G., Stern, B. D., Culotti, J. G., and Hedgecock, E. M. (1992). UNC-6, a laminin-related protein, guides cell and pioneer axon migrations in *C. elegans*. *Neuron* 9, 873-881.

Jessell, T. M. (2000). Neuronal specification in the spinal cord: inductive signals and transcriptional codes. *Nat Rev Genet* 1, 20-29.

Kantor, D. B., Chivatakarn, O., Peer, K. L., Oster, S. F., Inatani, M., Hansen, M. J., Flanagan, J. G., Yamaguchi, Y., Sretavan, D. W., Giger, R. J., and Kolodkin, A. L. (2004). Semaphorin 5A is a bifunctional axon guidance cue regulated by heparan and chondroitin sulfate proteoglycans. *Neuron* 44, 961-975.

Karlstrom, R. O., Trowe, T., Klostermann, S., Baier, H., Brand, M., Crawford, A. D., Grunewald, B., Haffter, P., Hoffmann, H., Meyer, S. U., *et al.* (1996). Zebrafish mutations affecting retinotectal axon pathfinding. *Development* 123, 427-438.

Keino-Masu, K., Masu, M., Hinck, L., Leonardo, E. D., Chan, S. S., Culotti, J. G., and Tessier-Lavigne, M. (1996). Deleted in Colorectal Cancer (DCC) encodes a netrin receptor. *Cell* 87, 175-185.

Keleman, K., and Dickson, B. J. (2001). Short- and long-range repulsion by the *Drosophila* Unc5 netrin receptor. *Neuron* 32, 605-617.

Kennedy, T. E., Serafini, T., de la Torre, J. R., and Tessier-Lavigne, M. (1994). Netrins are diffusible chemotropic factors for commissural axons in the embryonic spinal cord. *Cell* 78, 425-435.

Kidd, T., Bland, K. S., and Goodman, C. S. (1999). Slit is the midline repellent for the robo receptor in *Drosophila*. *Cell* 96, 785-794.

Kidd, T., Brose, K., Mitchell, K. J., Fetter, R. D., Tessier-Lavigne, M., Goodman, C. S., and Tear, G. (1998). Roundabout controls axon crossing of the CNS midline and defines a novel subfamily of evolutionarily conserved guidance receptors. *Cell* 92, 205-215.

Kolodkin, A. L., Levengood, D. V., Rowe, E. G., Tai, Y. T., Giger, R. J., and Ginty, D. D. (1997). Neuropilin is a semaphorin III receptor. *Cell* 90, 753-762.

Kolodkin, A. L., Matthes, D. J., O'Connor, T. P., Patel, N. H., Admon, A., Bentley, D., and Goodman, C. S. (1992). Fasciclin IV: sequence, expression, and function during growth cone guidance in the grasshopper embryo. *Neuron* 9, 831-845.

Kullander, K., and Klein, R. (2002). Mechanisms and functions of Eph and ephrin signalling. *Nat Rev Mol Cell Biol* 3, 475-486.

Kullander, K., Mather, N. K., Diella, F., Dottori, M., Boyd, A. W., and Klein, R. (2001). Kinase-dependent and kinase-independent functions of EphA4 receptors in major axon tract formation in vivo. *Neuron* 29, 73-84.

Kumanogoh, A., and Kikutani, H. (2003). Immune semaphorins: a new area of semaphorin research. *J Cell Sci* 116, 3463-3470.

Kumanogoh, A., Marukawa, S., Suzuki, K., Takegahara, N., Watanabe, C., Ch'ng, E., Ishida, I., Fujimura, H., Sakoda, S., Yoshida, K., and Kikutani, H. (2002). Class IV semaphorin Sema4A enhances T-cell activation and interacts with Tim-2. *Nature* *419*, 629-633.

Kumanogoh, A., Watanabe, C., Lee, I., Wang, X., Shi, W., Araki, H., Hirata, H., Iwahori, K., Uchida, J., Yasui, T., *et al.* (2000). Identification of CD72 as a lymphocyte receptor for the class IV semaphorin CD100: a novel mechanism for regulating B cell signaling. *Immunity* *13*, 621-631.

Lee, H. Y., Kleber, M., Hari, L., Brault, V., Suter, U., Taketo, M. M., Kemler, R., and Sommer, L. (2004). Instructive role of Wnt/beta-catenin in sensory fate specification in neural crest stem cells. *Science* *303*, 1020-1023.

Leighton, P. A., Mitchell, K. J., Goodrich, L. V., Lu, X., Pinson, K., Scherz, P., Skarnes, W. C., and Tessier-Lavigne, M. (2001). Defining brain wiring patterns and mechanisms through gene trapping in mice. *Nature* *410*, 174-179.

Leonardo, E. D., Hinck, L., Masu, M., Keino-Masu, K., Ackerman, S. L., and Tessier-Lavigne, M. (1997). Vertebrate homologues of *C. elegans* UNC-5 are candidate netrin receptors. *Nature* *386*, 833-838.

Leung-Hagesteijn, C., Spence, A. M., Stern, B. D., Zhou, Y., Su, M. W., Hedgecock, E. M., and Culotti, J. G. (1992). UNC-5, a transmembrane protein with immunoglobulin and thrombospondin type 1 domains, guides cell and pioneer axon migrations in *C. elegans*. *Cell* *71*, 289-299.

Li, H. S., Chen, J. H., Wu, W., Fagaly, T., Zhou, L., Yuan, W., Dupuis, S., Jiang, Z. H., Nash, W., Gick, C., *et al.* (1999). Vertebrate slit, a secreted ligand for the transmembrane protein roundabout, is a repellent for olfactory bulb axons. *Cell* *96*, 807-818.

Lin, J. H., Saito, T., Anderson, D. J., Lance-Jones, C., Jessell, T. M., and Arber, S. (1998). Functionally related motor neuron pool and muscle sensory afferent subtypes defined by coordinate ETS gene expression. *Cell* *95*, 393-407.

- Livet J., Sigrist M., Stroebel S., De Paola V., Price S. R., Henderson C. E., Jessell T. M., Arber S. (2002). ETS gene *Pea3* controls the central position and terminal arborization of specific motor neuron pools. *Neuron* 35, 877-892.
- Long, H., Sabatier, C., Ma, L., Plump, A., Yuan, W., Ornitz, D. M., Tamada, A., Murakami, F., Goodman, C. S., and Tessier-Lavigne, M. (2004). Conserved roles for Slit and Robo proteins in midline commissural axon guidance. *Neuron* 42, 213-223.
- Luo, L. (2000). Rho GTPases in neuronal morphogenesis. *Nat Rev Neurosci* 1, 173-180.
- Luo, L. (2002). Actin cytoskeleton regulation in neuronal morphogenesis and structural plasticity. *Annu Rev Cell Dev Biol* 18, 601-635.
- Luo, Y., Raible, D., and Raper, J. A. (1993). Collapsin: a protein in brain that induces the collapse and paralysis of neuronal growth cones. *Cell* 75, 217-227.
- Lu, W., Yamamoto, V., Ortega, B., and Baltimore, D. (2004). Mammalian Ryk is a Wnt coreceptor required for stimulation of neurite outgrowth. *Cell* 119, 97-108.
- Lyuksyutova, A. I., Lu, C. C., Milanesio, N., King, L. A., Guo, N., Wang, Y., Nathans, J., Tessier-Lavigne, M., and Zou, Y. (2003). Anterior-posterior guidance of commissural axons by Wnt-frizzled signaling. *Science* 302, 1984-1988.
- Mann, F., Ray, S., Harris, W., and Holt, C. (2002). Topographic mapping in dorsoventral axis of the *Xenopus* retinotectal system depends on signaling through ephrin-B ligands. *Neuron* 35, 461-473.
- Matsunaga, E., Tauszig-Delamasure, S., Monnier, P. P., Mueller, B. K., Strittmatter, S. M., Mehlen, P., and Chedotal, A. (2004). RGM and its receptor neogenin regulate neuronal survival. *Nat Cell Biol* 6, 749-755.
- McLaughlin, T., Hindges, R., and O'Leary, D. D. (2003a). Regulation of axial patterning of the retina and its topographic mapping in the brain. *Curr Opin Neurobiol* 13, 57-69.

McLaughlin, T., Hindges, R., Yates, P. A., and O'Leary, D. D. (2003b). Bifunctional action of ephrin-B1 as a repellent and attractant to control bidirectional branch extension in dorsal-ventral retinotopic mapping. *Development* *130*, 2407-2418.

Mitchell, K. J., Doyle, J. L., Serafini, T., Kennedy, T. E., Tessier-Lavigne, M., Goodman, C. S., and Dickson, B. J. (1996). Genetic analysis of Netrin genes in *Drosophila*: Netrins guide CNS commissural axons and peripheral motor axons. *Neuron* *17*, 203-215.

Monnier, P. P., Sierra, A., Macchi, P., Deitinghoff, L., Andersen, J. S., Mann, M., Flad, M., Hornberger, M. R., Stahl, B., Bonhoeffer, F., and Mueller, B. K. (2002). RGM is a repulsive guidance molecule for retinal axons. *Nature* *419*, 392-395.

Monschau B., Kremoser C., Ohta K., Tanaka H., Kaneko T., Yamada T., Handwerker C., Hornberger M. R., Loschinger J., Pasquale E. B., Siever D. A., Verderame M. F., Muller B. K., Bonhoeffer F., Drescher U. (1997). Shared and distinct functions of RAGS and ELF-1 in guiding retinal axons. *Embo J* *16*, 1258-1267.

Nakamoto M., Cheng H. J., Friedman G. C., McLaughlin T., Hansen M. J., Yoon C. H., O'Leary D. D., Flanagan J. G. (1996). Topographically specific effects of ELF-1 on retinal axon guidance in vitro and retinal axon mapping in vivo. *Cell* *86*, 755-766.

Nakamura, F., Tanaka, M., Takahashi, T., Kalb, R. G., and Strittmatter, S. M. (1998). Neuropilin-1 extracellular domains mediate semaphorin D/III-induced growth cone collapse. *Neuron* *21*, 1093-1100.

Neufeld, G., Cohen, T., Shraga, N., Lange, T., Kessler, O., and Herzog, Y. (2002). The neuropilins: multifunctional semaphorin and VEGF receptors that modulate axon guidance and angiogenesis. *Trends Cardiovasc Med* *12*, 13-19.

Neufeld, G., Shraga-Heled, N., Lange, T., Guttman-Raviv, N., Herzog, Y., and Kessler, O. (2005). Semaphorins in cancer. *Front Biosci* *10*, 751-760.

Niederkofler, V., Salie, R., Sigrist, M., and Arber, S. (2004). Repulsive guidance molecule (RGM) gene function is required for neural tube closure but not retinal topography in the mouse visual system. *J Neurosci* *24*, 808-818.

Nielsen H., Brunak S., von Heijne G. (1999). Machine learning approaches for the prediction of signal peptides and other protein sorting signals. *Protein Eng* *12*, 3-9.

Nishiyama, M., Hoshino, A., Tsai, L., Henley, J. R., Goshima, Y., Tessier-Lavigne, M., Poo, M. M., and Hong, K. (2003). Cyclic AMP/GMP-dependent modulation of Ca<sup>2+</sup> channels sets the polarity of nerve growth-cone turning. *Nature* *423*, 990-995.

Orioli, D., and Klein, R. (1997). The Eph receptor family: axonal guidance by contact repulsion. *Trends Genet* *13*, 354-359.

Packard, M., Mathew, D., and Budnik, V. (2003). Wnts and TGF beta in synaptogenesis: old friends signalling at new places. *Nat Rev Neurosci* *4*, 113-120.

Patapoutian, A., and Reichardt, L. F. (2000). Roles of Wnt proteins in neural development and maintenance. *Curr Opin Neurobiol* *10*, 392-399.

Pandey, A., Lindberg, R. A., and Dixit, V. M. (1995). Cell signalling. Receptor orphans find a family. *Curr Biol* *5*, 986-989.

Papanikolaou, G., Samuels, M. E., Ludwig, E. H., MacDonald, M. L., Franchini, P. L., Dube, M. P., Andres, L., MacFarlane, J., Sakellaropoulos, N., Politou, M., *et al.* (2004). Mutations in HFE2 cause iron overload in chromosome 1q-linked juvenile hemochromatosis. *Nat Genet* *36*, 77-82.

Pasterkamp, R. J., Peschon, J. J., Spriggs, M. K., and Kolodkin, A. L. (2003). Semaphorin 7A promotes axon outgrowth through integrins and MAPKs. *Nature* *424*, 398-405.

Plump, A. S., Erskine, L., Sabatier, C., Brose, K., Epstein, C. J., Goodman, C. S., Mason, C. A., and Tessier-Lavigne, M. (2002). Slit1 and Slit2 cooperate to prevent premature midline crossing of retinal axons in the mouse visual system. *Neuron* *33*, 219-232.

Rajagopalan, S., Deitinghoff, L., Davis, D., Conrad, S., Skutella, T., Chedotal, A., Mueller, B. K., and Strittmatter, S. M. (2004). Neogenin mediates the action of repulsive guidance molecule. *Nat Cell Biol* 6, 756-762.

Raper, J. A. (2000). Semaphorins and their receptors in vertebrates and invertebrates. *Curr Opin Neurobiol* 10, 88-94.

Roskies AL, O'Leary DD (1994) Control of topographic retinal axon branching by inhibitory membrane-bound molecules. *Science* 265:799-803.

Sabatier, C., Plump, A. S., Le, M., Brose, K., Tamada, A., Murakami, F., Lee, E. Y., and Tessier-Lavigne, M. (2004). The divergent Robo family protein rig-1/Robo3 is a negative regulator of slit responsiveness required for midline crossing by commissural axons. *Cell* 117, 157-169.

Samad, T. A., Rebbapragada, A., Bell, E., Zhang, Y., Sidis, Y., Jeong, S. J., Campagna, J. A., Perusini, S., Fabrizio, D. A., Schneyer, A. L., *et al.* (2005). DRAGON: a bone morphogenetic protein co-receptor. *J Biol Chem*.

Samad, T. A., Srinivasan, A., Karchewski, L. A., Jeong, S. J., Campagna, J. A., Ji, R. R., Fabrizio, D. A., Zhang, Y., Lin, H. Y., Bell, E., and Woolf, C. J. (2004). DRAGON: a member of the repulsive guidance molecule-related family of neuronal- and muscle-expressed membrane proteins is regulated by DRG11 and has neuronal adhesive properties. *J Neurosci* 24, 2027-2036.

Schaeren-Wiemers N., Gerfin-Moser A. (1993). A single protocol to detect transcripts of various types and expression levels in neural tissue and cultured cells: in situ hybridization using digoxigenin-labelled cRNA probes. *Histochemistry* 100, 431-440.

Seeger, M., Tear, G., Ferres-Marco, D., and Goodman, C. S. (1993). Mutations affecting growth cone guidance in *Drosophila*: genes necessary for guidance toward or away from the midline. *Neuron* 10, 409-426.

Serafini, T., Colamarino, S. A., Leonardo, E. D., Wang, H., Beddington, R., Skarnes, W. C., and Tessier-Lavigne, M. (1996). Netrin-1 is required for commissural axon guidance in the developing vertebrate nervous system. *Cell* 87, 1001-1014.

Serafini, T., Kennedy, T. E., Galko, M. J., Mirzayan, C., Jessell, T. M., and Tessier-Lavigne, M. (1994). The netrins define a family of axon outgrowth-promoting proteins homologous to *C. elegans* UNC-6. *Cell* 78, 409-424.

Sharom F. J., Lehto M. T. (2002). Glycosylphosphatidylinositol-anchored proteins: structure, function, and cleavage by phosphatidylinositol-specific phospholipase C. *Biochem Cell Biol* 80, 535-549.

Simon D. K., O'Leary D. D. (1992). Development of topographic order in the mammalian retinocollicular projection. *J Neurosci* 12,1212-1232.

Smith, S. J. (1988). Neuronal cytomechanics: the actin-based motility of growth cones. *Science* 242, 708-715.

Song, H., Ming, G., He, Z., Lehmann, M., McKerracher, L., Tessier-Lavigne, M., and Poo, M. (1998). Conversion of neuronal growth cone responses from repulsion to attraction by cyclic nucleotides. *Science* 281, 1515-1518.

Song, H. J., Ming, G. L., and Poo, M. M. (1997). cAMP-induced switching in turning direction of nerve growth cones. *Nature* 388, 275-279.

Song, H. J., and Poo, M. M. (1999). Signal transduction underlying growth cone guidance by diffusible factors. *Curr Opin Neurobiol* 9, 355-363.

Sperry R. (1963). Chemoaffinity in the orderly growth of nerve fiber patterns and connections. *Proc Natl Acad Sci USA* 50, 703-710.

Spriggs, M. K. (1999). Shared resources between the neural and immune systems: semaphorins join the ranks. *Curr Opin Immunol* 11, 387-391.



- Srinivasan, K., Strickland, P., Valdes, A., Shin, G. C., and Hinck, L. (2003). Netrin-1/neogenin interaction stabilizes multipotent progenitor cap cells during mammary gland morphogenesis. *Dev Cell* 4, 371-382.
- Stahl, B., Muller, B., von Boxberg, Y., Cox, E. C., and Bonhoeffer, F. (1990). Biochemical characterization of a putative axonal guidance molecule of the chick visual system. *Neuron* 5, 735-743.
- Takahashi, T., Fournier, A., Nakamura, F., Wang, L. H., Murakami, Y., Kalb, R. G., Fujisawa, H., and Strittmatter, S. M. (1999). Plexin-neuropilin-1 complexes form functional semaphorin-3A receptors. *Cell* 99, 59-69.
- Tamagnone, L., Artigiani, S., Chen, H., He, Z., Ming, G. I., Song, H., Chedotal, A., Winberg, M. L., Goodman, C. S., Poo, M., *et al.* (1999). Plexins are a large family of receptors for transmembrane, secreted, and GPI-anchored semaphorins in vertebrates. *Cell* 99, 71-80.
- Tessier-Lavigne, M., and Goodman, C. S. (1996). The molecular biology of axon guidance. *Science* 274, 1123-1133.
- Theiler K (1989) The house mouse: Atlas of embryonic development. New York: Springer-Verlag.
- Trusolino, L., and Comoglio, P. M. (2002). Scatter-factor and semaphorin receptors: cell signalling for invasive growth. *Nat Rev Cancer* 2, 289-300.
- Van Vactor, D., and Flanagan, J. G. (1999). The middle and the end: slit brings guidance and branching together in axon pathway selection. *Neuron* 22, 649-652.
- Walter, J., Henke-Fahle, S., and Bonhoeffer, F. (1987a). Avoidance of posterior tectal membranes by temporal retinal axons. *Development* 101, 909-913.
- Walter, J., Kern-Veits, B., Huf, J., Stolze, B., and Bonhoeffer, F. (1987b). Recognition of position-specific properties of tectal cell membranes by retinal axons in vitro. *Development* 101, 685-696.

Walter, J., Muller, B., and Bonhoeffer, F. (1990). Axonal guidance by an avoidance mechanism. *J Physiol (Paris)* *84*, 104-110.

Wang, H., Copeland, N. G., Gilbert, D. J., Jenkins, N. A., and Tessier-Lavigne, M. (1999a). Netrin-3, a mouse homolog of human NTN2L, is highly expressed in sensory ganglia and shows differential binding to netrin receptors. *J Neurosci* *19*, 4938-4947.

Wang, K. H., Brose, K., Arnott, D., Kidd, T., Goodman, C. S., Henzel, W., and Tessier-Lavigne, M. (1999b). Biochemical purification of a mammalian slit protein as a positive regulator of sensory axon elongation and branching. *Cell* *96*, 771-784.

Wen, Z., Guirland, C., Ming, G. L., and Zheng, J. Q. (2004). A CaMKII/calcineurin switch controls the direction of Ca(2+)-dependent growth cone guidance. *Neuron* *43*, 835-846.

Whitford, K. L., and Ghosh, A. (2001). Plexin signaling via off-track and rho family GTPases. *Neuron* *32*, 1-3.

Williams, S. E., Mann, F., Erskine, L., Sakurai, T., Wei, S., Rossi, D. J., Gale, N. W., Holt, C. E., Mason, C. A., and Henkemeyer, M. (2003). Ephrin-B2 and EphB1 mediate retinal axon divergence at the optic chiasm. *Neuron* *39*, 919-935.

Williams, S. E., Mason, C. A., and Herrera, E. (2004). The optic chiasm as a midline choice point. *Curr Opin Neurobiol* *14*, 51-60.

Winberg, M. L., Noordermeer, J. N., Tamagnone, L., Comoglio, P. M., Spriggs, M. K., Tessier-Lavigne, M., and Goodman, C. S. (1998). Plexin A is a neuronal semaphorin receptor that controls axon guidance. *Cell* *95*, 903-916.

Winberg, M. L., Tamagnone, L., Bai, J., Comoglio, P. M., Montell, D., and Goodman, C. S. (2001). The transmembrane protein Off-track associates with Plexins and functions downstream of Semaphorin signaling during axon guidance. *Neuron* *32*, 53-62.

Wolman, M. A., Liu, Y., Tawarayama, H., Shoji, W., and Halloran, M. C. (2004). Repulsion and attraction of axons by Semaphorin3D are mediated by different neuropilins in vivo. *J Neurosci* *24*, 8428-8435.

Wong, J. T., Wong, S. T., and O'Connor, T. P. (1999). Ectopic semaphorin-1a functions as an attractive guidance cue for developing peripheral neurons. *Nat Neurosci* *2*, 798-803.

Yates, P. A., Roskies, A. L., McLaughlin, T., and O'Leary, D. D. (2001). Topographic-specific axon branching controlled by ephrin-As is the critical event in retinotectal map development. *J Neurosci* *21*, 8548-8563.

Yu, T. W., and Bargmann, C. I. (2001). Dynamic regulation of axon guidance. *Nat Neurosci* *4 Suppl*, 1169-1176.

Zheng, J. Q., Wan, J. J., and Poo, M. M. (1996). Essential role of filopodia in chemotropic turning of nerve growth cone induced by a glutamate gradient. *J Neurosci* *16*, 1140-1149.

Zhou, F. Q., and Cohan, C. S. (2004). How actin filaments and microtubules steer growth cones to their targets. *J Neurobiol* *58*, 84-91.

Zinn, K., and Sun, Q. (1999). Slit branches out: a secreted protein mediates both attractive and repulsive axon guidance. *Cell* *97*, 1-4.

Zou, Y., Stoeckli, E., Chen, H., and Tessier-Lavigne, M. (2000). Squeezing axons out of the gray matter: a role for slit and semaphorin proteins from midline and ventral spinal cord. *Cell* *102*, 363-375.

# **Chapter 2**

## **Iron Homeostasis**

## 2.1 Balancing Iron

### Iron Homeostasis

Iron is an essential element incorporated in a variety of proteins in nearly all organisms (Aisen et al., 2001). In mammals, the majority of body iron is utilized for the production of heme proteins, such as hemoglobin, myoglobin and cytochromes. Iron has the capacity to accept and donate electrons readily, interconverting between ferric ( $\text{Fe}^{3+}$ ) and ferrous ( $\text{Fe}^{2+}$ ) forms. Free iron ( $\text{Fe}^{2+}$ ) catalyses the formation of dangerous free radicals (“Fenton-type” redox chemistry) that damage lipid membranes, proteins, and nucleic acids. Tight regulation of iron uptake, storage and export is essential to minimize free radical production. Any disturbance in iron metabolism can lead to hematological, metabolic and neurodegenerative disorders, which are potentially lethal to the organism (Andrews, 2000b; Hentze et al., 2004).

The human body contains ~3,000 mg to 4,000 mg iron, from which the vast majority (~70%) is utilized in erythroid cells for hemoglobin synthesis (Ponka, 1997; Andrews, 1999) (Figure 16). Each day only 1-2 mg is taken up by the duodenum while the same amount leaves the body through “passive” mechanisms like sloughing off mucosal cells of the gastrointestinal tract, desquamation, or blood losses (e.g. menstruation) (Figure 16). In comparison, approximately 20 mg iron is utilized in daily erythropoiesis. Recycling of iron from hemoglobin of senescent erythrocytes allows new red blood cell production with minimal iron absorption. Any excessive body iron is stored, for the most part, in hepatocytes and reticuloendothelial macrophages, from where it can be mobilized in response to acute need. As the body cannot actively excrete iron, the body iron levels must be tightly regulated at the point of absorption, across the mature enterocytes of the duodenum (Figure 16).

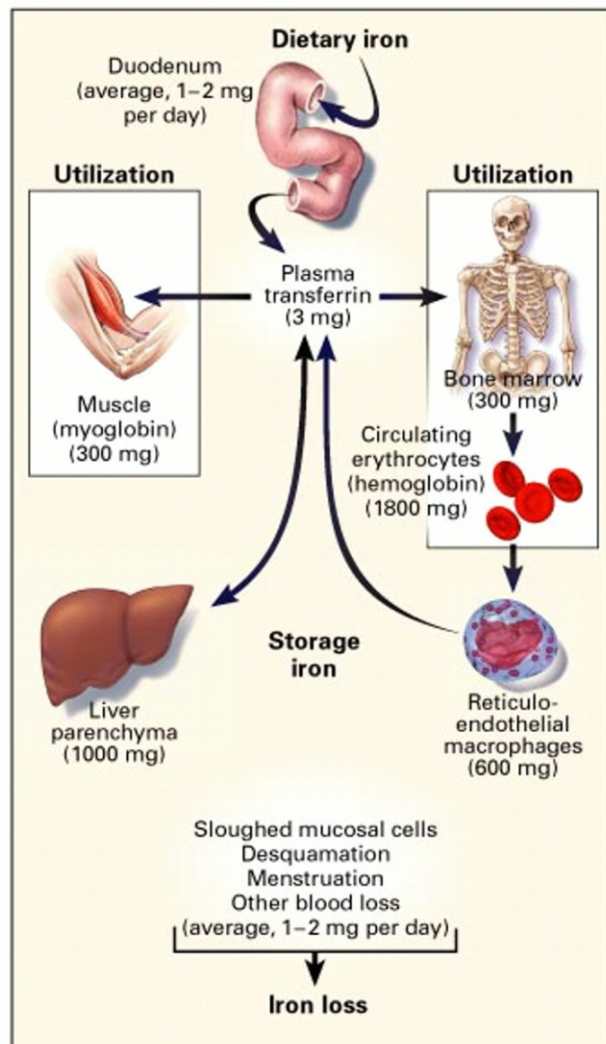


**Figure 16. Distribution of Iron in Adults.**

In the balanced state, 1 to 2 mg of iron enters and leaves the body each day. Dietary iron is absorbed by duodenal enterocytes. It circulates in plasma bound to transferrin. Most of the iron in the body is incorporated into hemoglobin in erythroid precursors and mature red cells. Approximately 10 to 15 percent is present in muscle fibers (in myoglobin) and other tissues (in enzymes and cytochromes). Iron is stored in parenchymal cells of the liver and reticuloendothelial macrophages. These macrophages provide most of the usable iron by degrading hemoglobin in senescent erythrocytes and reloading ferric iron onto transferrin for delivery to cells. (after Andrews, 1999)

## Regulation of Iron Absorption

Iron must pass from the gut lumen through both apical and basolateral membranes of the duodenal enterocyte to reach the plasma (Andrews, 2000b; Chorney et al., 2003) (Figure 17). The acidic milieu of gastric effluent facilitates enzymatic reduction of ferric iron to its ferrous form by a brush-border reductase, DcytB (a cytochrome b).  $\text{Fe}^{2+}$  is transported into the enterocyte by the divalent-metal transporter, DMT1. Once inside the absorptive enterocytes, iron is either stored in association with the protein ferritin or is transferred across the basolateral membrane via the iron exporter ferroportin (FPN1). After oxidation by hephaestin, a basolateral ferroxidase,  $\text{Fe}^{3+}$  is bound by transferrin (Tf) and transported across the vascular endothelium into the blood. Fe-Tf is recognized by the ubiquitously expressed transferrin receptor 1 (TfR1), and the entire Fe-Tf-TfR1 complex is endocytosed. Acidification of the vacuoles leads to conformational changes in the protein that release iron from transferrin and enables proton-coupled iron transport out of the endosomes through the activity of DMT1. Subsequently, Tf and TfR1 both return to the cell surface, where they dissociate at neutral pH. Both proteins participate in further rounds of iron delivery. In non-erythroid cells, iron may also be sequestered by ferritin (Figure 17).

## Cellular Iron Homeostasis via the IRE/IRP System

Cellular iron homeostasis is accomplished, in part, by the strictly regulated expression of proteins involved in iron uptake, storage, utilization, and export. The best understood regulatory mechanism to date engages two cytoplasmic iron regulatory proteins, IRP1 and IRP2 (Thomson et al., 1999; Cairo and Pietrangelo, 2000; Aisen et al., 2001; Eisenstein, 2003; Pantopoulos, 2004). IRPs interact with conserved mRNA stem loop structures, termed iron responsive elements (IREs), located either within the 5' or the 3' untranslated regions of mRNAs coding for central proteins in iron homeostasis, like ferritin, TfR1, ferroportin or DMT1 (McKie et al., 2000; Gunshin et al., 2001; Frazer et al., 2003). The IRE-binding affinity of IRPs is regulated by the availability of iron within a cell. When intracellular iron levels are high, binding affinity of IRPs to the IREs is low. In contrast, reduced cellular iron availability activates binding activity of IRPs, thus stabilizing mRNAs which bear their IREs within the 3' untranslated region, such as TfR1 and DMT1, and blocking translation of

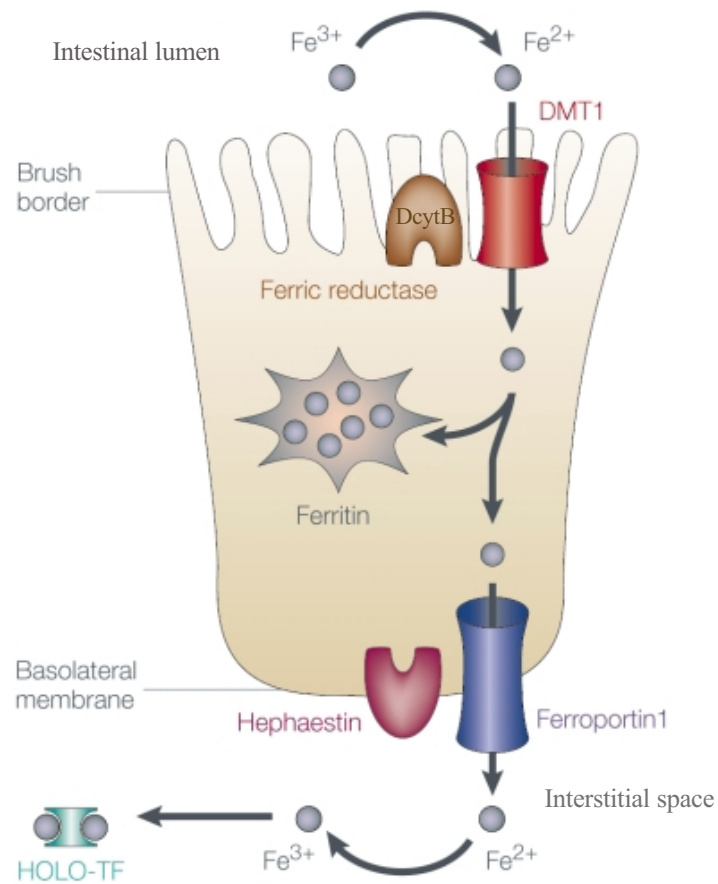


**Figure 17. Cellular Iron Transport.**

Duodenal enterocytes absorb iron from the diet. Non-haem iron is reduced by a ferric reductase (DcytB) in the brush border and is transported into the cell through the transmembrane iron transporter DMT1 (for divalent metal transporter 1). Some iron is stored within the cell in ferritin; the remainder must pass through the basolateral membrane to reach the plasma. An iron exporter, ferroportin, carries out basolateral iron transfer in cooperation with hephaestin, a ferroxidase. Absorbed iron is loaded onto transferrin (TF) to give holotransferrin (HOLO-TF) and transported across the vascular endothelium into the blood. (after Andrews, 2000b)



mRNAs with IREs located within the 5' untranslated region, like ferritin or ferroportin. By this posttranscriptional mechanism, TfR1 and DMT1 protein expression, and thus iron uptake into cells, is increased, while iron efflux, mediated by ferroportin and iron storage via ferritin is reduced.

## Regulation of Systemic Iron Homeostasis

Several mechanisms regulate intestinal iron uptake. First, iron uptake can be modulated by the amount of recently consumed iron in the diet, a mechanism referred to as the “dietary regulator” or “mucosal block” (Hahn et al, 1943; Stewart et al., 1950; O'Neil-Cutting and Crosby, 1987; Frazer et al., 2003). After the consumption of a high amount of iron, absorptive enterocytes transiently block any further uptake. This block seems to be caused by a rapid decrease of the divalent-metal transporter DMT1 and the brush-border reductase DcytB at both the transcriptional and translational levels, which is likely mediated by IRP-IRE interactions, decreasing iron absorption at the apical membrane (Frazer et al., 2003). The mucosal block may occur even in the presence of systemic iron deficiency (Stewart et al., 1950). Intestinal iron absorption is also regulated in response to the amount of iron in the body – the “stores regulator” (Finch, 1994; Gavin et al., 1994). When the amount of iron in the body stores decreases, iron absorption increases maintaining homeostatic levels. The “erythropoietic/hypoxia regulator” does not respond to iron levels at all, but rather modulates iron absorption in response to the requirements for erythropoiesis (Finch, 1994; Andrews, 1999). During periods of increased erythropoiesis, i.e. after severe blood loss, iron absorption from the diet increases and iron is released from hepatic and reticuloendothelial stores into the circulating iron pool. The “inflammatory regulator” is responsible for the withdrawal of iron to create a hostile environment to invading pathogens (Andrews, 1999; Hentze et al., 2004). Duodenal iron absorption is decreased and iron from senescent erythrocytes is withheld from recirculation into the transferrin pool by tissue macrophages. This generates a hypoferremic environment depriving pathogens of iron essential for their survival (Luft, 2004).

What is the regulatory effector underlying systemic iron homeostasis? Hepcidin, a small peptide hormone secreted predominantly by the liver, is the key regulator in iron absorption in response to dietary iron, iron stores, anemia/hypoxia and inflammation (Andrews, 1999; Andrews, 2004; Hentze et al., 2004).

## Hepcidin, the Iron Regulatory Hormone

Hepcidin was first identified as a 20-25 amino acid antimicrobial peptide in urine (Park et al., 2001) and plasma (Krause et al., 2000). In parallel, mRNA for mouse *Hamp*, the gene encoding hepcidin, was found to be increased in livers of mice fed a high iron diet (Pigeon et al., 2001), providing the first link to iron metabolism. Furthermore, evidence from transgenic mouse models indicates that hepcidin is the predominant negative regulator of iron absorption. *Hamp* mutant mice develop a disease called hereditary hemochromatosis (see below), characterized by progressive iron deposition in various organs (Nicolas et al., 2001). In contrast, mice overexpressing hepcidin under the control of a liver-specific promoter were born with lethal iron deficiency anemia (Nicolas et al., 2002a). Confirmation of the essential role of hepcidin in human iron metabolism came from two families suffering from juvenile hereditary hemochromatosis whose affected members were found to be homozygous for disruptive mutations in the hepcidin gene, *Hamp* (Roetto et al., 2003).

In humans, hepcidin is detectable in urine where it is increased during transfusion-induced iron overload, infections, and inflammatory states (Nemeth et al., 2003). Mice subjected to hypoxia or hemolytic anemia showed decreased hepatic *Hamp* mRNA compared to controls (Nicolas et al., 2002b). *Hamp* mRNA levels are increased in mice injected with the inflammatory agents bacterial lipopolysaccharide (LPS) or turpentine (Pigeon et al., 2001; Nicolas et al., 2002b) as well as in fish infected with pathogenic bacteria (Shike et al., 2002). Future studies will be required to elucidate the molecular circuitry that controls *Hamp* expression in response to iron, inflammation and hypoxia/anemia.

How does hepcidin fulfill its function? In the last two years, several research groups have observed an inverse relation between hepcidin and ferroportin mRNA and protein levels (Frazer et al., 2002; Yang et al., 2002; Mok et al., 2004; Yeh et al., 2004). This proposed interaction was recently confirmed by Nemeth et al. (Nemeth et al., 2004b) who showed in cell culture experiments that hepcidin binds to ferroportin on the cell surface, and induces its internalization and degradation. Since ferroportin is an iron exporter expressed by cells which release iron into the plasma like enterocytes, macrophages, hepatocytes and placental cells, its posttranslational regulation by hepcidin may complete a homeostatic loop: excess iron in the serum upregulates hepcidin, decreases ferroportin, and consequently decreases iron levels. The increase in *Hamp* mRNA which accompanies the decrease of *ferroportin* mRNA is most

likely not directly related, but rather the result of changes in binding activity of IRPs due to fluctuating iron levels, destabilizing *ferroportin* mRNA by binding to its 5' IRE.

## Iron Overload Diseases – Hereditary Hemochromatosis

There are several distinct iron-overload disorders that produce similar clinical symptoms, and causative mutations have been identified for some of them (Andrews, 2000b). The best understood iron overload disease is hereditary hemochromatosis, characterized by a hyperabsorption of iron, although the body iron stores are full (Andrews, 2000a; Beutler et al., 2003; Brissot et al., 2004; Pietrangelo, 2004). As a result various parenchymal tissues, mainly liver, pancreas, and heart, progressively accumulate iron. The main clinical features of this autosomal recessive iron overload disease are cirrhosis, cardiomyopathy, diabetes, and hypogonadism. In the past therapeutic phlebotomy (deliberate removal of venous blood) to reduce body iron levels was the only treatment for patients suffering from hereditary hemochromatosis (Beutler et al., 2003). Recently, iron chelators have been made available which bind iron and allow it to be excreted in urine and faeces (Beutler et al., 2003).

Four subclasses of hereditary hemochromatosis have been identified, each caused by disruption of a different protein (summarized in Figure 18) (Pietrangelo, 2004). The symptoms are very similar but their time of onset and severity varies. Type 1 and type 3 are caused by mutation of *HFE* or *transferrin receptor 2* respectively, and induce a mild, late onset form of hereditary hemochromatosis. Types 2A and 2B, also called juvenile hereditary hemochromatosis, are caused by mutations of *Hamp* or *HFE2* respectively, and result in a severe, early onset form of this disease, which is potentially lethal.

Clinical studies, as well as analysis of mutant animals, especially on *HFE* mutants, have lead to the conclusion that hepcidin is the major regulator of iron absorption (Andrews, 2000b; Pietrangelo, 2004). All subtypes of hereditary hemochromatosis show a reduction in hepcidin levels, as demonstrated by both patient studies and mutant mice analysis (Ahmad et al., 2002; Bridle et al., 2003; Papanikolaou et al., 2004; Kawabata et al., 2005; Nemeth et al., 2005). This implies that the hyperabsorption of iron may be due to failure to upregulate hepcidin upon high iron levels. Reduced hepcidin results in decreased ferroportin

Feature	<i>HFE</i> -Related Hereditary Hemochromatosis	Juvenile Hereditary Hemochromatosis		<i>TfR2</i> -Related Hereditary Hemochromatosis
	Type 1	Type 2, subtype A	Type 2, subtype B	Type 3
OMIM classification	Type 1	Type 2, subtype A	Type 2, subtype B	Type 3
Implicated gene and its chromosomal location	<i>HFE</i> , 6p21.3	<i>HJV</i> (originally called <i>HFE2</i> ), 1q21	<i>HAMP</i> , 19q13.1	<i>TfR2</i> , 7q22
Gene product name	HFE	Hemojuvelin	Hepcidin	Transferrin receptor 2
Known or postulated functions	Interaction with transferrin receptor 1, probably facilitating uptake of transferrin bound iron; possibly modulation of hepcidin expression	Unknown; possibly modulation of hepcidin expression	Down-regulation of iron release by enterocytes, macrophages, or placental cells	Possibly uptake of iron by hepatocytes
Pattern of inheritance	Autosomal recessive	Autosomal recessive	Autosomal recessive	Autosomal recessive
Potential for organ damage	Variable	High	High	Variable
Decade of onset of symptomatic organ disease	4th or 5th	2nd or 3rd	2nd or 3rd	4th or 5th

**Figure 18. Comparative Overview of Primary Iron-Overload Disorders Classified as Hereditary Hemochromatosis.** (after Pietrangelo, 2004)

internalization and degradation, causing more iron release by enterocytes and macrophages. The signaling mechanism by which hepcidin expression is regulated is currently unknown.

## **Aim of the Following Study (Chapter 2.2)**

Recently, mutation of a gene called *HFE2* on chromosome 1q has been linked by positional cloning to type 2B juvenile hereditary hemochromatosis in humans (Papanikolaou et al., 2004). The murine ortholog of human *HFE2* is *mRGMc*, a member of the GPI-anchored RGM protein family (Niederkofler et al., 2004). In the following study (Chapter 2.2) we show the functional characterization of mRGMc. We provide evidence that *mRGMc* mutant mice mimic the iron overload phenotype of human juvenile hereditary hemochromatosis and show a pronounced defect in the upregulation of *Hamp* upon increased iron loading. In contrast, *Hamp* remains inducible in these animals via the inflammatory pathway.

Furthermore, we identify mRGMc as the key component to resolve the conflict of dietary iron requirements of the body during hypoferremia induced by inflammation. Upon inflammation iron levels drop as a protection against iron dependent pathogens. This is achieved by upregulation of hepcidin, resulting in decreased intestinal iron absorption and increased iron retention by tissue macrophages, leaving the body in a transient hypoferremic state (Luft, 2004). To prevent the body from downregulating hepcidin, due to its dietary iron needs, an overriding mechanism is required. Here we demonstrate that the downregulation of *mRGMc* acts as a switch to suppress the iron-sensing pathway during inflammatory response, and provide an explanation of how the two conflicting pathways, dietary iron-sensing and inflammation, interact at the molecular level.

## 2.2 *mRGMc* Acts as a Switch to Suppress Dietary Iron-Sensing during Inflammatory Response

Vera Niederkofler<sup>\*</sup>, Rishard Salie<sup>\*</sup> & Silvia Arber (submitted Nature Genetics, 2005)

### Abstract

Iron homeostasis is controlled systemically by several upstream regulatory pathways, all of which converge on the regulation of *Hamp*, and its encoded peptide hepcidin (Nicolas et al., 2002b; Ganz, 2003; Andrews, 2004). In turn, hepcidin reduces cellular iron uptake by binding to the iron transporter ferroportin and inducing its internalization (Nemeth et al., 2004b). Normal iron balance is subverted during inflammation when hepcidin levels are elevated to create a transient hypoferremic environment inhibitory to pathogenic growth (Luft, 2004). It remains unclear however whether inflammatory and dietary iron-sensing pathways intersect or act in parallel to regulate hepcidin expression. Recently, human mutations in the GPI-anchored protein RGMc/HFE2/HJV have been shown to cause juvenile hemochromatosis (Papanikolaou et al., 2004), a severe iron overload disease (Beutler et al., 2003; Brissot et al., 2004; Hentze et al., 2004; Pietrangelo, 2004). Here we show that *mRGMc* mutant mice exhibit a dramatic decrease in hepatic *Hamp* expression and show iron overload, yet retain *Hamp* inducibility via the inflammatory pathway. Our findings define a key role for *mRGMc* in the normal iron-sensing pathway and also reveal how this homeostatic pathway is uncoupled during inflammation, through the coordinate extinction of *mRGMc* and activation of *Hamp* expression.

<sup>\*</sup> equal contribution

## Results and Discussion

The *RGM* gene family is comprised of three members (*RGMa*, *RGMb* and *RGMc*), the function of which has mainly been studied in the nervous system where *RGMa* has been implicated in axon guidance and neural tube closure (Monnier et al., 2002; Niederkofler et al., 2004). The recent genetic linkage of *RGMc* to the iron overload disease juvenile hemochromatosis in humans (Papanikolaou et al., 2004) has opened the way to elucidate the function of *RGMc* in iron homeostasis under normal physiological conditions and in disease by use of mouse genetics. We therefore generated *mRGMc* mutant mice, coordinately expressing LacZ from the *mRGMc* locus (Figure 19a, b). Previous work has shown that the strongest expression of *mRGMc* in mice is found in skeletal muscles, but lower expression was also detected in the liver (Niederkofler et al., 2004). Mice homozygous for the mutated *mRGMc* allele showed a complete absence of *mRGMc* mRNA in all tissues analyzed including skeletal muscles providing evidence for a complete null mutation (Figure 19c; data not shown). To determine the exact site of expression of *mRGMc* in the liver, we processed vibratome sections of adult liver from *mRGMc*<sup>+/-</sup> mice for the presence of LacZ activity (Figure 19e). Interestingly, we found a patterned distribution of *mRGMc* expression in the liver whereas skeletal muscles were stained uniformly (Figure 19e; data not shown). To determine the identity of these cells, we analyzed LacZ expression on thin sections and found labeled cells surrounding portal tracts but not central veins (Figure 19f, g). At high magnification, and as described to occur frequently in hepatocytes (Seglen, 1997; Guidotti et al., 2003), LacZ<sup>+</sup> cells often contained two nuclei (Figure 19g). In addition, double labeling immunohistochemistry with an antibody to HNF4 $\alpha$ , a transcription factor expressed in hepatocytes (Parviz et al., 2003), confirmed the hepatocytic identity of these LacZ<sup>+</sup> cells (Figure 19h-k). In contrast, no overlap in the expression of LacZ with several other cell types of the liver was seen (data not shown). Together, these findings indicate that *mRGMc* expression in the liver is restricted to hepatocytes surrounding the portal tracts.

To assess the consequences of *mRGMc* mutation for iron homeostasis in various organs, we used both histological staining procedures as well as quantitative determination of iron content. At 2.5 months of age, a severe increase in iron content was detected in liver, pancreas and heart of *mRGMc* mutant mice (Figure 20a-d; Figure 21a-d). In contrast, we found a reduction in iron accumulation in reticuloendothelial macrophages residing in the red pulp of the spleen (Figure 20e-h). These results were corroborated by quantitative

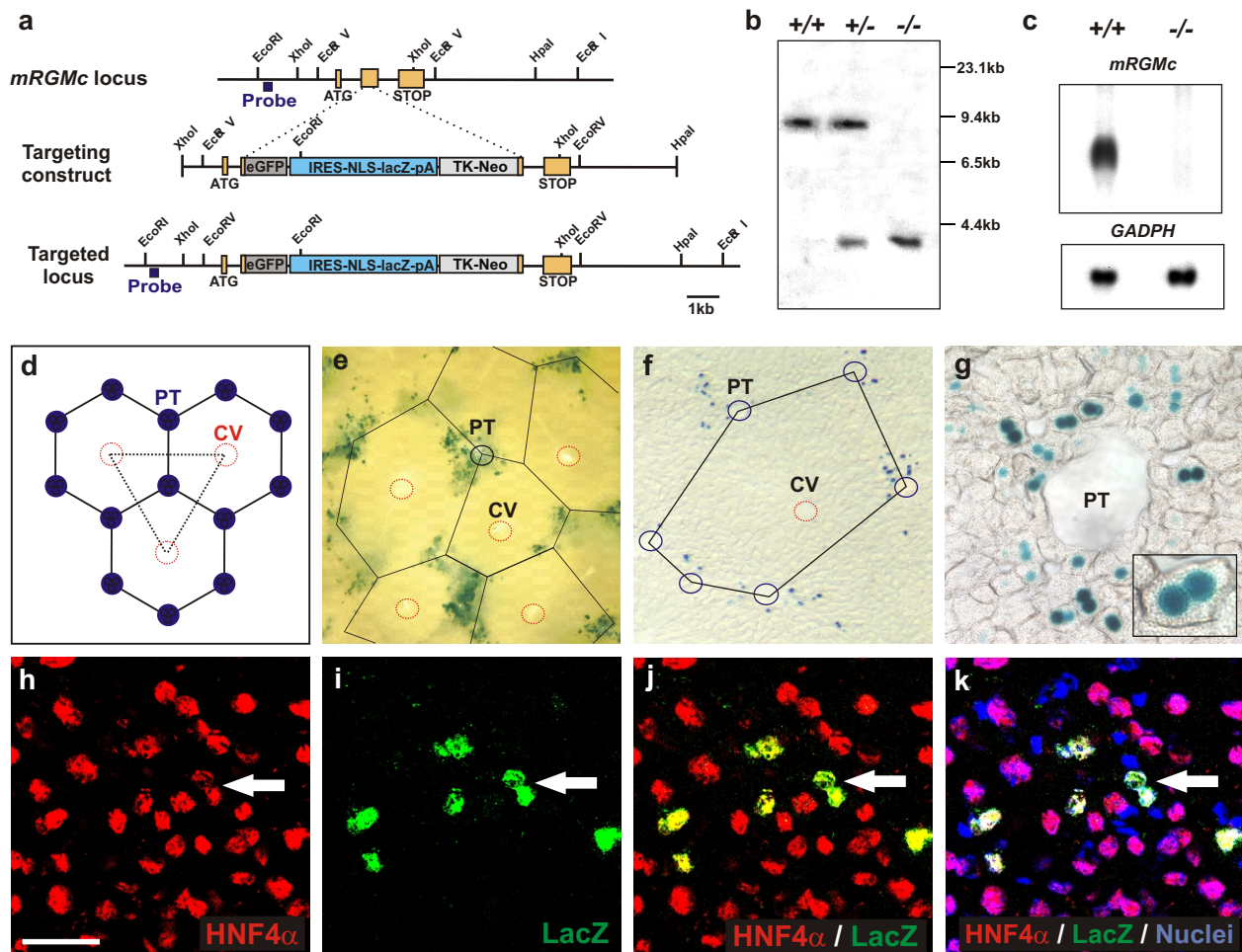


**Figure 19. *mRGMc* Expression in Periportal Hepatocytes.**

(a) Targeting strategy used for homologous recombination in ES cells to eliminate *mRGMc* gene function. The *mRGMc* locus contains three coding exons (yellow; amino-terminal methionine: ATG; carboxy-terminal stop codon: STOP) and a XhoI/HpaI genomic fragment was used to generate the targeting construct. eGFP (dark grey) followed by an IRES-NLS-LacZ-pA (blue) and TK-Neo (light grey) cassette was integrated in frame into the second coding exon of *mRGMc*. The probe used for genomic Southern analysis is indicated in blue. Integrated cassette is not drawn to scale.

(b) Genomic Southern of *mRGMc*<sup>+/+</sup>, *mRGMc*<sup>+/-</sup> and *mRGMc*<sup>-/-</sup> genomic DNA using the probe indicated in (a).

(c) Northern blot analysis of total RNA isolated from P21 hindlimb muscles of *mRGMc*<sup>+/+</sup> and *mRGMc*<sup>-/-</sup> mice probed for the expression of *mRGMc* (top) and *GADPH* (bottom).

(d) Schematic drawing depicting the territories of liver lobules. Portal tracts (PT) are indicated in blue, central veins (CV) are shown in red. Note that solid lines outline the hexagonally shaped hepatic lobule with PTs at the corners.

(e-g) Detection of enzymatic LacZ activity in liver from 3 months old *mRGMc*<sup>+/-</sup> mice analyzed on vibratome (e) or cryostat (f, g) sections. Red circles indicate central vein (CV), blue circles indicate portal tract (PT). Inset in (g) depicts high magnification of individual binuclear hepatocyte expressing LacZ.

(h-k) Immunohistochemical detection of HNF4α (h, j, k: red), LacZ (i, j, k: green), and SYTOX green (Nuclei; k: blue) on liver from 3 months old *mRGMc*<sup>+/-</sup> mice. Arrow points to binuclear *mRGMc* expressing hepatocyte.

Scale bar: (e)=530μm, (f)=260μm, (g)=70μm, (inset to g)=30μm, (h-k)=40μm.



measurements of iron content at the same ages (Figure 20i). A time course to determine the iron content in various tissues at different developmental stages postnatally showed a rapid and permanent increase in iron accumulation, reaching plateau levels by four months of age (Figure 20j; Figure 21e). The first signs of hepatic iron overload were detected already at postnatal day 30 (Figure 20j), consistent with the early onset of iron accumulation in patients suffering from juvenile hemochromatosis (Pietrangelo, 2004).

We next investigated the level of hepatic *Hamp* expression in *mRGMc* mutant mice by Northern blot analysis and *in situ* hybridization experiments. We found that it was virtually undetectable in adult *mRGMc* mutant mice when compared to wild-type littermates ( $\leq 0.3\%$  of wild-type; Figure 22a, b; Figure 23a). *Hamp* expression in the liver of wild-type mice occurs in two waves: an early postnatal (P0-P6) spike which declines rapidly is followed by a second increase during the third postnatal week remaining through to adulthood (Courselaud et al., 2002) (Figure 22c). In contrast to the dynamic expression of *Hamp*, *mRGMc* expression in the liver was already detected at E13.5 and reached a steady level by late embryonic stages (Figure 22c). Interestingly, hepatic *Hamp* expression in *mRGMc* mutant mice was reduced throughout both the early postnatal and adult expression phases (Figure 22a). These findings point to an essential role for *mRGMc* in iron-sensing upstream of hepcidin expression throughout life. Moreover, the massive reduction in hepcidin provides a molecular explanation for the continued iron accumulation and lack of effective regulatory mechanisms to decrease iron uptake in *mRGMc* mutant mice.

Does the lack of *Hamp* expression in *mRGMc* mutant mice represent an absolute inability to induce hepatic *Hamp* expression, or is it possible to bypass this deficiency by stimulation of the inflammatory pathway (Pigeon et al., 2001; Nemeth et al., 2004a)? We found that induction of acute inflammation by lipopolysaccharide (LPS) injection led to rapid and robust upregulation of *Hamp* in *mRGMc* mutant mice when compared to levels in sham injected mutant animals (Figure 23a). Furthermore, injections of either proinflammatory cytokine IL-6 or TNF $\alpha$ , both known to be downstream products of LPS injection (Zetterstrom et al., 1998), were sufficient to mimic the effect of LPS, albeit to a lower extent (Figure 23a). We also assessed whether, in *mRGMc* mutant mice, inflammation-mediated upregulation of *Hamp* expression was capable of effectively eliciting appropriate downstream responses. *Ferroportin* has been shown to be transcriptionally downregulated by high hepcidin levels

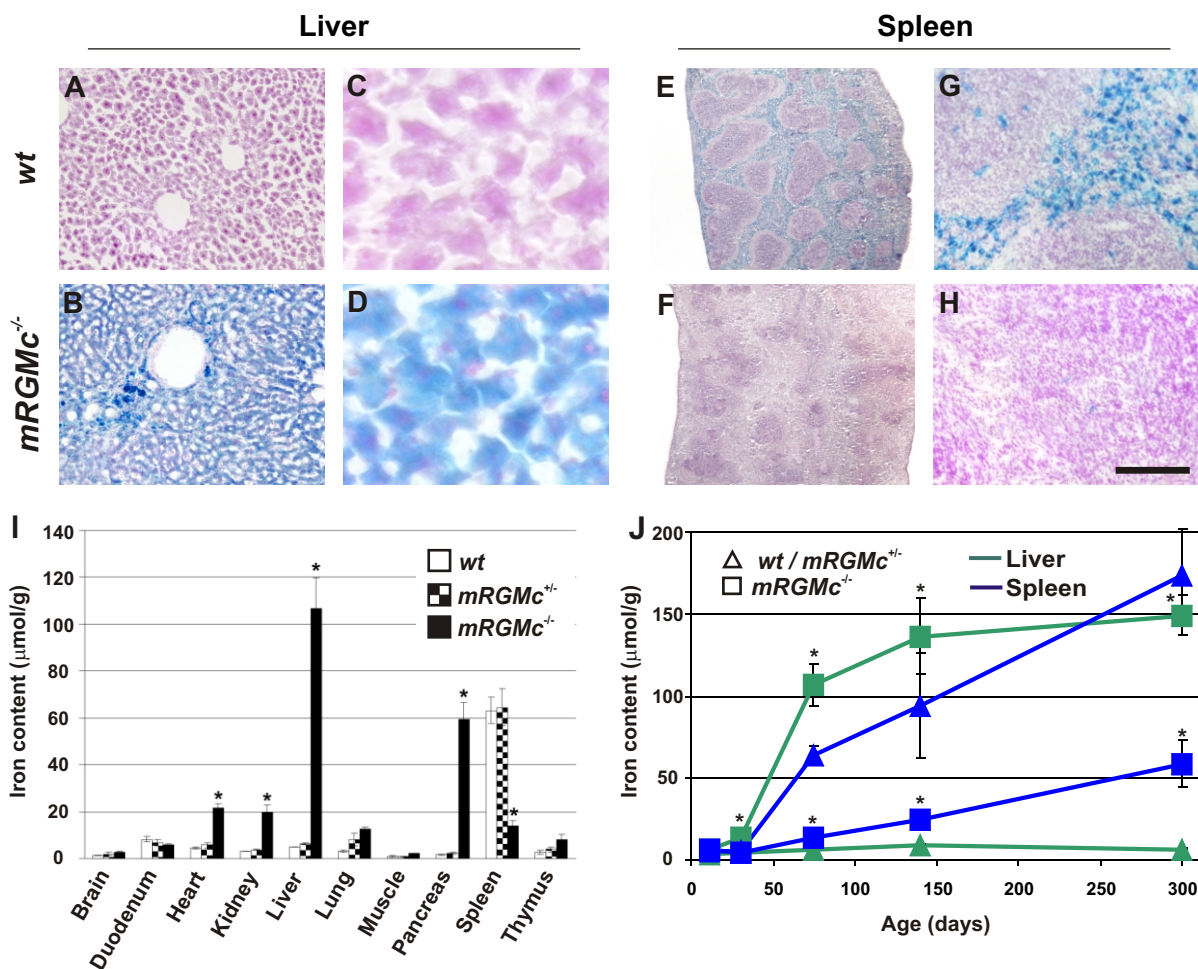


**Figure 20. Iron Accumulation in *mRGMc* Mutant Mice.**

(a-h) Histological detection of iron content on cryostat sections of liver (a-d) and spleen (e-h) of *wild-type* (a, c, e, g) and *mRGMc*<sup>-/-</sup> (b, d, f, h) mice.

(i) Quantitative determination of iron content ( $\mu\text{mol/g}$  dry weight) in various organs (brain, duodenum, heart, kidney, liver, lung, skeletal muscle, pancreas, spleen and thymus) of 2.5 months old *wild-type* (white), *mRGMc*<sup>+/-</sup> (checkerboard), and *mRGMc*<sup>-/-</sup> (black) mice (n=5 for each group). Asterisks indicate significant changes ( $P < 0.05$ ) in *mRGMc*<sup>-/-</sup> mice as compared to *wild-type* littermates.

(j) Time course (from P12 to P300; indicating days after birth) of iron content ( $\mu\text{mol/g}$  dry weight) determined in *mRGMc*<sup>-/-</sup> mice (squares) compared to pooled *wild-type* and *mRGMc*<sup>+/-</sup> mice (triangles). Liver (green) and spleen (blue) are depicted in the graph. At least 3 animals per time point and genotype were included in the analysis. Asterisks indicate significant changes ( $P < 0.05$ ) in *mRGMc*<sup>-/-</sup> mice as compared to pooled *wild-type* and *mRGMc*<sup>+/-</sup> littermates.

Scale bar: (a, b)=270 $\mu\text{m}$ , (c, d)=45 $\mu\text{m}$ , (e, f)=1.2mm, (g, h)=100 $\mu\text{m}$ .

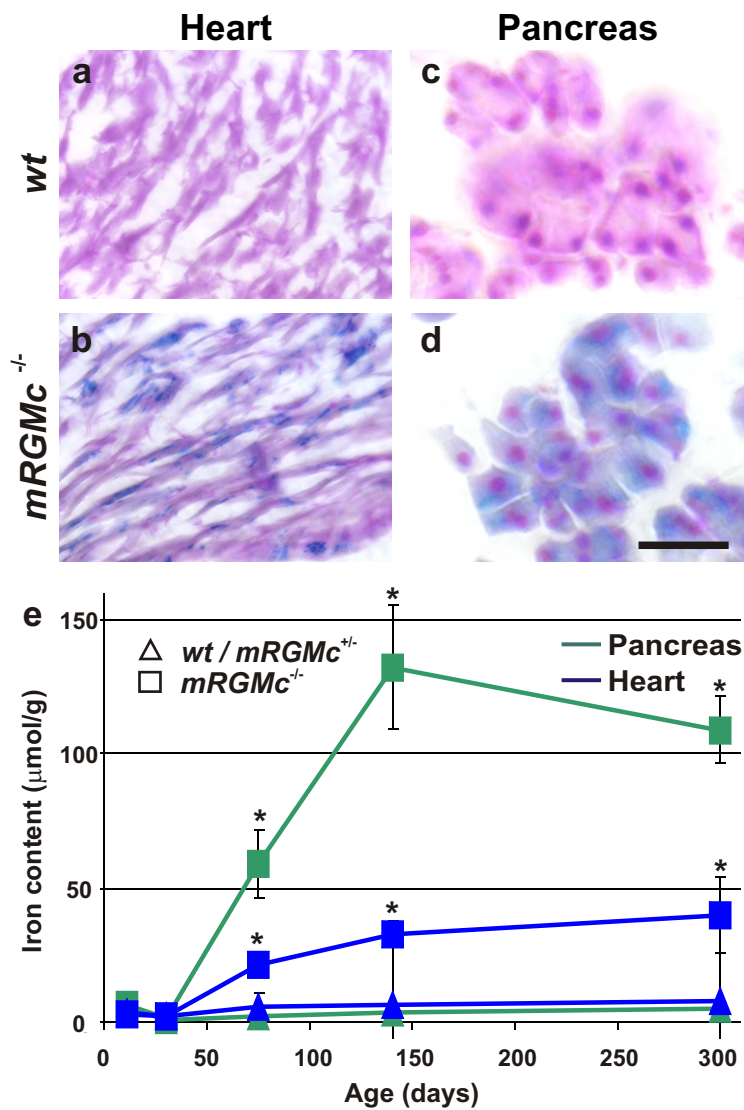


**Figure 21. Iron Accumulation in *mRGMc* Mutant Mice.**

(a-d) Histological detection of iron content on cryostat sections of heart (a, b) and pancreas (c, d) of *wild-type* (a, c) and *mRGMc<sup>-/-</sup>* (b, d) mice.

(e) Time course (from P12 to P300; indicating days after birth) of iron content ( $\mu\text{mol/g}$  dry weight) determined in *mRGMc<sup>-/-</sup>* mice (squares) compared to pooled *wild-type* and *mRGMc<sup>+/-</sup>* mice (triangles). Pancreas (green) and heart (blue) are depicted in the graph. At least 3 animals per time point and genotype were included in the analysis. Asterisks indicate significant changes ( $P < 0.05$ ) in *mRGMc<sup>-/-</sup>* mice as compared to pooled *wild-type* and *mRGMc<sup>+/-</sup>* littermates.

Scale bar: (a-d)=70 $\mu\text{m}$ , (c, d)=45 $\mu\text{m}$ .

(Yeh et al., 2004). Consistent with the observed lack of *Hamp* expression, *ferroportin* is highly expressed in untreated or sham-injected *mRGMc* mutant mice (Figure 23b; data not shown). In contrast, upon LPS injection (associated with *Hamp* induction), *ferroportin* is significantly reduced in *mRGMc* mutant mice as well as in wild-type mice (Figure 23b), indicating the presence of intact downstream responses to hepcidin in *mRGMc* mutant mice. These findings show that the inflammatory pathway can efficiently bypass a requirement for *mRGMc* in the induction of hepatic *Hamp* expression and assign a role to *mRGMc* specifically in the iron-sensing pathway upstream of hepcidin regulation.

The low serum iron concentration achieved during an inflammatory response should be perceived as hypoferremia by the dietary iron-sensing pathway and rapidly counteracted; however this is not the case. This raises the question of how these pathways can be prevented from conflicting at the molecular level. Interestingly, we found that *mRGMc* expression in the liver of wild-type mice was strongly downregulated upon induction of acute inflammation by LPS (Krijt et al., 2004), IL-6 or TNF $\alpha$  injection (Figure 23c). In contrast, no decrease in the expression of *mRGMc* expression in skeletal muscles was detected under these conditions (Figure 23d). To determine whether this effect is specific for *mRGMc* or whether other genes involved in iron metabolism (Beutler et al., 2003; Brissot et al., 2004; Hentze et al., 2004; Pietrangelo, 2004) are regulated in a similar manner, we assessed their level of expression before and after induction of inflammation. Surprisingly, we found that the expression levels of several genes analyzed in the liver (*Hfe*, *Tfr2*,  $\beta$ 2-microglobulin, *ceruloplasmin*) were unchanged following LPS injection (Figure 24) (Beutler et al., 2003; Brissot et al., 2004; Hentze et al., 2004; Pietrangelo, 2004). We conclude that *mRGMc* not only represents an essential element of the iron-sensing pathway but also is the key component mediating selective shutdown of this pathway upon inflammation.

This study provides evidence that the expression of *mRGMc* in the liver is restricted to a population of periportal hepatocytes (Fig. 19d-k). In contrast, *Hfe*, *Tfr2* and  $\beta$ 2-microglobulin have been described to be expressed broadly (Kawabata et al., 2001; Chorney et al., 2003; Zhang et al., 2004). Our results therefore suggest that the cellular source assigned to iron-sensing in the liver may be periportal hepatocytes, marked by the expression of *mRGMc*. These hepatocytes are located close to the portal veins which deliver blood to the liver from the gut and are thus in a prime position to detect the iron content of blood coming

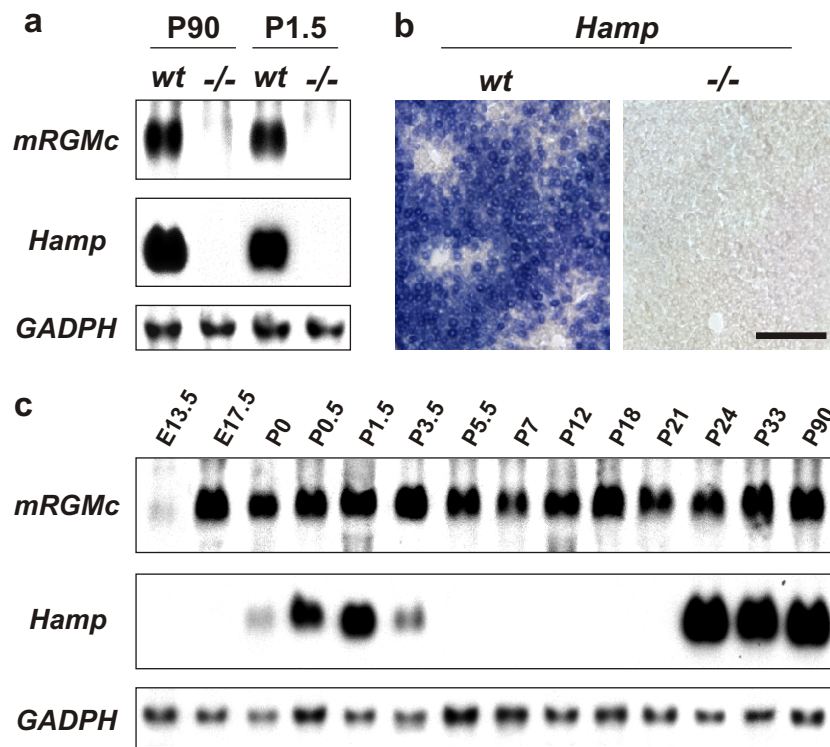


**Figure 22. Lack of *Hamp* Expression in *mRGMc* Mutant Mice.**

(a) Northern blot analysis of total RNA isolated from adult (P90) or P1.5 liver of *wild-type* and *mRGMc*<sup>-/-</sup> mice probed for the expression of *mRGMc*, *Hamp* and *GADPH*.

(b) *In situ* hybridization on cryostat sections of liver isolated from adult *wild-type* and *mRGMc*<sup>-/-</sup> mice probed for the expression of *Hamp*.

(c) Developmental time course (ages as indicated from E13.5 to P90) of *mRGMc*, *Hamp*, *GADPH* expression levels determined by Northern blot analysis on total RNA isolated from liver.

Scale bar: (b)= 100μm.

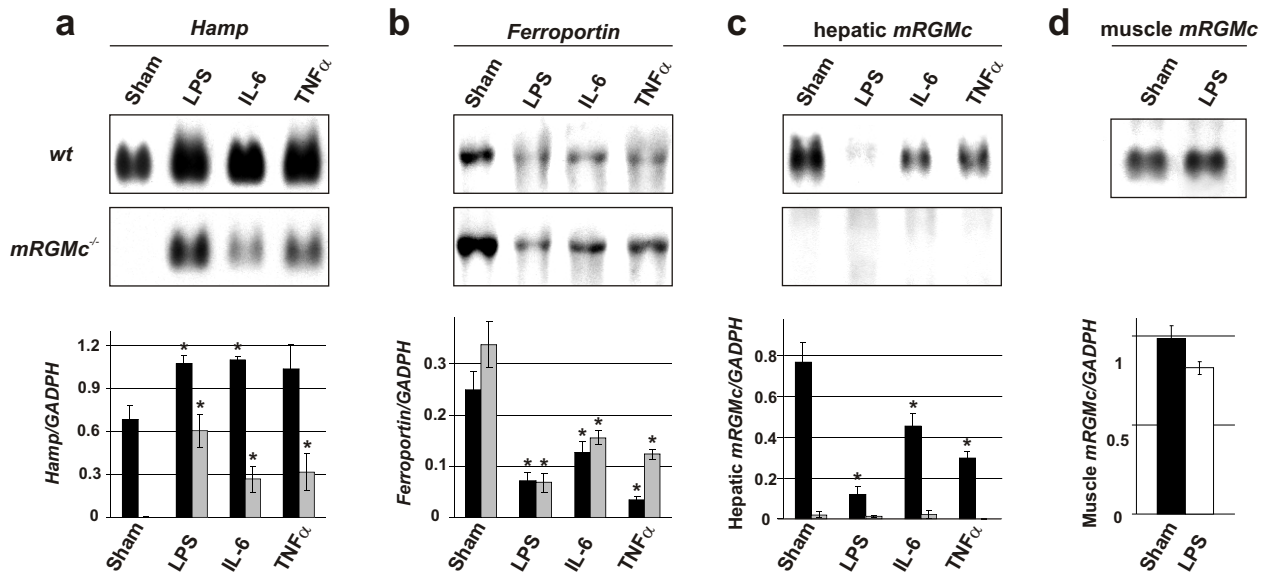


**Figure 23. Selective Suppression of *mRGMc* during Inflammatory Response.**

(a-c) Northern blot analysis of *Hamp* (a), *Ferroportin* (b) and *mRGMc* (c) expression on total RNA isolated from liver of *wild-type* or *mRGMc* mutant mice. Before isolation of total RNA, mice were injected intraperitoneally with PBS (sham), LPS, IL-6, or TNF $\alpha$ . At least three animals per experimental condition were analyzed and one representative example is shown. Quantification of expression levels was performed by normalization of each sample to *GADPH* expression probed sequentially on the same blots (data not shown). Histograms depict *wild-type* mice in black, *mRGMc* mutant mice in grey. Asterisks indicate significant changes ( $P < 0.05$ ) in animals treated with LPS, IL-6 or TNF $\alpha$  as compared to sham injected animals of the same genotype.

(d) Northern blot analysis of *mRGMc* expression on total RNA isolated from skeletal muscle of *wild-type* mice after sham or LPS injection. Quantification was performed as described in (a-c). Histogram depicts sham injected mice in black, LPS injected mice in white.

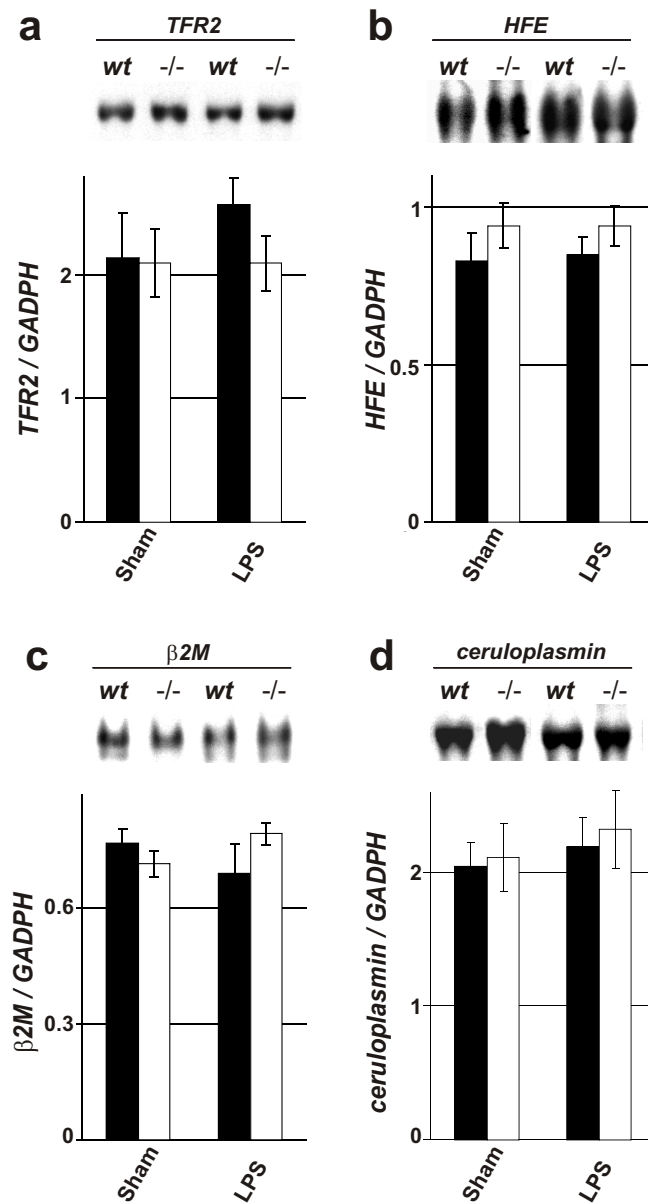


**Figure 24. LPS Injection Does Not Influence Expression of *TFR2*, *HFE*,  $\beta 2$ -microglobulin and *ceruloplasmin*.**

(a-d) Northern blot analysis of *TFR2*, *HFE*,  $\beta 2$ -microglobulin, *ceruloplasmin* and *GADPH* expression on total RNA isolated from liver of *wild-type* or *mRGMc* mutant mice. 6 hours before isolation of RNA, mice were injected intraperitoneally with PBS (sham) or LPS. At least four animals per experimental condition were analyzed and one representative example is shown. Quantification of expression levels was performed by normalization of each sample to *GADPH* expression probed sequentially on the same blots. Histograms depict *wild-type* mice in black, *mRGMc* mutant mice in white.

directly from the digestive tract. Since *Hamp* expression is not restricted to periportal hepatocytes (Figure 22b), this finding excludes a direct molecular link from mRGMc to the intracellular induction of *Hamp* expression. Instead, it suggests that intermediate, secreted factors in the liver might play a role in *Hamp* regulation associated with dietary iron-sensing.

The complex regulatory network underlying systemic regulation of iron homeostasis is tuned to respond to different stimuli by activation of distinct molecular pathways all of which funnel into the regulation of hepatic hepcidin expression (Figure 25a, b). To prevent interference of individual pathways, efficient and fast cross-regulatory interactions exist. This study provides evidence that the inflammatory pathway acts in parallel to the dietary iron-sensing pathway and controls its deactivation by rapid and selective extinction of *mRGMc* in the liver (Figure 25b). While it is still controversial whether acute inflammation influences *Hamp* expression in *Hfe* deficient mice (Lee et al., 2004; Roy et al., 2004), addition of LPS or IL-6 to cultured hepatocytes from *Tfr2* mutant mice has been shown to induce *Hamp* expression (Kawabata et al., 2005). Interestingly, we found that neither *Tfr2* nor *Hfe* expression levels are affected upon inflammation, thus assigning a unique role to *mRGMc* as a regulatory target in this process. The findings described in this study delineate a molecular and cellular mechanism for the selective suppression of the primary iron regulatory pathway, as well as the choice of an alternative pathway during inflammation, both of which converge on the downstream expression of the key regulatory peptide hepcidin. As such, they also provide important insights for future therapeutic strategies to treat diseases affecting iron metabolism.



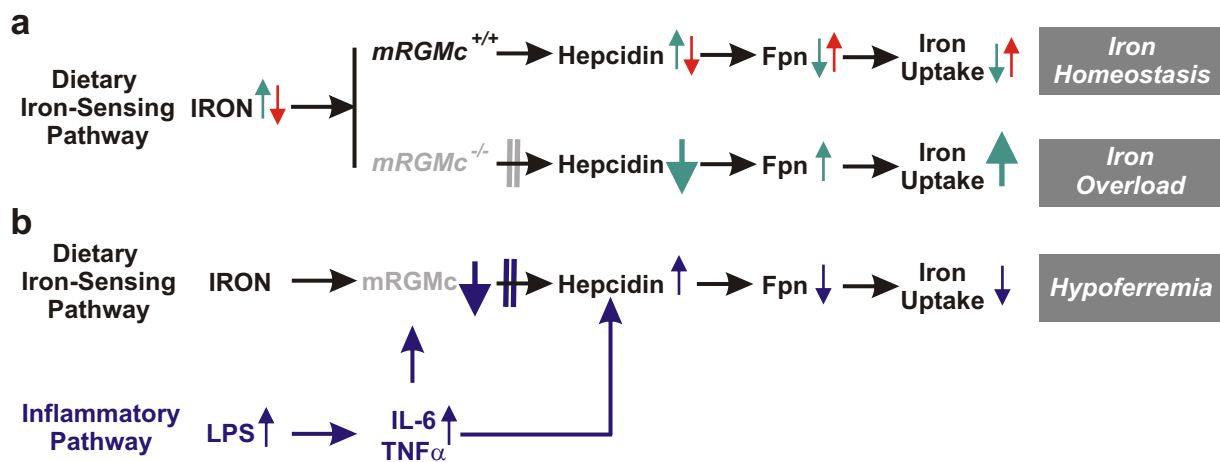


**Figure 25. *mRGMc* in the Iron-Sensing Pathway.**

(a) Schematic representation of dietary iron-sensing pathway in *wild-type* and *mRGMc* mutant mice. In *wild-type* mice, green arrows indicate responses in the presence of high iron, red arrows show responses in the presence of low iron. Balanced regulation of this pathway adjusts iron levels to the needs of the healthy organism (follow green or red arrows from left to right). In *mRGMc* mutant mice, iron-sensing is defective due to the absence of *mRGMc* (indicated by solid vertical double line). Despite high iron, this leads to an essentially complete absence of hepcidin expression, iron overload and hemochromatosis (green arrows in *mRGMc* mutant). Abbreviation: Fpn=Ferroportin.

(b) Schematic representation of the impact of acute inflammation on the iron-sensing pathway (blue arrows). Acute phase cytokines IL-6 and TNF $\alpha$  act to coordinately downregulate *mRGMc* expression in the liver while simultaneously inducing hepcidin expression. The reduction of *mRGMc* results in a blockade of the dietary iron-sensing pathway (indicated by solid vertical double line). This mechanism efficiently suppresses the iron-sensing pathway during inflammatory response resulting in a low iron serum concentration inhibiting pathogenic growth. Abbreviation: Fpn=Ferroportin.

## Material and Methods

### Generation and Analysis of *mRGMc* Mutant Mice

A mouse genomic library was screened using an *mRGMc*-specific probe. The second coding exon of *mRGMc* was disrupted by inserting a cassette containing an *eGFP* in frame with the endogenous ATG, followed by an *IRE5-NLS-LacZ-pA* and a thymidine kinase (TK)-neomycin cassette using homologous recombination in embryonic stem (ES) cells (targeting frequency, ~1:100). ES cell recombinants were screened by genomic Southern blot (EcoRI digest; 5' probe (~300bp): oligonucleotides (A) 5'-ctc agt gta tta tgt gta gaa-3' and (B) 5'-aat tcc agg aac gtt ggt ggc-3'; Fig. 1a). The identification of *mRGMc* mutant mice was performed by genomic Southern blotting (Fig. 1b) and PCR ([1] 5'-cca gtg caa gat cct ccg ctg c-3'; [2] 5'-tcc gga tgg tgg tag cgt tgg c-3').

### Northern Blot Analysis and Histology

Northern blot analysis and isolation of total RNA was performed as previously described (Niederkofler et al., 2004), using digoxigenin-labeled probes directed against mouse *mRGMc* (Niederkofler et al., 2004), *Hamp* (BC021587), *Tfr2* (BC013654),  $\beta$ 2-microglobulin (BI691504), *HFE* (AA255260), *Ferroportin* (BQ928442) and *GADPH* (gift from P. Matthias, FMI). Signals were quantified using FluoView500 (Olympus) and normalized to the expression level of *GADPH*. Average values were determined from at least 3 independent experiments for each data point. Cryostat sections (16 $\mu$ m) were processed for immunohistochemistry as described previously (Arber et al., 1999), using fluorophore-conjugated secondary antibodies (1:1000; Molecular Probes, Eugene, OR). Primary antibodies used in this study were rabbit anti-LacZ (Arber et al., 1999) and goat anti-HNF4 $\alpha$  (Santa Cruz). Nuclei were detected using SYTOX Green (Molecular Probes, Eugene, OR). Vibratome sections (100 $\mu$ m) were cut on a vibratome (Leica). Detection of LacZ enzymatic activity and *in situ* hybridization experiments were performed as previously described (Arber et al., 1999; Niederkofler et al., 2004).

### Iron Quantification, Induction of Inflammatory Response and Statistical Analysis

All experiments were performed using male mice and control littermates were processed in parallel for each experiment. Iron was detected on cryostat sections using the Accustain<sup>TM</sup> Iron Stain Kit (Sigma). Non heme-iron in dehydrated tissue was quantified according to a previously described method (Torrance, 1980). LPS (1 $\mu$ g/g body weight; serotype O111:B4;

Sigma), IL-6 (12.5ng/g body weight; R&D Systems) and TNF $\alpha$  (12.5ng/g body weight; R&D Systems) were injected intraperitoneally and organs were isolated for RNA preparation 6 hours after LPS and 4 hours after IL-6 or TNF $\alpha$  injections (Yeh et al., 2004). For statistical analysis, all *P* values were calculated in Microsoft Excel using a two tailed Student's *t*-test.

## REFERENCES

- Ahmad, K. A., Ahmann, J. R., Migas, M. C., Waheed, A., Britton, R. S., Bacon, B. R., Sly, W. S., and Fleming, R. E. (2002). Decreased liver hepcidin expression in the Hfe knockout mouse. *Blood Cells Mol Dis* 29, 361-366.
- Aisen, P., Enns, C., and Wessling-Resnick, M. (2001). Chemistry and biology of eukaryotic iron metabolism. *Int J Biochem Cell Biol* 33, 940-959.
- Andrews, N. C. (1999). Disorders of iron metabolism. *N Engl J Med* 341, 1986-1995.
- Andrews, N. C. (2000a). Inherited iron overload disorders. *Curr Opin Pediatr* 12, 596-602.
- Andrews, N. C. (2000b). Iron homeostasis: insights from genetics and animal models. *Nat Rev Genet* 1, 208-217.
- Andrews, N. C. (2004). Anemia of inflammation: the cytokine-hepcidin link. *J Clin Invest* 113, 1251-1253.
- Arber, S., Han, B., Mendelsohn, M., Smith, M., Jessell, T. M., and Sockanathan, S. (1999). Requirement for the homeobox gene Hb9 in the consolidation of motor neuron identity. *Neuron* 23, 659-674.
- Beutler, E., Hoffbrand, A. V., and Cook, J. D. (2003). Iron deficiency and overload. *Hematology (Am Soc Hematol Educ Program)*, 40-61.
- Bridle, K. R., Frazer, D. M., Wilkins, S. J., Dixon, J. L., Purdie, D. M., Crawford, D. H., Subramaniam, V. N., Powell, L. W., Anderson, G. J., and Ramm, G. A. (2003). Disrupted hepcidin regulation in HFE-associated haemochromatosis and the liver as a regulator of body iron homeostasis. *Lancet* 361, 669-673.
- Brissot, P., Troadec, M. B., and Loreal, O. (2004). The clinical relevance of new insights in iron transport and metabolism. *Curr Hematol Rep* 3, 107-115.

- Cairo, G., and Pietrangelo, A. (2000). Iron regulatory proteins in pathobiology. *Biochem J* 352 Pt 2, 241-250.
- Chorney, M. J., Yoshida, Y., Meyer, P. N., Yoshida, M., and Gerhard, G. S. (2003). The enigmatic role of the hemochromatosis protein (HFE) in iron absorption. *Trends Mol Med* 9, 118-125.
- Courselaud, B., Pigeon, C., Inoue, Y., Inoue, J., Gonzalez, F. J., Leroyer, P., Gilot, D., Boudjema, K., Guguen-Guillouzo, C., Brissot, P., *et al.* (2002). C/EBPalpha regulates hepatic transcription of hepcidin, an antimicrobial peptide and regulator of iron metabolism. Cross-talk between C/EBP pathway and iron metabolism. *J Biol Chem* 277, 41163-41170.
- Finch, C. (1994). Regulators of iron balance in humans. *Blood* 84, 1697-1702.
- Frazer, D. M., Wilkins, S. J., Becker, E. M., Murphy, T. L., Vulpe, C. D., McKie, A. T., and Anderson, G. J. (2003). A rapid decrease in the expression of DMT1 and Dcytb but not Ireg1 or hephaestin explains the mucosal block phenomenon of iron absorption. *Gut* 52, 340-346.
- Frazer, D. M., Wilkins, S. J., Becker, E. M., Vulpe, C. D., McKie, A. T., Trinder, D., and Anderson, G. J. (2002). Hepcidin expression inversely correlates with the expression of duodenal iron transporters and iron absorption in rats. *Gastroenterology* 123, 835-844.
- Ganz, T. (2003). Hepcidin, a key regulator of iron metabolism and mediator of anemia of inflammation. *Blood* 102, 783-788.
- Gavin, M. W., McCarthy, D. M., and Garry, P. J. (1994). Evidence that iron stores regulate iron absorption--a setpoint theory. *Am J Clin Nutr* 59, 1376-1380.
- Guidotti, J. E., Bregerie, O., Robert, A., Debey, P., Brechot, C., and Desdouets, C. (2003). Liver cell polyploidization: a pivotal role for binuclear hepatocytes. *J Biol Chem* 278, 19095-19101.

Gunshin, H., Allerson, C. R., Polycarpou-Schwarz, M., Rofts, A., Rogers, J. T., Kishi, F., Hentze, M. W., Rouault, T. A., Andrews, N. C., and Hediger, M. A. (2001). Iron-dependent regulation of the divalent metal ion transporter. *FEBS Lett* *509*, 309-316.

Hahn, P. F., Bale, W. F., Ross, J. F., Balfour, W. M., and Whipple, G. H. (1943). Radioactive iron absorption by the gastro-intestinal tract: influence of anemia, anoxia and antecedent feeding distribution in growing dogs. *J Exp Med* *78*, 169-88

Hentze, M. W., Muckenthaler, M. U., and Andrews, N. C. (2004). Balancing acts: molecular control of mammalian iron metabolism. *Cell* *117*, 285-297.

Kawabata, H., Fleming, R. E., Gui, D., Moon, S. Y., Saitoh, T., O'Kelly, J., Umehara, Y., Wano, Y., Said, J. W., and Koeffler, H. P. (2005). Expression of hepcidin is down-regulated in TfR2 mutant mice manifesting a phenotype of hereditary hemochromatosis. *Blood* *105*, 376-381.

Kawabata, H., Germain, R. S., Ikezoe, T., Tong, X., Green, E. M., Gombart, A. F., and Koeffler, H. P. (2001). Regulation of expression of murine transferrin receptor 2. *Blood* *98*, 1949-1954.

Krause, A., Neitz, S., Magert, H. J., Schulz, A., Forssmann, W. G., Schulz-Knappe, P., and Adermann, K. (2000). LEAP-1, a novel highly disulfide-bonded human peptide, exhibits antimicrobial activity. *FEBS Lett* *480*, 147-150.

Krijt, J., Vokurka, M., Chang, K. T., and Necas, E. (2004). Expression of Rgmc, the murine ortholog of hemojuvelin gene, is modulated by development and inflammation, but not by iron status or erythropoietin. *Blood* *104*, 4308-4310.

Lee, P., Peng, H., Gelbart, T., and Beutler, E. (2004). The IL-6- and lipopolysaccharide-induced transcription of hepcidin in HFE-, transferrin receptor 2-, and beta 2-microglobulin-deficient hepatocytes. *Proc Natl Acad Sci U S A* *101*, 9263-9265.

Luft, F. C. (2004). Hepcidin comes to the rescue. *J Mol Med* *82*, 345-347.

- McKie, A. T., Marciani, P., Rolfs, A., Brennan, K., Wehr, K., Barrow, D., Miret, S., Bomford, A., Peters, T. J., Farzaneh, F., *et al.* (2000). A novel duodenal iron-regulated transporter, IREG1, implicated in the basolateral transfer of iron to the circulation. *Mol Cell* 5, 299-309.
- Mok, H., Jelinek, J., Pai, S., Cattanaach, B. M., Prchal, J. T., Youssoufian, H., and Schumacher, A. (2004). Disruption of ferroportin 1 regulation causes dynamic alterations in iron homeostasis and erythropoiesis in polycythaemia mice. *Development* 131, 1859-1868.
- Monnier, P. P., Sierra, A., Macchi, P., Deitinghoff, L., Andersen, J. S., Mann, M., Flad, M., Hornberger, M. R., Stahl, B., Bonhoeffer, F., and Mueller, B. K. (2002). RGM is a repulsive guidance molecule for retinal axons. *Nature* 419, 392-395.
- Nemeth, E., Rivera, S., Gabayan, V., Keller, C., Taudorf, S., Pedersen, B. K., and Ganz, T. (2004a). IL-6 mediates hypoferremia of inflammation by inducing the synthesis of the iron regulatory hormone hepcidin. *J Clin Invest* 113, 1271-1276.
- Nemeth, E., Roetto, A., Garozzo, G., Ganz, T., and Camaschella, C. (2005). Hepcidin is decreased in TFR2 hemochromatosis. *Blood* 105, 1803-1806.
- Nemeth, E., Tuttle, M. S., Powelson, J., Vaughn, M. B., Donovan, A., Ward, D. M., Ganz, T., and Kaplan, J. (2004b). Hepcidin regulates cellular iron efflux by binding to ferroportin and inducing its internalization. *Science* 306, 2090-2093.
- Nemeth, E., Valore, E. V., Territo, M., Schiller, G., Lichtenstein, A., and Ganz, T. (2003). Hepcidin, a putative mediator of anemia of inflammation, is a type II acute-phase protein. *Blood* 101, 2461-2463.
- Nicolas, G., Bennoun, M., Devaux, I., Beaumont, C., Grandchamp, B., Kahn, A., and Vaulont, S. (2001). Lack of hepcidin gene expression and severe tissue iron overload in upstream stimulatory factor 2 (USF2) knockout mice. *Proc Natl Acad Sci U S A* 98, 8780-8785.

Nicolas, G., Bennoun, M., Porteu, A., Mativet, S., Beaumont, C., Grandchamp, B., Sirtito, M., Sawadogo, M., Kahn, A., and Vaulont, S. (2002a). Severe iron deficiency anemia in transgenic mice expressing liver hepcidin. *Proc Natl Acad Sci U S A* 99, 4596-4601.

Nicolas, G., Chauvet, C., Viatte, L., Danan, J. L., Bigard, X., Devaux, I., Beaumont, C., Kahn, A., and Vaulont, S. (2002b). The gene encoding the iron regulatory peptide hepcidin is regulated by anemia, hypoxia, and inflammation. *J Clin Invest* 110, 1037-1044.

Niederkofler, V., Salie, R., Sigrist, M., and Arber, S. (2004). Repulsive guidance molecule (RGM) gene function is required for neural tube closure but not retinal topography in the mouse visual system. *J Neurosci* 24, 808-818.

O'Neil-Cutting, M. A., and Crosby, W. H. (1987). Blocking of iron absorption by a preliminary oral dose of iron. *Arch Intern Med* 147, 489-491.

Pantopoulos, K. (2004). Iron metabolism and the IRE/IRP regulatory system: an update. *Ann N Y Acad Sci* 1012, 1-13.

Papanikolaou, G., Samuels, M. E., Ludwig, E. H., MacDonald, M. L., Franchini, P. L., Dube, M. P., Andres, L., MacFarlane, J., Sakellaropoulos, N., Politou, M., *et al.* (2004). Mutations in HFE2 cause iron overload in chromosome 1q-linked juvenile hemochromatosis. *Nat Genet* 36, 77-82.

Park, C. H., Valore, E. V., Waring, A. J., and Ganz, T. (2001). Hepcidin, a urinary antimicrobial peptide synthesized in the liver. *J Biol Chem* 276, 7806-7810.

Parviz, F., Matullo, C., Garrison, W. D., Savatski, L., Adamson, J. W., Ning, G., Kaestner, K. H., Rossi, J. M., Zaret, K. S., and Duncan, S. A. (2003). Hepatocyte nuclear factor 4alpha controls the development of a hepatic epithelium and liver morphogenesis. *Nat Genet* 34, 292-296.

Pietrangolo, A. (2004). Hereditary hemochromatosis--a new look at an old disease. *N Engl J Med* 350, 2383-2397.



- Pigeon, C., Ilyin, G., Courselaud, B., Leroyer, P., Turlin, B., Brissot, P., and Loreal, O. (2001). A new mouse liver-specific gene, encoding a protein homologous to human antimicrobial peptide hepcidin, is overexpressed during iron overload. *J Biol Chem* 276, 7811-7819.
- Ponka, P. (1997). Tissue-specific regulation of iron metabolism and heme synthesis: distinct control mechanisms in erythroid cells. *Blood* 89, 1-25.
- Roetto, A., Papanikolaou, G., Politou, M., Alberti, F., Girelli, D., Christakis, J., Loukopoulos, D., and Camaschella, C. (2003). Mutant antimicrobial peptide hepcidin is associated with severe juvenile hemochromatosis. *Nat Genet* 33, 21-22.
- Roy, C. N., Custodio, A. O., de Graaf, J., Schneider, S., Akpan, I., Montross, L. K., Sanchez, M., Gaudino, A., Hentze, M. W., Andrews, N. C., and Muckenthaler, M. U. (2004). An Hfe-dependent pathway mediates hyposideremia in response to lipopolysaccharide-induced inflammation in mice. *Nat Genet* 36, 481-485.
- Seglen, P. O. (1997). DNA ploidy and autophagic protein degradation as determinants of hepatocellular growth and survival. *Cell Biol Toxicol* 13, 301-315.
- Shike, H., Lauth, X., Westerman, M. E., Ostland, V. E., Carlberg, J. M., Van Olst, J. C., Shimizu, C., Bulet, P., and Burns, J. C. (2002). Bass hepcidin is a novel antimicrobial peptide induced by bacterial challenge. *Eur J Biochem* 269, 2232-2237.
- Stewart, W. B., Yuile, C. L., Claiborne, H. A., Snowman, R. T., and Whipple, G. H. (1950). Radioiron absorption in anemic dogs; fluctuations in the mucosal block and evidence for a gradient of absorption in the gastrointestinal tract. *J Exp Med* 92, 375-382.
- Thomson, A. M., Rogers, J. T., and Leedman, P. J. (1999). Iron-regulatory proteins, iron-responsive elements and ferritin mRNA translation. *Int J Biochem Cell Biol* 31, 1139-1152.
- Torrance, J. D., Bothwell, T.H. (1980). *Tissue iron stores* (New York, Churchill Livingstone Press).

Yang, F., Liu, X. B., Quinones, M., Melby, P. C., Ghio, A., and Haile, D. J. (2002). Regulation of reticuloendothelial iron transporter MTP1 (Slc11a3) by inflammation. *J Biol Chem* 277, 39786-39791.

Yeh, K. Y., Yeh, M., and Glass, J. (2004). Hepcidin regulation of ferroportin 1 expression in the liver and intestine of the rat. *Am J Physiol Gastrointest Liver Physiol* 286, G385-394.

Zhang, A. S., Xiong, S., Tsukamoto, H., and Enns, C. A. (2004). Localization of iron metabolism-related mRNAs in rat liver indicate that HFE is expressed predominantly in hepatocytes. *Blood* 103, 1509-1514.

Zetterstrom, M., Sundgren-Andersson, A. K., Ostlund, P., and Bartfai, T. (1998). Delineation of the proinflammatory cytokine cascade in fever induction. *Ann N Y Acad Sci* 856, 48-52.

# **Chapter 3**

## **Monosynaptic Stretch Reflex Circuit**

## **3.1 The Role of ETS Transcription Factors in Neuronal Circuit Formation**

### **The Monosynaptic Stretch Reflex Circuit**

During normal movement the central nervous system uses information from a vast array of sensory receptors to ensure the generation of correct patterns of muscle activity. Somatosensory-motor reflexes play an essential role in transmitting sensory information from muscles, joints, or skin into fast, coordinated motor output. Reflexes have traditionally been viewed as automatic, stereotyped movements in response to stimulation of peripheral receptors. Due to connections to higher brain centers, reflexes can be modified to adapt to a task. This flexibility allows reflexes to be smoothly incorporated into complex movements initiated by central commands (Clarac et al., 2000; Chen et al., 2003).

The most studied spinal reflex is the stretch reflex, a contraction of the muscle that occurs when the muscle is stretched. The neural circuit responsible for the stretch reflex was one of the first reflex pathways to be examined in detail. It basically consists of a monosynaptic and a disynaptic component formed between Ia muscle sensory (proprioceptive) neurons, and  $\alpha$ -motor neurons. The proprioceptive afferents convey information about the stretch status of a muscle, which they obtain from muscle spindles (sensory organs located within the muscle), to motor neurons located in the ventral spinal cord. Importantly, not only motor neurons innervating the same muscle as the sensory neuron (homonymous connections) but also those innervating muscles having a similar mechanical action (synergistic muscles) obtain excitatory input (heteronymous connections). In contrast,  $\alpha$ -motor neurons innervating antagonistic muscles receive inhibition from Ia fibers via the Ia inhibitory interneurons. This disynaptic inhibitory pathway is the basis for reciprocal innervation so that when a muscle is stretched, the antagonistic muscles relax.

Reciprocal innervation is essential not only for stretch reflexes but also for voluntary movements. Relaxation of the antagonistic muscle during movement enhances speed and efficiency because the muscles that act as prime movers are not working against the contraction of opposing muscles.

## **The ETS Transcription Factors, ER81 and PEA3 Are Essential for Establishment of the Spinal Monosynaptic Reflex Circuit**

The vertebrate spinal stretch reflex circuit has been the focus of many studies due to its relative simplicity. It is generally believed that initial phases of neuronal differentiation are already established at cell cycle exit, while extrinsic cues appear to be required for later events in building the stretch reflex circuit (Edlund and Jessell, 1999; Jessell, 2000; Shirasaki and Pfaff, 2002; Bertrand et al., 2002). PEA3 and ER81, two members of the ETS family of transcription factors (Sharrocks, 2001), have been implicated in this later phase of neuronal circuit formation (Arber et al., 2000; Haase et al., 2002; Livet et al., 2002). Both genes are only expressed by a distinct subset of motor and sensory neurons, once their axons have reached the base of the limb (Lin et al., 1998; Arber et al., 2000). Limb ablation experiments in chick have shown that the initiation of *Pea3* and *Er81* are strictly dependent on signals from their peripheral target (Lin et al., 1998).

In the developing brachial spinal cord, motor neurons innervating two distinct muscles start to express *Pea3* once their axons have reached the vicinity of their peripheral targets (Haase et al., 2002; Livet et al., 2002). In the absence of *Pea3* these motor neurons project axons to the periphery but fail to branch properly within their target. In addition, the corresponding motor neuron cell bodies are mispositioned in the ventral horn. Interestingly, *GDNF* (glial cell line-derived neurotrophic factor) or *GFR $\alpha$ 1* (a GDNF-binding receptor component) deficient mice exhibit a very similar phenotype. GDNF, initially characterized for its role as a survival factor, is specifically expressed in the two muscles that are innervated by *Pea3* positive motor neurons. Mice lacking *GDNF* signaling fail to induce *Pea3* in brachial motor neurons, demonstrating that GDNF is the peripheral signal that turns on the ETS transcription factor *Pea3*, which in turn is required for late differentiation processes of motor neurons.

In *Er81* mutant mice, Ia afferents fail to invade the ventral spinal cord and thus cannot make direct contact with motor neurons (Arber et al., 2000). As a consequence, *Er81* mutant mice develop a severe defect in motor coordination. *Er81* is expressed by proprioceptive neurons, muscle spindles and distinct motor pools. The primary locus of action of ER81 has been assigned to proprioceptive neurons due to several lines of evidence: First, *Er81* starts to be expressed in muscle spindles only by E18.5, a timepoint when Ia afferents already have formed synapses with motor neurons. Second, in the *Er81* mutant, all proprioceptive neurons are affected, although *Er81* is only expressed in a few motor neuron pools (Arber et al., 2000). And thirdly, proprioceptive neurons invade the ventral horn even if motor neurons are genetically eliminated as soon as they are postmitotic, long before Ia afferents project to the ventral spinal cord (Patel et al., 2003). However, the peripheral signal that induces *Er81* in proprioceptive afferents remains unknown.

### **Aim of the Following Study (Chapter 3.2)**

The following study is aimed at the identification of the inductive peripheral signal of *Er81* in proprioceptive neurons, the location where ER81 is thought to fulfill its function. Neurotrophins are known to be essential for the survival of DRG sensory neurons which express *Trk* (receptor tyrosine kinase) receptors (Snider, 1994; Bibel and Barde, 2000; Huang and Reichardt, 2001). DRG sensory neurons fall into three major functional classes, depending on which *Trk* receptor they express. Each Trk receptor transmits the signal of a different neurotrophin, e.g. neurotrophin-3 (NT3) is essential for proprioceptive neurons which express *TrkC*. Mice lacking TrkC signaling show a loss of 20-30% of sensory neurons and an absence of central proprioceptive projections (Ernfors et al., 1994; Farinas et al., 1994; Klein et al., 1994; Tessarollo et al., 1994). The dependence on neurotrophin signaling for survival at early developmental stages has prevented the analysis of these factors in regulating later events. In the following study the early cell death of sensory neurons in *NT3* mutant mice was elegantly circumvented by crossing them into the *Bax* mutant background. The lack of *Bax*, a pro-apoptotic gene allowed for functional analysis of proprioceptive neurons lacking TrkC signaling at a stage, when these neurons start to form connections to their synaptic partners (Deckwerth et al., 1996). We show that NT3 is the peripheral signal in target muscles

that induces *Er81* expression in proprioceptive sensory neurons, which in turn promotes the invasion of the ventral horn.

## 3.2 Peripheral NT3 Signaling Is Required for ETS Protein Expression and Central Patterning of Proprioceptive Sensory Afferents

Tushar D. Patel, Ina Kramer, Jan Kucera, Vera Niederkofler, Thomas M. Jessell, Silvia Arber & William D. Snider (Neuron 38, 403-416, 2003)

### Abstract

To study the role of NT3 in directing axonal projections of proprioceptive dorsal root ganglion (DRG) neurons,  $NT3^{-/-}$  mice were crossed with mice carrying a targeted deletion of the proapoptotic gene *Bax*. In  $Bax^{-/-}/NT3^{-/-}$  mice, NT3-dependent neurons survived and expressed the proprioceptive neuronal marker parvalbumin. Initial extension and collateralization of proprioceptive axons into the spinal cord occurred normally, but proprioceptive axons extended only as far as the intermediate spinal cord. This projection defect is similar to the defect in mice lacking the ETS transcription factor ER81 (Arber et al., 2000). Few if any DRG neurons from  $Bax^{-/-}/NT3^{-/-}$  mice expressed ER81 protein. Expression of a NT3 transgene in muscle restored DRG ER81 expression in  $NT3^{-/-}$  mice. Finally, addition of NT3 to DRG explant cultures resulted in induction of ER81 protein. Our data indicate that NT3 mediates the formation of proprioceptive afferent-motor neuron connections via regulation of ER81.

(contribution: analysis of  $ER81^{lox}$  mice)



## Introduction

Neurons of the dorsal root ganglia (DRG) are specialized to convey distinct somatic sensory modalities from the periphery to the central nervous system. Proprioceptive sensory neurons supply skeletal muscle and serve to provide information about muscle length and tension essential for coordinated motor function. Peripherally, group Ia and II proprioceptive neurons terminate on muscle spindles, whereas group Ib afferents innervate Golgi tendon receptors (Zelena, 1994). The central branches of proprioceptors project to the spinal cord and form synaptic connections with interneurons in the intermediate zone of the spinal cord (group Ia, Ib, and II afferents) or directly with motor neurons in the ventral horn of the spinal cord (group Ia and group II afferents; Brown, 1981). The specificity of connections between proprioceptive afferents and motor neurons in the mature spinal cord is well characterized (Eccles et al., 1957; Brown, 1981), but much less is known about the factors regulating proprioceptive axon extension and targeting during development.

Members of the ETS family of transcription factors have been implicated in regulating the formation of synaptic connections between group Ia sensory afferents and motor neurons (Lin et al., 1998; Arber et al., 2000). Two ETS family members, ER81 and PEA3, are expressed by developing proprioceptive sensory neurons as well as by motor neurons in the spinal cord (Lin et al., 1998; Arber et al., 2000; Livet et al., 2002). In the chick embryo, proprioceptive sensory neurons and motor neuron pools projecting to a given muscle exhibit the same pattern of ETS gene expression, and this coordinated expression is regulated by signals from peripheral target tissue (Lin et al., 1998; see also Haase et al., 2002). In mouse, ER81 is initially expressed by most or all proprioceptive neurons in the DRG (Arber et al., 2000). Consistent with this observation, virtually all proprioceptive neurons fail to establish direct monosynaptic connections with motor neurons of *Er81*<sup>-/-</sup> mice, and terminate instead in the intermediate zone of the spinal cord (Arber et al., 2000). Since proprioceptive neuronal survival is not affected in *Er81*<sup>-/-</sup> mice, ER81 expression is likely to regulate the expression of molecules necessary for the establishment of the appropriate terminal arborization of group Ia and II afferents within the ventral spinal cord (Arber et al., 2000). Although interactions with the periphery appear to be important in the regulation of ER81 expression (Lin et al., 1998), the identity of the relevant inductive factor(s) responsible for this regulation is unknown.

The two major functional classes of DRG neurons, proprioceptive and cutaneous sensory neurons, are distinguished by their expression of different receptor tyrosine kinases (Trks) that transduce signals provided by different members of the neurotrophin family of polypeptide growth factors (for reviews see Snider, 1994; Bibel and Barde, 2000; Huang and Reichardt, 2001). Neurotrophin signaling via receptor tyrosine kinases underlies, in large part, the target dependence of peripheral neurons during critical developmental periods. Proprioceptive DRG neurons, which comprise ~20% of the adult DRG neuronal population, express TrkC and require neurotrophin-3 (NT3) signaling for their survival during development. Elimination of TrkC signaling in mice results in a 20%–35% loss of DRG neurons and the absence of central proprioceptive projections (Klein et al., 1994; Tessarollo et al., 1994; see also Ernfors et al., 1994; Farinas et al., 1994). In contrast, inactivation of *NT3* in mice results in a ~70% reduction in the number of DRG neurons and thus appears to result in an additional loss of nonproprioceptive sensory neurons (Ernfors et al. 1994; Farinas et al., 1994; Tessarollo et al., 1994).

In addition to their role in regulating neuronal survival, there is emerging evidence that neurotrophins have regulatory effects on neuronal morphology, notably functions related to axonal growth and arborization in target fields (for reviews see McAllister et al., 1999; Bibel and Barde, 2000; Huang and Reichardt, 2001; Markus et al.; 2002). However, the dependence of peripheral neurons on neurotrophin signaling for survival at early developmental stages has limited our understanding of the requirements for neurotrophins in regulating late developmental events *in vivo*. Our previous work has demonstrated that genetic elimination of the *Bcl2* family member *Bax*, which is required for apoptosis upon neurotrophin withdrawal (Deckwerth et al., 1996), permits TrkA-expressing cutaneous DRG neurons to survive in the absence of neurotrophin signaling *in vivo* (Patel et al., 2000). These neurons extend central processes through the dorsal roots into the spinal cord, but the growth of the peripheral process in the limb is markedly impaired (Patel et al., 2000). Thus, elimination of *Bax*, in principle, might provide a tool to explore axon growth and targeting of proprioceptive neurons in the absence of *NT3*.

NT3 appears to play a complex role in the regulation of proprioceptive axon extension and targeting. During development, NT3 is expressed by skeletal muscle, by mesenchyme surrounding peripheral projection pathways and by motor neurons in the spinal cord

(Schechterson and Bothwell, 1992; Ernfors et al., 1992; Patapoutian et al., 1999). Injection of blocking anti-NT3 antibodies into the limb during the period of naturally occurring cell death results in a decrease in the number of proprioceptive neurons (Oakley et al., 1995), indicating that NT3 derived from peripheral tissues is required for the survival of proprioceptive neurons. Furthermore, developing peripheral sensory axons can be directed to grow toward local sources of NT3 and other neurotrophins (Tucker et al., 2001), raising the possibility that endogenous NT3 might play a role in supporting interstitial axon extension in the developing limb. It also seems plausible that NT3 derived from either peripheral or spinal cord sources might influence central proprioceptive axon projections. However, it remains to be established whether NT3 regulates the collateralization and targeting of central proprioceptive axons to motor neurons, and if so, by what mechanism.

In order to assess the role of NT3 on proprioceptive axon extension and ER81 expression, we crossed mice carrying a targeted deletion of the *Bax* gene with *NT3*<sup>-/-</sup> mice. We report here that proprioceptive sensory neurons survive in *Bax*<sup>-/-</sup>/*NT3*<sup>-/-</sup> mice. However, peripheral proprioceptive axons and their associated muscle spindles are absent at birth in these mice. Furthermore, although the initial collateralization of central proprioceptive axons into the spinal cord proceeds normally in *Bax*<sup>-/-</sup>/*NT3*<sup>-/-</sup> mice, these axons do not project toward motor neurons and instead terminate in the intermediate spinal cord, a phenotype similar to that observed in *Er81*<sup>-/-</sup> mice (Arber et al., 2000). Consistent with this observation, we find that DRG neurons from *Bax*<sup>-/-</sup>/*NT3*<sup>-/-</sup> mice express markedly reduced levels of ER81 protein, and we show that exogenous NT3 can induce the expression of ER81 in proprioceptive neurons of DRG explant cultures. Furthermore, we provide evidence that a peripheral rather than a central source of NT3 is required for ER81 expression and central targeting of group Ia and II afferents toward motor neurons.

## Results

### Elimination of *Bax* Restores DRG Neuronal Number in the Absence of NT3/Trk Signaling

DRG neurons survive in the absence of neurotrophin signaling *in vivo* if *Bax* is also deleted (Patel et al., 2000). To study the effects of NT3 on the development of proprioceptive sensory neurons, *Bax*<sup>-/-</sup>/*NT3*<sup>-/-</sup> mice were generated by crossing heterozygotes from each line. At birth, *Bax*<sup>-/-</sup>/*NT3*<sup>-/-</sup> mice were overtly indistinguishable from their wild-type littermates. However, *Bax*<sup>-/-</sup>/*NT3*<sup>-/-</sup> mice did not survive beyond the first postnatal week, as is the case with *NT3*<sup>-/-</sup> mice (Ernfors et al., 1994).

We assessed peripheral sensory neuron survival in the progeny of *Bax/NT3* crosses by counting lumbar level 4 (L4) DRG neurons in semi thin sections at P0 (Figure 26A). As expected, there was a ~70% loss of DRG neurons in *Bax*<sup>+/+</sup>/*NT3*<sup>-/-</sup> mice compared to wild-type. Strikingly, no neuronal loss occurred in the L4 DRG of *Bax*<sup>-/-</sup>/*NT3*<sup>-/-</sup> mice. Rather, we found a ~50% increase in the total number of DRG neurons in the *Bax*<sup>-/-</sup>/*NT3*<sup>-/-</sup> mice (12,932 ± 758), comparable to that found in *Bax*<sup>-/-</sup>/*NT3*<sup>+/+</sup> mice (14,160 ± 1013). These findings indicate that the elimination of *BAX* restores neuronal number in the DRG in the absence of NT3. The supranormal number of neurons in both *Bax*<sup>-/-</sup>/*NT3*<sup>+/+</sup> and *Bax*<sup>-/-</sup>/*NT3*<sup>-/-</sup> mice is presumably due to the absence of naturally occurring neuron death in the *Bax* null mutants (White et al., 1998; Patel et al. 2000).

To assess whether proprioceptive neurons survived in the absence of NT3 signaling, we examined DRG sections from P0 mice for expression of the calcium binding protein Parvalbumin (Figures 26B–26D). Parvalbumin is an established marker of NT3-dependent proprioceptive neurons (Coprav et al., 1994; Ernfors et al., 1994; Honda 1995). We found Parvalbumin immunoreactivity in large-diameter DRG neurons of wild-type mice (Figure 26B), and consistent with the loss of proprioceptive neurons in *Bax*<sup>+/+</sup>/*NT3*<sup>-/-</sup> mice, the number of Parvalbumin-expressing neurons in the DRG was dramatically reduced (Figure 26C). In contrast, we found numerous Parvalbumin-expressing neurons in *Bax*<sup>-/-</sup>/*NT3*<sup>-/-</sup> mice, demonstrating that proprioceptive neurons had survived NT3 deprivation in the absence of *Bax*. However, the cross-sectional area of Parvalbumin<sup>+</sup> DRG neuronal somata from *Bax*<sup>-/-</sup>/*NT3*<sup>-/-</sup> mice was reduced by ~70% as compared to wild-type mice at P0, presumably

<b>A DRG Neuron and Dorsal Root Axon Counts at P0</b>				
Genotype	<i>Bax</i> <sup>+/+</sup> , <i>NT3</i> <sup>+/+</sup>	<i>Bax</i> <sup>-/-</sup> , <i>NT3</i> <sup>+/+</sup>	<i>Bax</i> <sup>+/+</sup> , <i>NT3</i> <sup>-/-</sup>	<i>Bax</i> <sup>-/-</sup> , <i>NT3</i> <sup>-/-</sup>
L4 DRG Neuron Counts	8618 ± 483 (100%)	14,160 ± 1013 (164%)	2531 (30%, n=2)	12,932 ± 758 (150%)
L4 Dorsal Root Axons	8800	13,003	2603 (n=2)	14,485

n=5 for DRG neuron counts; n=3 for dorsal root axon counts

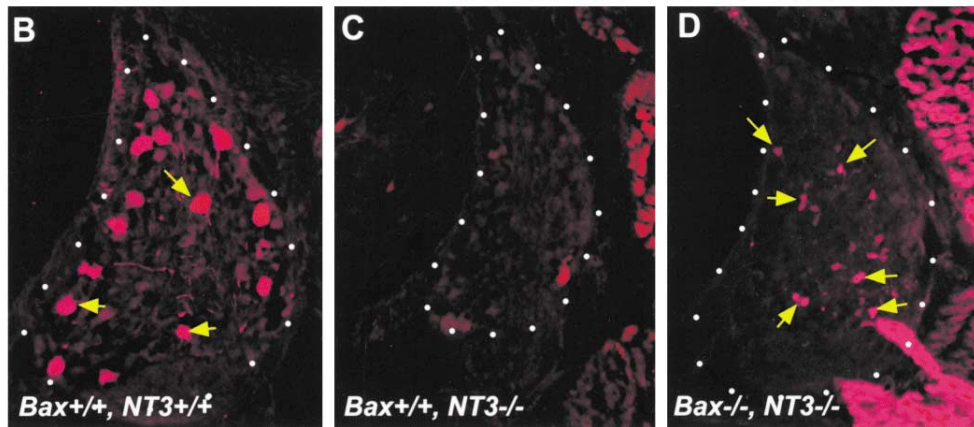


**Figure 26. Proprioceptive DRG Neurons Survive in *Bax*<sup>-/-</sup>/*NT3*<sup>-/-</sup> Mice.**

(A) L4 DRG neuron and L4 dorsal root axon counts at P0. There is no significant difference in the number of DRG neurons between *Bax*<sup>-/-</sup>/*NT3*<sup>+/+</sup> (14,160 ± 1013) and *Bax*<sup>+/+</sup>/*NT3*<sup>-/-</sup> (12,932 ± 758) mice. These values represent a 64% and 50% increase, respectively, over wild-type (8618 ± 483). Note that the number of dorsal root axons corresponds well with the number of DRG neurons for each genotype, demonstrating that the additional DRG neurons in *Bax*<sup>-/-</sup>/*NT3*<sup>+/+</sup> and *Bax*<sup>-/-</sup>/*NT3*<sup>-/-</sup> mice extend their central axons through the dorsal roots toward the spinal cord.

(B–D) Parvalbumin immunohistochemistry in P0 DRG sections. In wild-type DRG (B), Parvalbumin expression is found in large neurons (arrows), consistent with expression by proprioceptive neurons. As expected, Parvalbumin immunoreactivity is virtually absent in DRG sections from the *Bax*<sup>+/+</sup>/*NT3*<sup>-/-</sup> mice (C), consistent with the complete loss of proprioceptive neurons in these mice. In contrast, numerous Parvalbumin<sup>+</sup> neurons can be seen in DRG sections from *Bax*<sup>-/-</sup>/*NT3*<sup>-/-</sup> mice (D; arrows). Note, however, that these rescued Parvalbumin<sup>+</sup> neurons are considerably smaller than Parvalbumin<sup>+</sup> neurons in wild-type DRG.

due to the sustained loss of NT3 trophic support (Figure 26D). Further evidence that proprioceptive neurons survived until P0 in  $Bax^{-/-}/NT3^{-/-}$  mice is provided by analysis of their axonal projections into the spinal cord (see below).

### **A Peripheral Defect in Proprioceptive Axon Projections in $Bax^{-/-}/NT3^{-/-}$ Mice**

To determine in  $Bax^{-/-}/NT3^{-/-}$  mice whether the peripheral axons of proprioceptive neurons innervate muscles in the absence of NT3 signaling, we searched for the presence of Parvalbumin<sup>+</sup> axons in the soleus nerve at P0 (Figure 27). Parvalbumin<sup>+</sup> axons were found to extend through the soleus nerve and penetrated the soleus muscle in P0 wild-type ( $Bax^{+/+}/NT3^{+/+}$ ) mice (Figure 27B). In contrast, in the  $Bax^{-/-}/NT3^{-/-}$  mice (Figure 27C), no Parvalbumin<sup>+</sup> axons were detected in the soleus nerve at P0, despite the fact that Parvalbumin<sup>+</sup> axons could be detected in the spinal cord (see below). Because NT3 could, in principle, regulate the levels of Parvalbumin expression rather than the presence of peripheral axons themselves, we characterized further the extent of peripheral innervation through axon counts in the soleus nerve at P0 (Figure 27A). We detected a 64% decrease in the number of axons in the  $Bax^{-/-}/NT3^{-/-}$  mice when compared with the  $Bax^{-/-}/NT3^{+/+}$  mice even though the number of DRG neurons in the two mutants were similar (see Figure 26A). These findings indicate that proprioceptive sensory axons fail to innervate their target muscles *in*  $Bax^{-/-}/NT3^{-/-}$  mice.

Muscle spindles are peripheral end organs innervated by proprioceptive neurons, and their development and maintenance are regulated by contacts of group Ia and II afferents with myotubes (Kucera and Walro; 1987; Kucera and Walro 1988). The morphology and number of muscle spindles in the soleus muscle were identical in  $Bax^{-/-}/NT3^{+/+}$  and wild-type mice (Figure 27A). In contrast, we found no muscle spindles in soleus muscles of  $Bax^{+/+}/NT3^{-/-}$  or  $Bax^{-/-}/NT3^{-/-}$  mice at P0 (Figure 27A). Collectively, the failure to detect Parvalbumin<sup>+</sup> axons in the soleus nerve, the deficiency in axon number, and the absence of muscle spindles in the soleus muscle demonstrate a developmental failure of proprioceptive neurons to innervate their peripheral muscle targets or an early retraction of these axonal processes.

To distinguish between these two possibilities, we assessed the development of peripheral proprioceptive projections in  $Bax^{-/-}/NT3^{-/-}$  embryos at E15 and E17. E15 represents the earliest stage at which muscle spindle formation in the mouse embryo can be detected, as assessed by the expression of the zinc finger transcription factor *Egr3* and the

<b>A Soleus Nerve Axon Counts and Soleus Muscle Spindle Counts</b>				
Genotype	<i>Bax</i> <sup>+/+</sup> , <i>NT3</i> <sup>+/+</sup>	<i>Bax</i> <sup>-/-</sup> , <i>NT3</i> <sup>+/+</sup>	<i>Bax</i> <sup>+/+</sup> , <i>NT3</i> <sup>-/-</sup>	<i>Bax</i> <sup>-/-</sup> , <i>NT3</i> <sup>-/-</sup>
Soleus Nerve Axon Counts	78 ± 1	126 ± 23	37 ± 0.6	70 ± 4
Soleus Muscle Spindle Counts	11.2	11.5 (n=2)	0	0

n ≥ 3 for axon and spindle counts

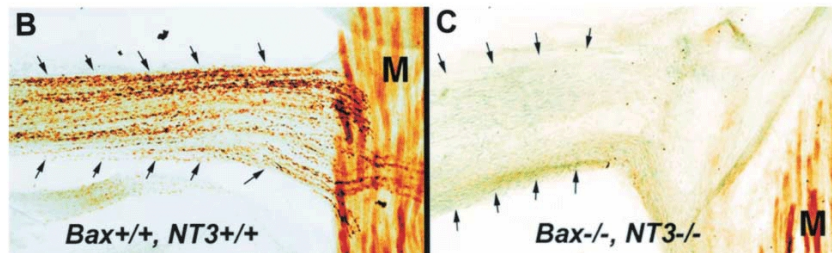


**Figure 27. Peripheral Proprioceptive Axons and Muscle Spindles Are Absent at P0 in *Bax*<sup>-/-</sup>/*NT3*<sup>-/-</sup> Mice.**

(A) Axon counts in the nerve to the soleus muscle at P0 reveal that the number of axons is reduced in *Bax*<sup>-/-</sup>/*NT3*<sup>-/-</sup> (70 ± 4) mice compared to *Bax*<sup>-/-</sup>/*NT3*<sup>+/+</sup> (126 ± 23), even though the number of DRG neurons is equivalent in the two mutants. Furthermore, muscle spindle counts reveal the absence of soleus muscle spindles in *Bax*<sup>+/+</sup>/*NT3*<sup>-/-</sup> and *Bax*<sup>-/-</sup>/*NT3*<sup>-/-</sup> mice.

(B and C) Parvalbumin<sup>+</sup> axons can be seen in the nerve to the soleus muscle (outlined by arrows) from wild-type P0 mice. These axons extend through the nerve and penetrate the muscle (M) in the wild-type controls. However, in the *Bax*<sup>-/-</sup>/*NT3*<sup>-/-</sup> mice, Parvalbumin immunoreactivity is absent in the nerve to the soleus.

ETS protein PEA3 (Tourtellotte et al., 2001; Hippenmeyer et al. 2002). At E15, we detected Egr3 immunoreactivity in the distal hindlimb muscles of wild-type embryos in approximately 15% of the longitudinal sections examined (n = 3, data not shown). In contrast, in E15 *Bax*<sup>-/-</sup>/*NT3*<sup>-/-</sup> embryos, we did not detect Egr3 immunoreactivity in distal hindlimb muscles in any of the sections examined (n = 3). At E17, Egr3 is robustly expressed by intrafusal muscle fibers in wild-type embryos, and clusters of Egr3<sup>+</sup> fibers could be detected in roughly 15% of the sections through both forelimb and hindlimb muscles (arrows in Figures 28A–28C and 3E). In contrast, in *Bax*<sup>-/-</sup>/*NT3*<sup>-/-</sup> embryos analyzed at E17, no Egr3<sup>+</sup> fibers were detected in distal forelimb and hindlimb (n = 3; Figures 28D and 28F).

As in P0 mice, no Parvalbumin<sup>+</sup> axons were detected in hindlimb nerves of *Bax*<sup>-/-</sup>/*NT3*<sup>-/-</sup> embryos at E15 or E17 (data not shown). To assess whether the expression of Parvalbumin may not reveal the full extent of peripheral projections in *Bax*<sup>-/-</sup>/*NT3*<sup>-/-</sup> embryos, we used DiI crystals applied to sciatic nerves as an independent means of tracing peripheral projections. In wild-type embryos, this method readily revealed annulospiral endings characteristic of spindle afferents in soleus and plantaris muscles at E17 (Figure 28G, arrows). Interestingly, some axons with similar morphology were labeled in soleus and plantaris muscles of *Bax*<sup>-/-</sup>/*NT3*<sup>-/-</sup> embryos, analyzed at the same age (Figures 28H and 28I). These axons were invariably in close proximity to the main nerve trunk and did not extend to lateral aspects of the muscle. Since no Parvalbumin or Egr3 expression could be detected in these preparations, our results do not resolve definitively whether these axons correspond to proprioceptive afferents. Nevertheless, these findings reveal an embryonic defect in the development of peripheral projections of proprioceptive afferents and a corresponding defect in the initiation of muscle spindle differentiation by these proprioceptive afferents.

### **Proprioceptive Axons Fail to Extend into the Ventral Horn in *Bax*<sup>-/-</sup>/*NT3*<sup>-/-</sup> Mice**

The growth of the central and peripheral axon branches of TrkA-expressing DRG neurons is differentially regulated by NGF signaling (Patel et al., 2000). In order to assess whether proprioceptive neurons extend their axons centrally into the spinal cord in the absence of NT3 signaling, we counted dorsal root axons at P0 by sampling electron micrographs of lumbar dorsal root sections (Figure 26A). Across all genotypes, there was a tight correspondence between DRG neuronal number and dorsal root axon counts, indicating that surviving neurons in *Bax*<sup>-/-</sup>/*NT3*<sup>-/-</sup> embryos do extend their central processes into the dorsal roots, toward the spinal cord (Figure 26A).



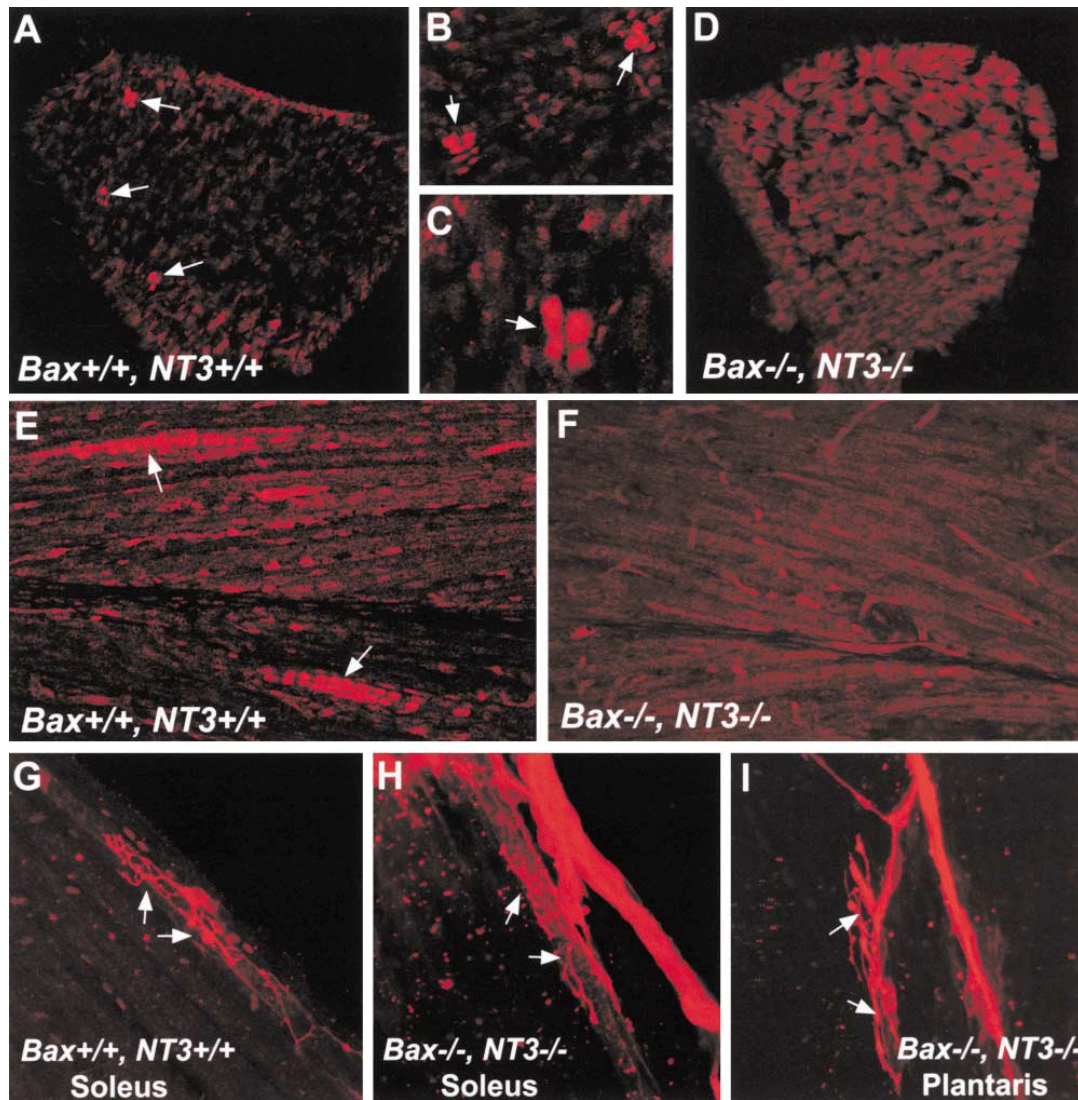


**Figure 28. Muscle Spindles Do Not Develop in the Absence of NT3 Signaling in *Bax*<sup>-/-</sup>/*NT3*<sup>-/-</sup> Mice.**

(A–F) Egr3 immunoreactivity in distal hindlimb and forelimb skeletal muscle. In cross-sections through wild-type soleus muscle (A–C) and longitudinal sections through the distal forelimb (E), Egr3 immunoreactivity is present in intrafusal muscle fibers at E17. Egr3 immunoreactivity is absent in hindlimb (soleus in D) and forelimb (F) muscles in *Bax*<sup>-/-</sup>/*NT3*<sup>-/-</sup> mice.

(G–I) DiI-labeled peripheral axons in distal hindlimb muscles at E17. The endings of proprioceptive afferents exhibit a characteristic annulospiral structure in the wild-type soleus muscle (G; arrow). A few spiral-like axonal endings are found in the soleus and plantaris muscles from *Bax*<sup>-/-</sup>/*NT3*<sup>-/-</sup> mice (H and I, arrows). In contrast to controls, such endings in *Bax*<sup>-/-</sup>/*NT3*<sup>-/-</sup> mice are invariably in close proximity to the major nerve trunk.

To characterize further the central projections of proprioceptive afferents, we traced the axons into the spinal cord at E15, by DiI labeling (Figure 29). By E15, proprioceptive afferents have started to invade the ventral horn at all levels of the spinal cord in wild-type mice (Figure 29A). In  $Bax^{+/+}/NT3^{-/-}$  embryos, DiI-labeled axons projected only into the dorsal laminae of the spinal cord, consistent with the early death of proprioceptive neurons observed in the absence of NT3 (Figure 29B). In contrast, in  $Bax^{-/-}/NT3^{-/-}$  embryos, proprioceptive axons entered the spinal cord and followed a trajectory similar to that in wild-type controls ( $n = 4$ ; Figure 29C, arrows). However, in  $Bax^{-/-}/NT3^{-/-}$  embryos, proprioceptive axons stopped in the intermediate zone of the spinal cord and failed to project toward motor neurons in the ventral horn (Figure 29, yellow asterisks). Parvalbumin immunostaining in  $Bax^{-/-}/NT3^{+/+}$  revealed the presence of proprioceptive afferents in the ventral horn of the spinal cord, indicating that the projection defect observed in  $Bax^{-/-}/NT3^{-/-}$  mice is due to the absence of NT3 rather than the absence of BAX (data not shown). In order to quantify DiI-labeled proprioceptive afferents, we measured the fluorescence intensity of DiI-labeled afferents in  $Bax^{-/-}/NT3^{-/-}$  and  $Bax^{+/+}/NT3^{+/+}$  mice at E15. The mean fluorescence intensity measurements of DiI-labeled afferents in the intermediate zone of  $Bax^{-/-}/NT3^{-/-}$  mice were comparable to the mean density measurements of DiI-labeled afferents in the ventral horn of  $Bax^{+/+}/NT3^{+/+}$  mice with a ratio of 1.02 ( $Bax^{-/-}/NT3^{-/-}$  versus  $Bax^{+/+}/NT3^{+/+}$ ), indicating that the overall number of proprioceptive collaterals was roughly comparable in the two mutants.

To examine whether axonal projections into the ventral spinal cord were simply delayed developmentally, we traced central projections with DiI at E17 (Figures 29D and 29E) and P0 (Figures 29F and 29G). No afferent projections were detected in the ventral horn at either of these ages in  $Bax^{-/-}/NT3^{-/-}$  embryos (E17,  $n = 3$ ; P0,  $n = 2$ ). Parvalbumin staining at P0 verified that these axons were indeed from proprioceptive afferents ( $n = 3$ , data not shown).

### **Proprioceptive DRG Neurons Show Reduced ER81 Expression in the Absence of NT3 Signaling**

A defect in the central projections of proprioceptive afferents similar to that in  $Bax^{-/-}/NT3^{-/-}$  mice occurs in mice lacking the ETS transcription factor *Er81* (Arber et al., 2000). The failure of proprioceptive axons to project into the ventral horn in both  $Bax^{-/-}/NT3^{-/-}$  and  $Er81^{-/-}$  mutants raised the possibility that the central projection defect observed in  $Bax^{-/-}/NT3^{-/-}$

express ER81 coexpress TrkC and Parvalbumin and correspond to proprioceptive afferents (Arber et al., 2000). We examined whether proprioceptive DRG neurons expressed ER81 in *Bax*<sup>-/-</sup>/*NT3*<sup>-/-</sup> mice. Unlike at P0, the cross-sectional area of Parvalbumin<sup>+</sup> DRG neurons in wild-type and *Bax*<sup>-/-</sup>/*NT3*<sup>-/-</sup> mice was equivalent at E15 (781 ± 37 μm<sup>2</sup> in wild-type and 727 ± 32 μm<sup>2</sup> in *Bax*<sup>-/-</sup>/*NT3*<sup>-/-</sup> embryos; Figures 30A–30C). The intensity of Parvalbumin staining, however, appeared to be fainter in DRG from the *Bax*<sup>-/-</sup>/*NT3*<sup>-/-</sup> mice than wild-type. At E15, numerous ER81<sup>+</sup> neurons were detected in DRGs from wild-type (Figure 30E) and *Bax*<sup>-/-</sup>/*NT3*<sup>+/+</sup> mice (not shown), but no ER81 protein expression was detected in DRG sections from *Bax*<sup>-/-</sup>/*NT3*<sup>-/-</sup> embryos (n = 4; Figure 30G). ER81 expression was also not detected in DRGs of *Bax*<sup>+/+</sup>/*NT3*<sup>-/-</sup> mice, but this reflects the loss of all proprioceptive neurons (Figure 30F).

To assess whether there was a similar reduction in *Er81* mRNA in the *Bax*<sup>-/-</sup>/*NT3*<sup>-/-</sup> embryos, we examined *Er81* mRNA levels in E15 lumbar level DRGs by in situ hybridization (n = 2; Figures 30I–30K). Compared to wild-type, we observed a marked reduction in the number of DRG neurons expressing *Er81* mRNA in DRG from *Bax*<sup>-/-</sup>/*NT3*<sup>-/-</sup> embryos. In addition, the intensity of the *Er81* mRNA labeling in individual neurons was reduced in the *Bax*<sup>-/-</sup>/*NT3*<sup>-/-</sup> DRG compared to wild-type.

The effect of NT3 on ER81 expression appears to be selective to DRG neurons. Subsets of motor neurons in the ventral horn of the spinal cord also express ER81 (Arber et al., 2000). At E15, *Er81* mRNA and ER81 protein (Figures 30L–30O) were expressed in similar patterns in lumbar regions of the spinal cord in wild-type and *Bax*<sup>-/-</sup>/*NT3*<sup>-/-</sup> embryos. In addition, to assess whether the regulation of ETS genes by NT3 is restricted to ER81, we assessed the expression of PEA3, a member of the ETS gene family closely related to *Er81*, in DRG neurons of *Bax*<sup>-/-</sup>/*NT3*<sup>-/-</sup> embryos. PEA3 is expressed by both a subset of proprioceptive afferents and a subset of cutaneous DRG neurons (Arber et al., 2000). There was no noticeable difference in patterns or levels of *Pea3* mRNA expression between DRGs from wild-type and *Bax*<sup>-/-</sup>/*NT3*<sup>-/-</sup> embryos (Figures 30P and 30Q). This result provides evidence for specificity of NT3 in regulating ER81 expression in DRG neurons although it does not absolutely exclude the possibility that PEA3 expression in proprioceptive but not cutaneous sensory neurons is affected.

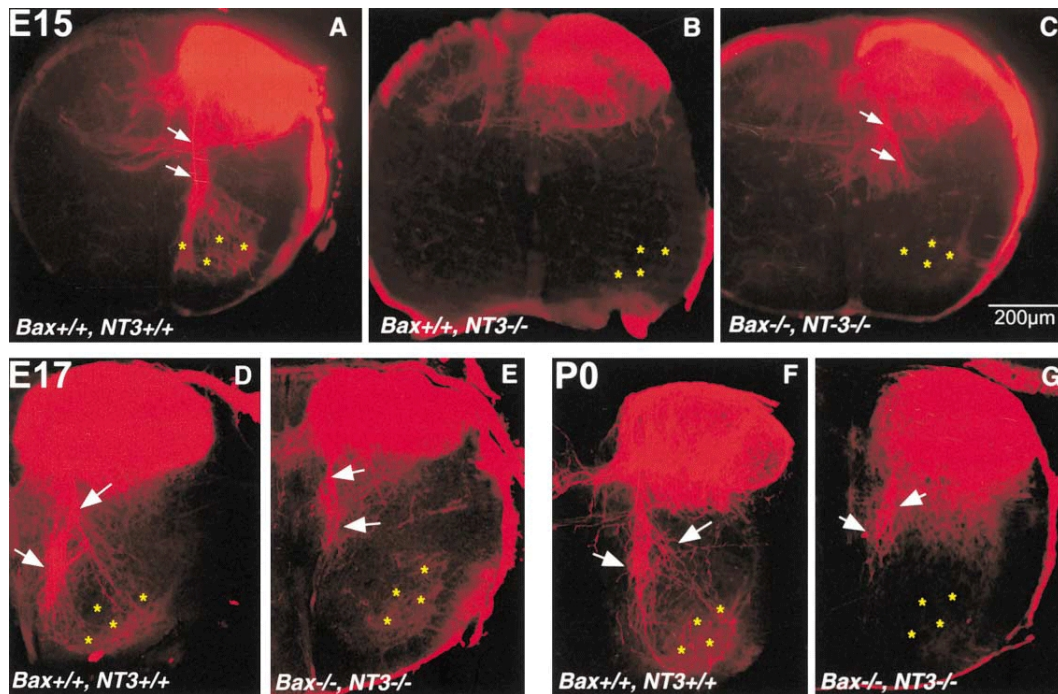


**Figure 29. Central Proprioceptive Projections Do Not Reach the Ventral Spinal Cord in *Bax*<sup>-/-</sup>/*NT3*<sup>-/-</sup> Mice.**

DiI tracing of the central DRG projections at E15 (A–C), E17 (D and E), and P0 (F and G). In E15 wild-type embryos (A), proprioceptive axons (arrows) penetrate the spinal cord and project ventrally to the motor neurons in the ventral horn (yellow asterisks) of the spinal cord. As expected, the ventrally projecting proprioceptive axons are absent in the spinal cord of E15 *Bax*<sup>+/+</sup>/*NT3*<sup>-/-</sup> mice (B). In E15 *Bax*<sup>-/-</sup>/*NT3*<sup>-/-</sup> mice (C), the axons (arrows) of the rescued proprioceptive neurons penetrate the spinal cord but extend only as far as the intermediate spinal cord and do not project to the motor neurons in the ventral horn (yellow asterisks). DiI-labeled central projections at E17 (D and E) and P0 (F and G) reveal that the proprioceptive axons of *Bax*<sup>-/-</sup>/*NT3*<sup>-/-</sup> mice never innervate the motor neurons in the ventral horn of the spinal cord.



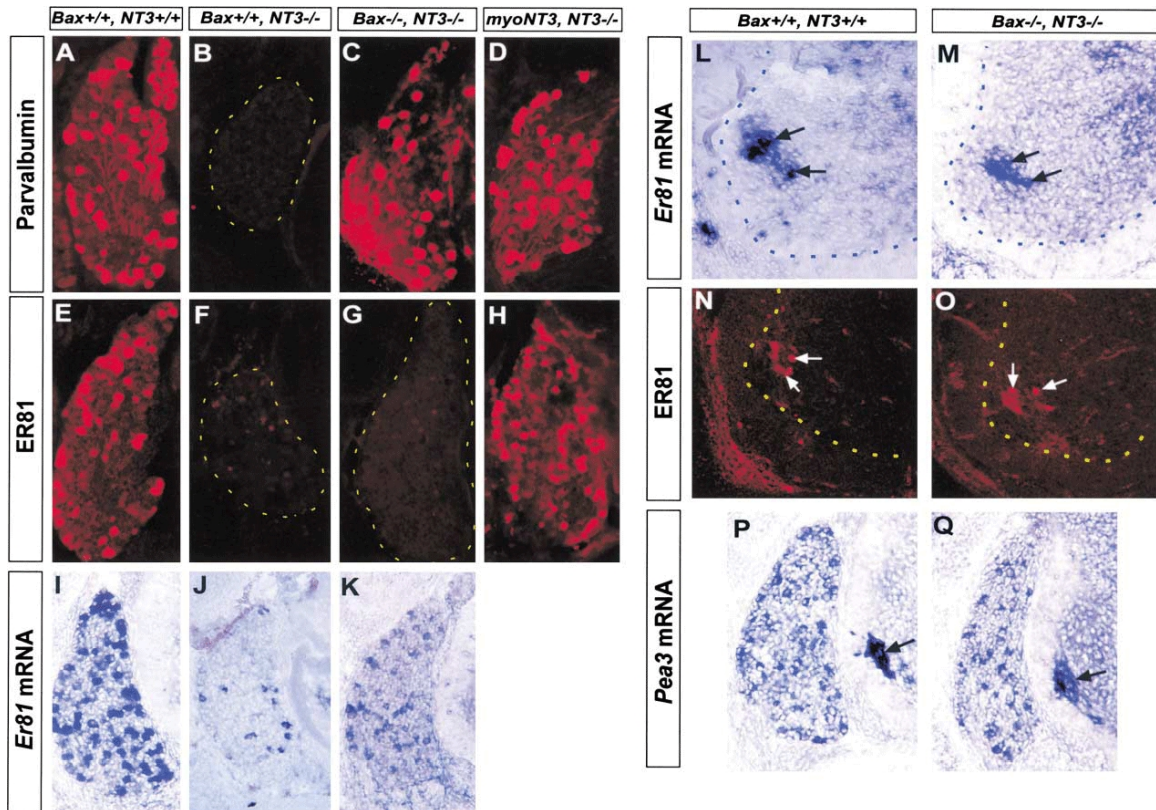


**Figure 30. Proprioceptive DRG Neurons Do Not Express ER81 in the Absence of NT3 Signaling.**

(A–D) Parvalbumin<sup>+</sup> neurons are found in lumbar DRG sections from E15 wild-type and *Bax*<sup>-/-</sup>/*NT3*<sup>-/-</sup> mice. As expected, Parvalbumin<sup>+</sup> neurons are not found in DRG sections from *Bax*<sup>+/+</sup>/*NT3*<sup>-/-</sup> mice. Parvalbumin-expressing neurons are also rescued in *myoNT3*/*NT3*<sup>-/-</sup> mice.

(E–H) Numerous ER81-expressing neurons are present in the wild-type E15 DRG. In contrast, ER81 immunoreactivity is absent in DRG sections from the E15 *Bax*<sup>-/-</sup>/*NT3*<sup>-/-</sup> mice even though the proprioceptive neurons survive and express Parvalbumin in these mice. ER81 expression is rescued in DRG neurons from *myoNT3*/*NT3*<sup>-/-</sup> mice.

(I–K) Consistent with the absence of ER81 immunoreactivity in *Bax*<sup>-/-</sup>/*NT3*<sup>-/-</sup> DRG neurons, there is also a marked reduction in *Er81* mRNA levels as revealed by in situ hybridization. However, mRNA expression is not abolished in *Bax*<sup>-/-</sup>/*NT3*<sup>-/-</sup> DRG neurons.

(L–O) In situ hybridization and immunohistochemistry reveal that expression of *Er81* mRNA (L and M) and protein (N and O) in a subset of spinal motor neurons (arrows) is unaffected in *Bax*<sup>-/-</sup>/*NT3*<sup>-/-</sup> mice (dots demarcate the boundary of the ventral horn).

(P and Q) In situ hybridization reveals no qualitative difference in pattern or levels *Pea3* mRNA expression between DRGs from E15.5 wild-type and *Bax*<sup>-/-</sup>/*NT3*<sup>-/-</sup> mice. Also note that *Pea3* mRNA is present in motor neurons of both wild-type and *Bax*<sup>-/-</sup>/*NT3*<sup>-/-</sup> mice (arrows).

### **NT3 Induces ER81 Expression in Proprioceptive DRG Neurons**

The absence of ER81 expression in DRG from *Bax*<sup>-/-</sup>/*NT3*<sup>-/-</sup> mice and the similarity in the central projection phenotype with *Er81*<sup>-/-</sup> mice raises the possibility that NT3 is responsible for the induction of ER81 in DRG neurons. To test this hypothesis, we cultured wild-type mouse DRG *in vitro* in the presence or absence of NT3 and assessed ER81 protein expression. Since the onset of ER81 expression in DRG does not occur until E13 *in vivo* (Arber et al., 2000), DRG explants were cultured from E11.5 and E12.5 (not shown) embryos. We did not detect ER81 immunoreactivity in DRG explants cultured in the absence of NT3 at any time point up to 18 hr even though many DRG neurons expressed the LIM homeodomain protein *Isl1*. In the presence of NT3, induction of ER81 expression was detected in a subset of *Isl1*<sup>+</sup> neurons within 3 hr of culturing the explants, and expression was maintained for up to 18 hr *in vitro* (Figure 31). In contrast, no expression of ER81 was detected in DRG explants cultured in the presence of NGF for 18 hr (Figure 31).

To rule out the possibility that NT3-dependent DRG neurons die within a few hours of NT3 deprivation *in vitro*, we cultured E12.5 DRG explants from *Bax*<sup>-/-</sup> embryos for 18 hr in the presence or absence of NT3. Both NGF- and NT3-dependent neurons from *Bax*<sup>-/-</sup> DRG neurons survive several days *in vitro* in the absence of neurotrophin signaling (Lentz et al., 1999). Consistent with the results from wild-type explants, we found numerous ER81<sup>+</sup> neurons in *Bax*<sup>-/-</sup> DRG explants cultured in the presence of NT3 for 18 hr *in vitro* (Figures 32E and 32F). In contrast, few if any ER81<sup>+</sup> neurons were found in DRG explants cultured in the absence of NT3 (Figures 32B and 32C).

### **Sources of NT3 Regulating ER81 Expression and the Development of Central Projections of Proprioceptive Neurons**

We next addressed the question of whether the source of NT3 responsible for regulating ER81 expression in proprioceptive neurons and the development of ventral projections by group Ia and II afferents is located peripherally or within the spinal cord. Within the developing spinal cord, motor neurons are known to be a major source of NT3 (see Wright et al., 1997, and references therein). We therefore analyzed a mouse mutant in which motor neurons are ablated genetically by diphtheria toxin expression as soon as they are postmitotic, and thus long before group Ia and II afferents project into the ventral spinal cord (Yang et al., 2001; Pun et al., 2002). In these mice we found normal expression of both ER81 and Parvalbumin in DRG neurons at E17.5 (Figures 33A–33F). Group Ia and II afferents innervated the muscles

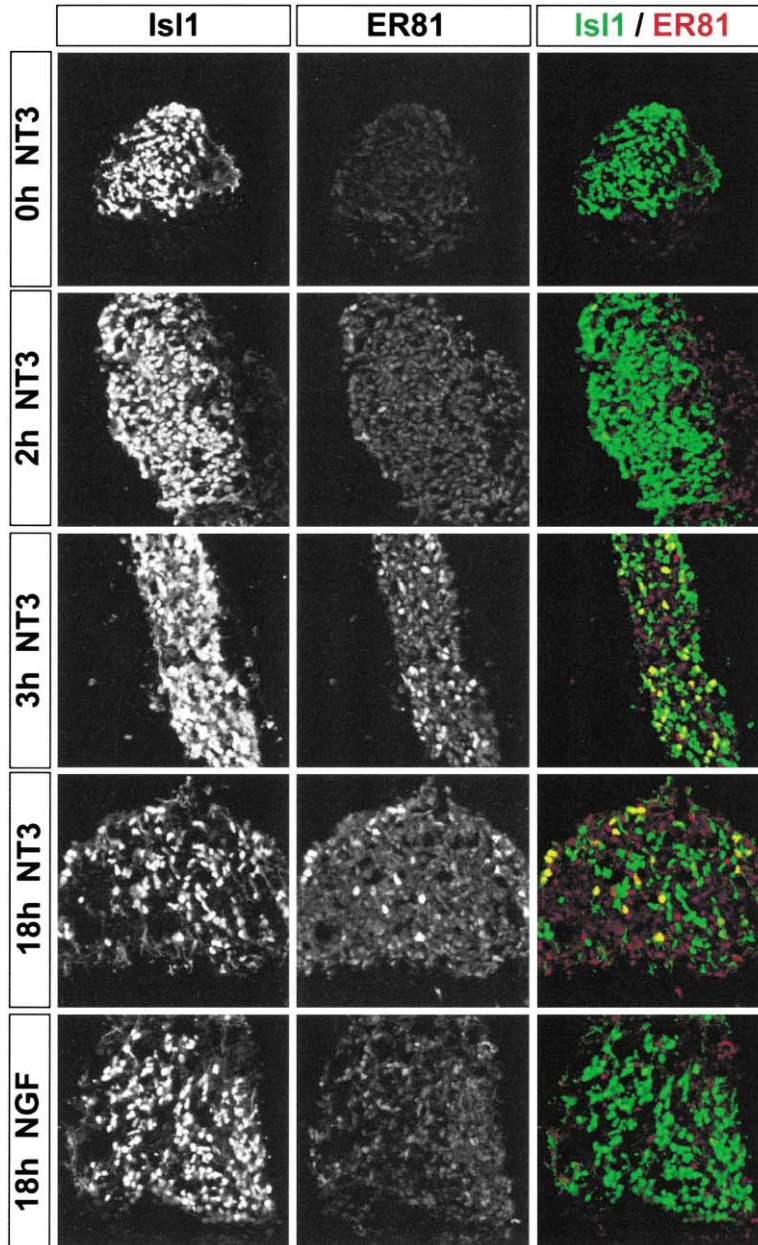


**Figure 31. Rapid Induction of ER81 Expression by NT3 in E11.5 DRG Explants.**

ER81 expression is induced in the presence of NT3 in a subset of Isl1+ DRG neurons within 3 hr of culturing the explants. In the presence of NGF, however, even after 18 hr in vitro, ER81 expression is not induced in DRG neurons.

and were capable of inducing muscle spindles expressing *Pea3* (Figures 33G–33J). In addition, the central projections of proprioceptive afferents in these mice were not impaired in their ability to project into the ventral spinal cord (Figures 33K–33N), arguing against a role for motor neuron-derived NT3 in the induction of ER81 in proprioceptive afferents and the control of the central patterning of group Ia and II afferents.

Second, to assess whether peripheral NT3 is sufficient to restore the expression of ER81 in *NT3*<sup>-/-</sup> mice, we crossed *NT3*<sup>-/-</sup> mice with a strain of mice selectively overexpressing NT3 in skeletal muscles under the control of the myogenin promoter (*myoNT3* mice). In *myoNT3/NT3*<sup>-/-</sup> mice, Parvalbumin<sup>+</sup> proprioceptive neurons are rescued from apoptotic cell death and these rescued neurons project their axons to the ventral horn of spinal cord (Wright et al., 1997). We examined ER81 expression in lumbar DRGs from E15 *myoNT3/NT3*<sup>-/-</sup> mice. As reported previously (Wright et al., 1997), Parvalbumin expression was restored by NT3 expression in muscle (Figure 30D). Furthermore, we found that in these animals, numerous DRG neurons express ER81 (Figure 30H).

Finally, in order to define the neuronal cell type in which ER81 exerts its role in controlling the development of central projections of proprioceptive afferents in the ventral spinal cord, we generated a targeted allele of *Er81* in which the first exon coding for the DNA binding ETS domain was flanked by loxP sites (Figure 34A). This mouse strain was crossed to *Isl1*<sup>Cre</sup> mice to eliminate *Er81* expression exclusively in DRG neurons, motor neurons, and a subpopulation of dorsal interneurons in the spinal cord (Srinivas et al., 2001) but not in ER81 expressing interneurons in the intermediate and dorsal spinal cord. In *Isl1*<sup>Cre</sup>/*Er81*<sup>lox/-</sup> mice, ER81 protein failed to be expressed in DRG neurons (Figures 34D and 34E), and Parvalbumin<sup>+</sup> proprioceptive afferents entered the spinal cord appropriately but terminated prematurely in the intermediate zone of the spinal cord (Figure 34G), similar to the findings in constitutive *Er81*<sup>-/-</sup> mice (Arber et al., 2000). These findings thus exclude a role for ER81-expressing interneurons in the intermediate zone of the spinal cord or ER81-expressing muscle spindles in affecting the targeting of proprioceptive afferents to the ventral spinal cord.

Taken together, our findings suggest a model in which NT3 derived from the periphery is required to control expression of ER81 in proprioceptive DRG neurons. This ETS protein in turn controls, in a cell-intrinsic manner, the development of proprioceptive projections to the ventral spinal cord.



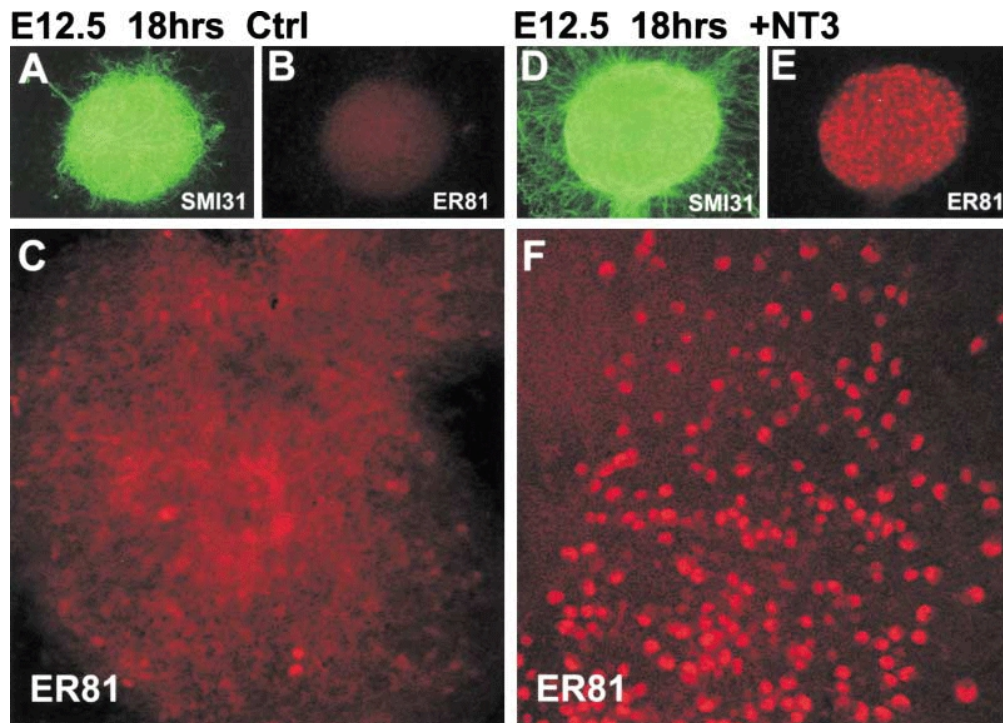


**Figure 32. Induction of ER81 Expression in E12.5 *Bax*<sup>-/-</sup> DRG Explants Is NT3 Dependent.** Confocal images of neurofilament (SMI31; [A and D]) and ER81 and staining (B and E) in DRG explants from E12.5 *Bax*<sup>-/-</sup> mice. ER81+ neurons are found after 18 hr *in vitro* in the presence of NT3 (E and F). Few if any *Bax*<sup>-/-</sup> DRG neurons exhibit ER81 immunoreactivity in the absence of NT3 (B and C), even after 18 hr. Neurofilament staining demonstrates that *Bax*<sup>-/-</sup> DRG neurons survive *in vitro* for 18 hr even in the absence of neurotrophin signaling.

## Discussion

NT3 is a powerful regulator of DRG neuronal number *in vivo* and proprioceptive neuron morphology *in vitro*, but relatively little is known about the effects of NT3 on proprioceptive axon extension and targeting during development *in vivo*. In this study, we have shown that in *Bax*<sup>-/-</sup>/*NT3*<sup>-/-</sup> mice, proprioceptive DRG neurons survive through embryonic development. However, the surviving NT3-deprived neurons exhibit both peripheral and central projection defects. The peripheral processes of proprioceptive neurons fail to support muscle spindle differentiation and there is a reduction in the number of axons in the soleus nerve at P0. Central processes extend through the dorsal roots into the dorsal columns and branch and arborize in the intermediate spinal cord but fail to reach the motor neurons in the ventral horn. Furthermore, we find that in the absence of NT3 signaling, proprioceptive DRG neurons do not express the ETS family transcription factor ER81, and conversely NT3 is able to induce ER81 expression in E11 and E12 DRG neurons. Finally, we find that a peripheral source of NT3 is sufficient to induce ER81 expression by DRG neurons *in vivo*. These findings establish a role for peripheral NT3 in the regulation of proprioceptive afferent projections to motor neuron via the regulation of ER81 expression.

### NT3 Regulates DRG Neuron Number via Control of Apoptosis

Our findings demonstrate that elimination of BAX restores DRG neuronal number, as evidenced by a ~50% increase in the number of DRG neurons even in the absence of NT3 signaling. The increase in the number of DRG neurons in *Bax*<sup>-/-</sup>/*NT3*<sup>-/-</sup> mice is comparable to that found in *Bax*<sup>-/-</sup> mice and is presumably due to the elimination of naturally occurring cell death.

There are two important aspects to NT-3 regulation of DRG neuronal number. First, ~20% of DRG neurons, including the entire proprioceptive afferent population, express TrkC from E11 through postnatal life (Mu et al., 1993; Wright and Snider, 1995; White et al., 1996), and 20%–35% of DRG neurons are lost in *TrkC* mutant mice (Klein et al., 1994 and Tessarollo et al., 1997). Therefore, NT3/TrkC signaling is thought to regulate survival of proprioceptive neurons in a manner analogous to regulation of the nociceptive population by NGF/TrkA signaling (Crowley et al., 1994; Smeyne et al., 1994). In contrast to findings in *TrkC*<sup>-/-</sup> mice, *NT3*<sup>-/-</sup> mice exhibit reductions of 60%–70% in DRG neuron number (Ernfors

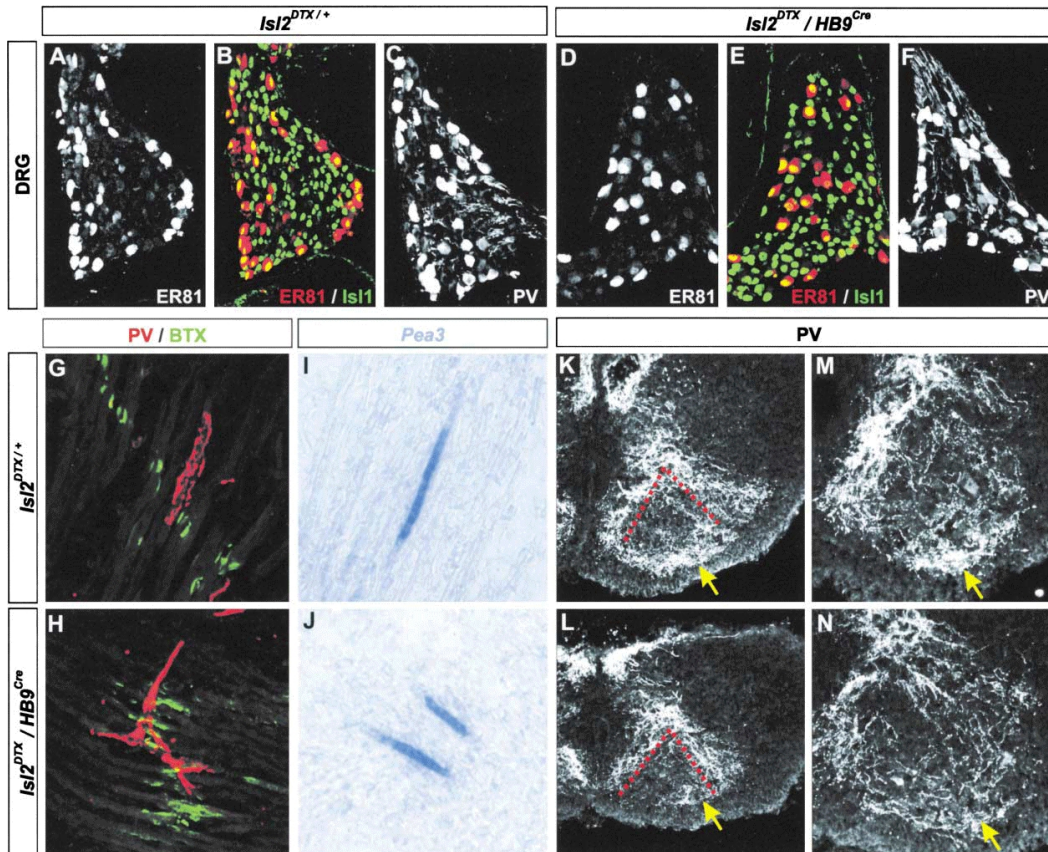


**Figure 33. Proprioceptive Afferent Development in the Absence of Motor Neurons.**

(A–F) ER81 (A and D), ER81 and Is11 (B and E), and Parvalbumin (C and F) immunocytochemistry on E17.5 brachial DRG from *Isl2*<sup>DTX</sup> (A–C) and *Isl2*<sup>DTX</sup>/*Hb9*<sup>Cre</sup> (D–F) embryos.

(G–J) Analysis of muscle spindle differentiation by Parvalbumin (PV) and -bungarotoxin (G and H) immunocytochemistry or *Pea3* *in situ* hybridization (I and J) on forelimb muscles of E17.5 *Isl2*<sup>DTX</sup> (G and I) and *Isl2*<sup>DTX</sup>/*Hb9*<sup>Cre</sup> (H and J) embryos.

(K–N) Analysis of central projections of proprioceptive afferents by Parvalbumin immunocytochemistry on spinal cords of E17.5 *Isl2*<sup>DTX</sup> (K and M) and *Isl2*<sup>DTX</sup>/*Hb9*<sup>Cre</sup> (L and N) embryos. Arrows point to the ventral horn of the spinal cord where group Ia and II afferents normally terminate.

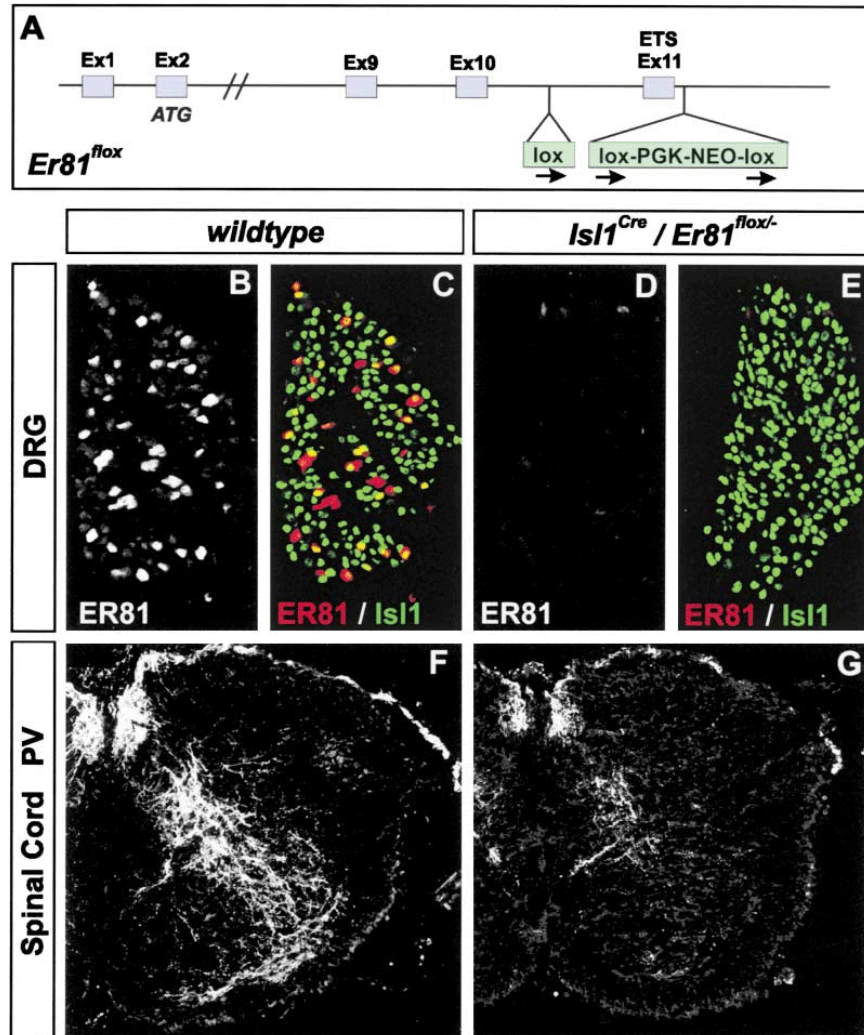


**Figure 34. ER81 Acts in Proprioceptive Afferents to Control Central Connectivity.**

(A) Schematic diagram of targeting strategy for the *Er81<sup>lox</sup>* allele.

(B–E) ER81 (B and D) and ER81/Is1 (C and E) immunocytochemistry on E17.5 lumbar DRG from wild-type (B and C) and *Isl1<sup>Cre</sup>/Er81<sup>lox/-</sup>* (D and E) embryos demonstrates absence of ER81 protein in DRG of *Isl1<sup>Cre</sup>/Er81<sup>lox/-</sup>*.

(F and G) Analysis of central projections of proprioceptive afferents by Parvalbumin immunocytochemistry on E17.5 lumbar spinal cords of wild-type (F) and *Isl1<sup>Cre</sup>/Er81<sup>lox/-</sup>* (G) embryos.



et al., 1994; Farinas et al., 1994; see also results from this study), raising the question as to the mechanism of action of NT3 on DRG neuron survival at early developmental stages.

The mechanism by which NT3 regulates DRG neuronal number remains unclear but several hypotheses have been put forward to explain the severe neuronal losses observed in the *NT3*<sup>-/-</sup> mice. Some studies have favored direct regulation of the cell cycle by NT3 (Verdi et al., 1996, Ockel et al., 1996) and therefore imply a control of neuron number through the regulation of precursor cell proliferation. Other studies have suggested that the proliferating precursors in the DRG that express TrkC undergo apoptosis in the absence of NT3, resulting in a depletion of neuronal precursors and in the generation of fewer neurons (ElShamy and Ernfors, 1996). Finally, still other studies of *TrkC*<sup>-/-</sup> and *NT3*<sup>-/-</sup> mice have suggested that failure of NT3 to activate TrkB during the proliferation stage of neurogenesis causes DRG precursors to exit the cell cycle prematurely, resulting in a smaller precursor pool (Farinas et al., 1996; Farinas et al., 1998). Characterization of Trk protein expression has demonstrated that sensory neuron precursors do not express TrkB or TrkC, suggesting that effects on the proliferating population are indirect (Farinas et al., 1998).

The current findings demonstrate that deletion of *Bax* restores DRG neuron number in the absence of NT3 signaling. Since the *Bax* deletion is thought selectively to affect the ability of DRG neurons or their precursors to enter an apoptotic cell death program and does not influence their capacity to proliferate (Deckwerth et al., 1996; White et al., 1998), our findings suggest that the effects of NT3 on DRG neuronal number are mediated via the inhibition of apoptosis. This conclusion leaves open the question of whether NT3 regulates the survival of precursors and/or postmitotic neurons. It is also possible that the early death of TrkB and TrkC neurons, or their precursors, could decrease the proliferation of neighboring cells. Our results do, however, argue against the idea that the direct regulation of proliferation by NT3 is likely to be a critical determinant of DRG neuronal number.

### **NT3 Regulates Peripheral Components of the Proprioceptive System**

Proprioceptive DRG neurons survive in *Bax*<sup>-/-</sup>/*NT3*<sup>-/-</sup> mice, but we find that their peripheral projections and associated muscle spindles are absent at P0. Thus, in the absence of NT3 signaling, there is a failure of peripheral proprioceptive axons either to grow toward their skeletal muscle targets during development, or alternatively a retraction of these processes with subsequent degeneration of the muscle spindles. Analysis of the expression of the zinc

finger transcription factor *Egr3* (Tourtellotte and Milbrandt, 1998) in muscles of *Bax<sup>-/-</sup>/NT3<sup>-/-</sup>* at E15 and E17 revealed no staining for *Egr3*, arguing that *Egr3* expression is never initiated in these mice. While we also never detected Parvalbumin<sup>+</sup> proprioceptive afferents in muscles of *Bax<sup>-/-</sup>/NT3<sup>-/-</sup>*, which may be caused by the low expression level of Parvalbumin by these afferents, an independent tracing experiment revealed some peripheral axons in distal limb muscles with a morphology similar to annulospiral endings of group Ia or II afferents. An intriguing possibility would thus be that proprioceptive afferents are present transiently in muscle nerves of *Bax<sup>-/-</sup>/NT3<sup>-/-</sup>* mice, but do not release Neuregulin-1, which is thought to mediate initiation of muscle spindle differentiation (Hippenmeyer et al., 2002).

The lack of appropriate development of peripheral endings of proprioceptive afferents and associated sensory organs observed in *Bax<sup>-/-</sup>/NT3<sup>-/-</sup>* mice is analogous to our previous observations in *Bax<sup>-/-</sup>/NGF<sup>-/-</sup>* mice in which *TrkA<sup>+</sup>* nociceptive DRG neurons survive but their peripheral cutaneous projections are absent at P0 (Patel et al., 2000). Together, these findings suggest a generality in the principle that neurotrophins are essential for the establishment and/or maintenance of peripheral sensory projections *in vivo*.

### **NT3 Regulates Proprioceptive Afferent Projections into the Ventral Spinal Cord via Regulation of ER81 Expression**

A striking finding of this study is that proprioceptive group Ia and II afferents fail to extend into the ventral spinal cord in the absence of NT3 signaling. Nevertheless, the initial extension of proprioceptive afferents into the dorsal roots and their initial arborization into the dorsal spinal cord proceed normally in the *Bax<sup>-/-</sup>/NT3<sup>-/-</sup>* mutants. This finding is consistent with our observations in *Bax<sup>-/-</sup>/NGF<sup>-/-</sup>* and *Bax<sup>-/-</sup>/TrkA<sup>-/-</sup>* mice in which the extension of the central nociceptive projections into spinal cord proceeds normally in the absence of NGF/*TrkA* signaling (Patel et al., 2000). Since neither NT3 nor NGF are expressed in the dorsal roots or the dorsal horn of the spinal cord, the extension of the central sensory axonal processes appears not to require neurotrophin signaling.

Why, in *Bax<sup>-/-</sup>/NT3<sup>-/-</sup>* mice, do the central group Ia and II projections extend only as far as the intermediate spinal cord and fail to project into the ventral horn? The targeting defect in *Bax<sup>-/-</sup>/NT3<sup>-/-</sup>* mice is similar to that seen in mice lacking the ETS family transcription factor ER81. We find that proprioceptive DRG neurons in the *Bax<sup>-/-</sup>/NT3<sup>-/-</sup>* do not express ER81 protein and that ER81 expression can be induced rapidly by application of

NT3 in DRG explant cultures. NT3 expression by motor neurons does not appear to be required for the induction of ER81 in DRG. Moreover, peripheral NT3 can restore both the expression of ER81 in DRG as well as the development of central projections of proprioceptive afferents into the ventral spinal cord in *NT3*<sup>-/-</sup> mice. Since selective elimination of ER81 in DRG and motor neurons recapitulated the *Er81*<sup>-/-</sup> phenotype, ER81 expression by interneurons in the intermediate zone of the spinal cord and by intrafusal muscle fibers is not crucial to proprioceptive-motor neuron targeting. Together, these findings suggest that peripheral NT3 regulates central proprioceptive afferent projections through its ability to regulate ER81 in proprioceptive afferents.

ER81 is a member of the ETS family of transcription factors, an evolutionary conserved gene family characterized by sequence homology within the DNA binding ETS domain (reviewed in Bartel et al., 2000). It is unclear how ER81 regulates the targeting of proprioceptive afferents to motor neurons in the ventral horn of the spinal cord, but there is growing evidence that ETS family members play a role in regulating late steps in the establishment of sensory-motoneuron connectivity. In *Pea3*<sup>-/-</sup> mice, the axons of specific pools of motor neurons fail to invade and branch normally within their target muscles and the cell bodies of these motor neurons are mispositioned within the spinal cord (Livet et al., 2002). Limb-derived signals, mediated in part by GDNF, regulate the expression of ETS proteins in motor neurons (Livet et al., 2002; Haase et al., 2002). Thus, an important implication of our findings, together with studies on PEA3, is that ETS genes act cooperatively at a late step of development to establish functional sensory-motor circuitry. In turn, ETS gene expression is regulated by neurotrophic factors released from peripheral target tissues.

It is interesting that NT3 regulates ER81 expression in proprioceptive sensory but not spinal motor neurons even though both of these neuronal classes express the NT3 receptor TrkC during embryonic development (Yan et al., 1993). This is one of several examples of differences in NT3 actions on these two types of neurons; for example, unlike proprioceptors, motor neurons do not require NT3 for survival. Little is known about differences in Trk intracellular signaling mediators that may be responsible for neuron class-specific effects.

One important question is the identity of downstream targets of ER81 that regulate the projection of proprioceptive axons. Given the specificity of the central proprioceptive

targeting defect in *Er81*<sup>-/-</sup> and *Bax*<sup>-/-</sup>/*NT3*<sup>-/-</sup> mice, ER81 may be involved in regulating the expression of axon guidance and/or cell recognition molecules. Candidates include the type II cadherins. In developing chick DRG, type II cadherin family members are coexpressed with ETS family members ER81 and PEA3 in proprioceptive neurons and spinal motor neurons. A matching of cadherin expression in proprioceptive sensory and motor neurons could therefore provide a basis for the selectivity with which sensory-motoneuron connections are formed (Price et al., 2002). It is possible that NT3 regulation of ER81 expression regulates the expression of type II cadherins in proprioceptive DRG neurons. Indeed, ectopic expression of ER81 results in the deregulation of at least one type II cadherin family member in the chick spinal cord (Price et al., 2002), and *Pea3*<sup>-/-</sup> mice show an altered profile of type II cadherin expression in motor neurons (Livet et al., 2002).

Finally, ER81 is unlikely to be the only transcription factor involved in controlling the development of central connectivity of group Ia and II afferents. Recently, a Runx family transcription factor Runx3 has been shown to be an essential regulator of proprioceptive DRG neuron development (Levanon et al., 2002; Inoue et al., 2002). *Runx3* mutant mice exhibit severe limb ataxia due to disruption of monosynaptic connectivity between proprioceptive afferents and motor neurons. The central projection defect in the *Runx3*<sup>-/-</sup> mice is more severe than that reported in *Er81*<sup>-/-</sup> mice (Arber et al., 2000) and than that reported here in the *Bax*<sup>-/-</sup>/*NT3*<sup>-/-</sup> mice. Specifically, in *Runx3*<sup>-/-</sup> mice, proprioceptive DRG neurons fail to extend central processes into the intermediate spinal cord. In contrast, in the *Bax*<sup>-/-</sup>/*NT3*<sup>-/-</sup> and *Er81*<sup>-/-</sup> mice, proprioceptive afferents extend as far as the intermediate zone but fail to extend into the ventral horn. These findings raise the possibility that Runx3 and ER81 function coordinately for proper targeting of group Ia and II afferents to the ventral horn.

### **Roles of Neurotrophic Factors in Axon Targeting**

Our study and the prior studies of Haase et al. (2002) and Ma et al. (2002) establish an important role for neurotrophic molecules in regulating axon targeting. Surprisingly, their effect on targeting is not due to the intensively studied chemotropic function of these molecules (see O'Connor and Tessier-Lavigne, 1999; Tucker et al., 2001, and references therein). In the circuit considered here, NT3 is expressed by motor neurons well prior to projection of proprioceptive afferents into the ventral horn (see Wright et al., 1997, and references therein). We show here that proprioceptive afferents project toward the ventral horn even if motor neurons are ablated genetically. In addition, it has been shown that a



central source of NT3 is unimportant in the central targeting of proprioceptive axons since central NT3 can be neutralized by anti-NT3 antibodies without affecting the projections of proprioceptive afferents (Oakley et al., 1995). Our evidence demonstrates that NT3 regulates targeting of proprioceptive afferents to motor neurons via a different mechanism — the regulation of ER81 expression and presumed subsequent effects on gene transcription through a peripheral source of NT3. At a later stage, local regulation of proprioceptive axon branching in the vicinity of the motor pools may involve Wnt signals derived from motor neurons (Krylova et al., 2002).

Since there is a peripheral projection defect in *Bax*<sup>-/-</sup>/*NT3*<sup>-/-</sup> mice, it could also be argued that target-derived factors in addition to NT3 are required to direct proprioceptive afferents to the ventral horn. Two lines of evidence suggest that NT3 has the predominant role. In chick, when proprioceptive axons are deprived of their peripheral targets by limb bud ablation, exogenous application of NT3 is sufficient to direct projection of muscle afferents appropriately within the spinal cord (Oakley et al., 1997). Furthermore, peripherally supplied NT3 is sufficient to direct central projections to motor pools even if the peripheral proprioceptive axon is misrouted in the periphery and therefore exposed to atypical peripheral influences (Oakley and Karpinski, 2002). Interestingly, target-derived NT3 also exerts important influences on proprioceptive afferent-motor neuron connections at later developmental stages and into maturity. Thus, intramuscular injections of NT3 rescue the functional deficit in group Ia and II synaptic transmission observed in *Egr3*<sup>-/-</sup> mice where proprioceptors lose their peripheral target end organ due to progressive degeneration of muscle spindles after birth (Tourtellotte and Milbrandt, 1998; Chen et al., 2002). Furthermore, administration of NT3 rescues the defect in group Ia and II synaptic transmission that results from separation of proprioceptive afferents from their targets by axotomy in fully mature animals (Mendell et al., 1999). Thus, a single target-derived neurotrophic factor appears to regulate both the development and function of this sensory-motor circuit.

## Material and Methods

### Animals

*Bax*<sup>-/-</sup> mice on a 129/B16 background (from Dr. Stan Korsmeyer) were crossed with *NT3*<sup>+/-</sup> mice also on a 129/B16 background to generate *Bax*<sup>-/-</sup>/*NT3*<sup>-/-</sup> mice. *Bax*<sup>-/-</sup> and *NT3*<sup>-/-</sup> mice maintained on a pure C57Bl/6 genetic background (Jackson Labs) were also crossed to produce *Bax*<sup>-/-</sup>/*NT3*<sup>-/-</sup> mice. Results from the two genetic backgrounds were indistinguishable. Genotypes were confirmed by tail DNA PCR (Deckwerth et al., 1996; Wright et al., 1997). *Er81*<sup>flox</sup> mice were generated by the integration of loxP sites 5' and 3' of Exon11 in the *Er81* locus in a targeting strategy analogous to Arber et al. (2000). *Isl1*<sup>Cre</sup>, *Hb9*<sup>Cre</sup>, and *Isl2*<sup>DTX</sup> mice have been described previously (Srinivas et al., 2001; Yang et al., 2001; Pun et al., 2002). The generation of *myo-NT3* mice was described previously (Wright et al., 1997).

### Neuron and Nerve Fiber Counts

Neuron and axon counts in the different mutants were conducted as described previously in detail in Patel et al. (2000). To measure the cross-sectional area of Parvalbumin+ DRG neurons at E15 and P0, images of lumbar DRG sections were captured at 20× magnification and analyzed using the NIH image software. A minimum of 15 lumbar DRG sections from each mouse was captured. The outline of Parvalbumin<sup>+</sup> cell bodies were manually traced and diameter and cross-sectional area measurements were recorded.

### Immunohistochemistry

E15, E17, and P0 mice were intracardially perfused with 4% paraformaldehyde (PFA). Tissue was dissected, postfixed in 4% PFA, washed extensively in PBS, and incubated in 30% sucrose/PBS. DRG, spinal cord, and limb sections were cut on a cryostat at 10 to 20 μm. Sections were incubated in primary antibody overnight. The following antibodies were used: goat anti-Parvalbumin (1:500, Swant, Switzerland), guinea pig anti-*Isl1* (Arber et al., 2000), rabbit anti-Parvalbumin (1:5000, Swant, Switzerland), rabbit anti-*Egr3* (1:500, Santa Cruz, Santa Cruz, CA), and rabbit anti-*ER81* (1:12,500; Arber et al., 2000). Sections were washed in PBS and incubated with the appropriate Cy-2- or Cy-3-conjugated secondary antibodies (Jackson ImmunoResearch, West Grove, PA), Alexa-488-conjugated secondary antibodies (Molecular Probes), or fluorescently labeled -bungarotoxin (Molecular Probes) and prepared

for visualization. To confirm the absence of *Egr3* immunoreactivity in E15 and E17 *Bax*<sup>-/-</sup>/*NT3*<sup>-/-</sup> muscles, we examined more than 100 hindlimb and forelimb sections at E15 and more than 200 sections at E17 from a total of three animals at each age.

### **DiI Labeling**

To label the central DRG axon projections, DiI crystals (Molecular Probes) were placed directly in the DRG at E15, E17, and P0. The tissue was incubated at 37°C in 4% paraformaldehyde and monitored periodically to assess the extent of labeling. Spinal cords were sectioned at 75 µm on a vibratome for visualization. For labeling of peripheral axon projections, DiI crystals were placed in the sciatic nerve proximal to the tibial and common peroneal branch points of E17 embryos and processed as above.

To quantify DiI labeled afferents, mean intensity measurements in defined regions of the intermediate zone and ventral horn of spinal cord were obtained using the NIH Image analysis software. Photoshop images were first converted to gray scale and inverted. Images were then imported into NIH Image, and mean intensity measurements of DiI-labeled afferents in a given area were recorded. Background corrections were made for each section. Measurements were made in a fixed area at a defined point for all sections examined. The data were expressed as the ratio of mean density measurements in the *Bax*<sup>-/-</sup>/*NT3*<sup>-/-</sup> mice versus the *Bax*<sup>+/+</sup>/*NT3*<sup>+/+</sup> mice.

### **In Situ Hybridization**

In situ hybridization was performed on fixed tissue sections according to previously described protocols (Wright and Snider, 1995; Patel et al., 2000) using digoxigenin-labeled sense and antisense riboprobes for *Er81* and *Pea3*.

### **Explant Cultures**

For ER81 induction studies, E11.5 and E12.5 wild-type DRG were dissected and whole explants cultured in DMEM/F12 medium supplemented with 10% FCS and 2 mM L-glutamine. Cultures were maintained under conditions of no neurotrophin, 10 ng/ml NT3, or 50 ng/ml NGF up to 18 hr. At different time intervals, explants were washed once for 5 min in PBS, fixed for 20 min on ice in 4% PFA, washed again in PBS, incubated in 30% sucrose/PBS overnight, and embedded the next morning using the Tissue-Tek OCT compound. After freezing, 9-µm-thick sections were cut and antibody staining performed

according to standard procedures. *Bax*<sup>-/-</sup> DRG explant cultures were performed as described in Patel et al. (2000).

## REFERENCES

- Arber, S., Ladle, D. R., Lin, J. H., Frank, E., and Jessell, T. M. (2000). ETS gene Er81 controls the formation of functional connections between group Ia sensory afferents and motor neurons. *Cell* *101*, 485-498.
- Bartel, F. O., Higuchi, T., and Spyropoulos, D. D. (2000). Mouse models in the study of the Ets family of transcription factors. *Oncogene* *19*, 6443-6454.
- Bertrand, N., Castro, D. S., and Guillemot, F. (2002). Proneural genes and the specification of neural cell types. *Nat Rev Neurosci* *3*, 517-530.
- Bibel, M., and Barde, Y. A. (2000). Neurotrophins: key regulators of cell fate and cell shape in the vertebrate nervous system. *Genes Dev* *14*, 2919-2937.
- Brown, A. G. (1981). *Organization in the Spinal Cord* (New York:Springer)
- Chen, H. H., Hippenmeyer, S., Arber, S., and Frank, E. (2003). Development of the monosynaptic stretch reflex circuit. *Curr Opin Neurobiol* *13*, 96-102.
- Chen, H. H., Tourtellotte, W. G., and Frank, E. (2002). Muscle spindle-derived neurotrophin 3 regulates synaptic connectivity between muscle sensory and motor neurons. *J Neurosci* *22*, 3512-3519.
- Clarac, F., Cattaert, D., and Le Ray, D. (2000). Central control components of a 'simple' stretch reflex. *Trends Neurosci* *23*, 199-208.
- Copray, J. C., Mantingh-Otter, I. J., and Brouwer, N. (1994). Expression of calcium-binding proteins in the neurotrophin-3-dependent subpopulation of rat embryonic dorsal root ganglion cells in culture. *Brain Res Dev Brain Res* *81*, 57-65.
- Crowley, C., Spencer, S. D., Nishimura, M. C., Chen, K. S., Pitts-Meek, S., Armanini, M. P., Ling, L. H., MacMahon, S. B., Shelton, D. L., Levinson, A. D., and et al. (1994). Mice

lacking nerve growth factor display perinatal loss of sensory and sympathetic neurons yet develop basal forebrain cholinergic neurons. *Cell* 76, 1001-1011.

Deckwerth, T. L., Elliott, J. L., Knudson, C. M., Johnson, E. M., Jr., Snider, W. D., and Korsmeyer, S. J. (1996). BAX is required for neuronal death after trophic factor deprivation and during development. *Neuron* 17, 401-411.

Eccles, J. C., Eccles, R. M., and Lundberg, A. (1957). The convergence of monosynaptic excitatory afferents on to many different species of alpha motoneurons. *J Physiol* 137, 22-50.

Edlund, T., and Jessell, T. M. (1999). Progression from extrinsic to intrinsic signaling in cell fate specification: a view from the nervous system. *Cell* 96, 211-224.

ElShamy, W. M., and Ernfors, P. (1996). A local action of neurotrophin-3 prevents the death of proliferating sensory neuron precursor cells. *Neuron* 16, 963-972.

Ernfors, P., Lee, K. F., Kucera, J., and Jaenisch, R. (1994). Lack of neurotrophin-3 leads to deficiencies in the peripheral nervous system and loss of limb proprioceptive afferents. *Cell* 77, 503-512.

Ernfors, P., Merlio, J. P., and Persson, H. (1992). Cells Expressing mRNA for Neurotrophins and their Receptors During Embryonic Rat Development. *Eur J Neurosci* 4, 1140-1158.

Farinas, I., Jones, K. R., Backus, C., Wang, X. Y., and Reichardt, L. F. (1994). Severe sensory and sympathetic deficits in mice lacking neurotrophin-3. *Nature* 369, 658-661.

Farinas, I., Wilkinson, G. A., Backus, C., Reichardt, L. F., and Patapoutian, A. (1998). Characterization of neurotrophin and Trk receptor functions in developing sensory ganglia: direct NT-3 activation of TrkB neurons in vivo. *Neuron* 21, 325-334.

Farinas, I., Yoshida, C. K., Backus, C., and Reichardt, L. F. (1996). Lack of neurotrophin-3 results in death of spinal sensory neurons and premature differentiation of their precursors. *Neuron* 17, 1065-1078.

Haase, G., Dessaud, E., Garces, A., de Bovis, B., Birling, M., Filippi, P., Schmalbruch, H., Arber, S., and deLapeyriere, O. (2002). GDNF acts through PEA3 to regulate cell body positioning and muscle innervation of specific motor neuron pools. *Neuron* 35, 893-905.

Hippenmeyer, S., Shneider, N. A., Birchmeier, C., Burden, S. J., Jessell, T. M., and Arber, S. (2002). A role for neuregulin1 signaling in muscle spindle differentiation. *Neuron* 36, 1035-1049.

Honda, C. N. (1995). Differential distribution of calbindin-D28k and parvalbumin in somatic and visceral sensory neurons. *Neuroscience* 68, 883-892.

Huang, E. J., and Reichardt, L. F. (2001). Neurotrophins: roles in neuronal development and function. *Annu Rev Neurosci* 24, 677-736.

Jessell, T. M. (2000). Neuronal specification in the spinal cord: inductive signals and transcriptional codes. *Nat Rev Genet* 1, 20-29.

Inoue, K., Ozaki, S., Shiga, T., Ito, K., Masuda, T., Okado, N., Iseda, T., Kawaguchi, S., Ogawa, M., Bae, S. C., *et al.* (2002). Runx3 controls the axonal projection of proprioceptive dorsal root ganglion neurons. *Nat Neurosci* 5, 946-954.

Klein, R., Silos-Santiago, I., Smeyne, R. J., Lira, S. A., Brambilla, R., Bryant, S., Zhang, L., Snider, W. D., and Barbacid, M. (1994). Disruption of the neurotrophin-3 receptor gene *trkC* eliminates la muscle afferents and results in abnormal movements. *Nature* 368, 249-251.

Krylova, O., Herreros, J., Cleverley, K. E., Ehler, E., Henriquez, J. P., Hughes, S. M., and Salinas, P. C. (2002). WNT-3, expressed by motoneurons, regulates terminal arborization of neurotrophin-3-responsive spinal sensory neurons. *Neuron* 35, 1043-1056.

Kucera, J., and Walro, J. M. (1987). Postnatal maturation of spindles in deafferented rat soleus muscles. *Anat Embryol (Berl)* 176, 449-461.

- Kucera, J., and Walro, J. M. (1988). The effect of neonatal deafferentation or deafferentation on myosin heavy chain expression in intrafusal muscle fibers of the rat. *Histochemistry* *90*, 151-160.
- Lentz, S. I., Knudson, C. M., Korsmeyer, S. J., and Snider, W. D. (1999). Neurotrophins support the development of diverse sensory axon morphologies. *J Neurosci* *19*, 1038-1048.
- Levanon, D., Bettoun, D., Harris-Cerruti, C., Woolf, E., Negreanu, V., Eilam, R., Bernstein, Y., Goldenberg, D., Xiao, C., Fliegau, M., *et al.* (2002). The Runx3 transcription factor regulates development and survival of TrkC dorsal root ganglia neurons. *Embo J* *21*, 3454-3463.
- Lin, J. H., Saito, T., Anderson, D. J., Lance-Jones, C., Jessell, T. M., and Arber, S. (1998). Functionally related motor neuron pool and muscle sensory afferent subtypes defined by coordinate ETS gene expression. *Cell* *95*, 393-407.
- Livet, J., Sigrist, M., Stroebel, S., De Paola, V., Price, S. R., Henderson, C. E., Jessell, T. M., and Arber, S. (2002). ETS gene Pea3 controls the central position and terminal arborization of specific motor neuron pools. *Neuron* *35*, 877-892.
- Ma, L., Harada, T., Harada, C., Romero, M., Hebert, J. M., McConnell, S. K., and Parada, L. F. (2002). Neurotrophin-3 is required for appropriate establishment of thalamocortical connections. *Neuron* *36*, 623-634.
- Markus, A., Zhong, J., and Snider, W. D. (2002). Raf and akt mediate distinct aspects of sensory axon growth. *Neuron* *35*, 65-76.
- McAllister, A. K., Katz, L. C., and Lo, D. C. (1999). Neurotrophins and synaptic plasticity. *Annu Rev Neurosci* *22*, 295-318.
- Mendell, L. M., Johnson, R. D., and Munson, J. B. (1999). Neurotrophin modulation of the monosynaptic reflex after peripheral nerve transection. *J Neurosci* *19*, 3162-3170.



Mu, X., Silos-Santiago, I., Carroll, S. L., and Snider, W. D. (1993). Neurotrophin receptor genes are expressed in distinct patterns in developing dorsal root ganglia. *J Neurosci* *13*, 4029-4041.

Oakley, R. A., Garner, A. S., Large, T. H., and Frank, E. (1995). Muscle sensory neurons require neurotrophin-3 from peripheral tissues during the period of normal cell death. *Development* *121*, 1341-1350.

Oakley, R. A., and Karpinski, B. A. (2002). Target-independent specification of proprioceptive sensory neurons. *Dev Biol* *249*, 255-269.

Oakley, R. A., Lefcort, F. B., Clary, D. O., Reichardt, L. F., Prevet, D., Oppenheim, R. W., and Frank, E. (1997). Neurotrophin-3 promotes the differentiation of muscle spindle afferents in the absence of peripheral targets. *J Neurosci* *17*, 4262-4274.

Ockel, M., Lewin, G. R., and Barde, Y. A. (1996). In vivo effects of neurotrophin-3 during sensory neurogenesis. *Development* *122*, 301-307.

O'Connor, R., and Tessier-Lavigne, M. (1999). Identification of maxillary factor, a maxillary process-derived chemoattractant for developing trigeminal sensory axons. *Neuron* *24*, 165-178.

Patapoutian, A., Backus, C., Kispert, A., and Reichardt, L. F. (1999). Regulation of neurotrophin-3 expression by epithelial-mesenchymal interactions: the role of Wnt factors. *Science* *283*, 1180-1183.

Patel, T. D., Kramer, I., Kucera, J., Niederkofler, V., Jessell, T. M., Arber, S., and Snider, W. D. (2003). Peripheral NT3 signaling is required for ETS protein expression and central patterning of proprioceptive sensory afferents. *Neuron* *38*, 403-416.

Patel, T. D., Jackman, A., Rice, F. L., Kucera, J., and Snider, W. D. (2000). Development of sensory neurons in the absence of NGF/TrkA signaling in vivo. *Neuron* *25*, 345-357.

Price, S. R., De Marco Garcia, N. V., Ranscht, B., and Jessell, T. M. (2002). Regulation of motor neuron pool sorting by differential expression of type II cadherins. *Cell* 109, 205-216.

Pun, S., Sigrist, M., Santos, A. F., Ruegg, M. A., Sanes, J. R., Jessell, T. M., Arber, S., and Caroni, P. (2002). An intrinsic distinction in neuromuscular junction assembly and maintenance in different skeletal muscles. *Neuron* 34, 357-370.

Schechter, L. C., and Bothwell, M. (1992). Novel roles for neurotrophins are suggested by BDNF and NT-3 mRNA expression in developing neurons. *Neuron* 9, 449-463.

Sharrocks, A. D. (2001). The ETS-domain transcription factor family. *Nat Rev Mol Cell Biol* 2, 827-837.

Shirasaki, R., and Pfaff, S. L. (2002). Transcriptional codes and the control of neuronal identity. *Annu Rev Neurosci* 25, 251-281.

Smeyne, R. J., Klein, R., Schnapp, A., Long, L. K., Bryant, S., Lewin, A., Lira, S. A., and Barbacid, M. (1994). Severe sensory and sympathetic neuropathies in mice carrying a disrupted Trk/NGF receptor gene. *Nature* 368, 246-249.

Snider, W. D. (1994). Functions of the neurotrophins during nervous system development: what the knockouts are teaching us. *Cell* 77, 627-638.

Srinivas, S., Watanabe, T., Lin, C. S., Williams, C. M., Tanabe, Y., Jessell, T. M., and Costantini, F. (2001). Cre reporter strains produced by targeted insertion of EYFP and ECFP into the ROSA26 locus. *BMC Dev Biol* 1, 4.

Tessarollo, L., Tsoulfas, P., Donovan, M. J., Palko, M. E., Blair-Flynn, J., Hempstead, B. L., and Parada, L. F. (1997). Targeted deletion of all isoforms of the trkC gene suggests the use of alternate receptors by its ligand neurotrophin-3 in neuronal development and implicates trkC in normal cardiogenesis. *Proc Natl Acad Sci U S A* 94, 14776-14781.

Tessarollo, L., Vogel, K. S., Palko, M. E., Reid, S. W., and Parada, L. F. (1994). Targeted mutation in the neurotrophin-3 gene results in loss of muscle sensory neurons. *Proc Natl Acad Sci U S A* *91*, 11844-11848.

Tourtellotte, W. G., and Milbrandt, J. (1998). Sensory ataxia and muscle spindle agenesis in mice lacking the transcription factor *Egr3*. *Nat Genet* *20*, 87-91.

Tourtellotte, W. G., Keller-Peck, C., Milbrandt, J., and Kucera, J. (2001). The transcription factor *Egr3* modulates sensory axon-myotube interactions during muscle spindle morphogenesis. *Dev Biol* *232*, 388-399.

Tucker, K. L., Meyer, M., and Barde, Y. A. (2001). Neurotrophins are required for nerve growth during development. *Nat Neurosci* *4*, 29-37.

Verdi, J. M., Groves, A. K., Farinas, I., Jones, K., Marchionni, M. A., Reichardt, L. F., and Anderson, D. J. (1996). A reciprocal cell-cell interaction mediated by NT-3 and neuregulins controls the early survival and development of sympathetic neuroblasts. *Neuron* *16*, 515-527.

White, F. A., Keller-Peck, C. R., Knudson, C. M., Korsmeyer, S. J., and Snider, W. D. (1998). Widespread elimination of naturally occurring neuronal death in *Bax*-deficient mice. *J Neurosci* *18*, 1428-1439.

White, F. A., Silos-Santiago, I., Molliver, D. C., Nishimura, M., Phillips, H., Barbacid, M., and Snider, W. D. (1996). Synchronous onset of NGF and TrkA survival dependence in developing dorsal root ganglia. *J Neurosci* *16*, 4662-4672.

Wright, D. E., and Snider, W. D. (1995). Neurotrophin receptor mRNA expression defines distinct populations of neurons in rat dorsal root ganglia. *J Comp Neurol* *351*, 329-338.

Wright, D. E., Zhou, L., Kucera, J., and Snider, W. D. (1997). Introduction of a neurotrophin-3 transgene into muscle selectively rescues proprioceptive neurons in mice lacking endogenous neurotrophin-3. *Neuron* *19*, 503-517.

Yan, Q., Elliott, J. L., Matheson, C., Sun, J., Zhang, L., Mu, X., Rex, K. L., and Snider, W. D. (1993). Influences of neurotrophins on mammalian motoneurons in vivo. *J Neurobiol* 24, 1555-1577.

Yang, X., Arber, S., William, C., Li, L., Tanabe, Y., Jessell, T. M., Birchmeier, C., and Burden, S. J. (2001). Patterning of muscle acetylcholine receptor gene expression in the absence of motor innervation. *Neuron* 30, 399-410.

Zelena, J. (1994). *Nerves and Mechanoreceptors – The Role of Innervation in the Development and Maintenance of Mammalian Mechanoreceptors* (New York: Chapman and Hall)

# Appendix

## **A Acknowledgments**

I am deeply obliged to Prof. Dr. Silvia Arber for giving me the unique opportunity to do my Ph. D. in her laboratory. Especially I would like to thank her for her great supervision, dedication and generosity.

Furthermore, I am very grateful for such having such a wonderful collaborator as Rishard Salie. I very much appreciate our constructive scientific atmosphere.

Finally I thank the whole lab for trying to tolerate my “organized chaos”.

## B Curriculum vitae

### Personal:

**Birth:** January 23<sup>rd</sup>, 1976 in Kroonstad, South Africa

**Address:** Socinstrasse 1, CH-4051 Basel, Switzerland

**Citizenships:** Austrian, South African

**Marital Status:** single

**Children:** none

### Education:

<b>1982 – 1986</b>	Elementary school in Dornbirn, Austria
<b>1986 – 1994</b>	High school, Bundesrealgymnasium Dornbirn, Austria (graduation with distinction)
<b>October 1994 – March 2000</b>	Studies in Biology (Human Biology) at the University of Vienna, Austria
<b>October 1998 – February 2000</b>	Diploma thesis (with distinction) (Prof. R. J. Schweyen, Institute for Microbiology and Genetics, Campus Vienna Biocenter, University of Vienna, Austria)
<b>April 2000 – June 2000</b>	Practical training using <i>C. elegans</i> (PD T. Buerklin, Biozentrum, Department of Cell Biology, University of Basel, Switzerland)
<b>Since July 2000</b>	Ph.D. candidate (Prof. S. Arber, Biozentrum, Department of Cell Biology, University of Basel, Switzerland)

## **Publications:**

Patel TD, Kramer I, Kucera J, Niederkofler V, Jessell TM, Arber S, Snider WD (2003). Peripheral NT3 signaling is required for ETS protein expression and central patterning of proprioceptive sensory afferents. *Neuron* 38:403-16

Niederkofler V\*, Salie R\*, Sigrist M, Arber S (2004). Repulsive guidance molecule (RGM) gene function is required for neural tube closure but not retinal topography in the mouse visual system. *J Neurosci.* 24:808-18.

Salie R\*, Niederkofler V\*, Arber S (2005). Patterning molecules; multitasking in the nervous system. *Neuron* 45:189-92

Niederkofler V\*, Salie R\*, Arber S (2005). *mRGMc* acts as a switch to suppress dietary iron-sensing during inflammatory response. *Nat Genet.* (submitted)

\* equal contribution



Ich erkläre, dass ich die Dissertation, *Identification and Functional Characterization of the RGM Family in Mouse*, nur mit der darin angegebenen Hilfe verfasst und bei keiner anderen Fakultät eingereicht habe.